NTIA-REPORT-79-20

Ground Wave Propagation Over Irregular, Inhomogeneous Terrain: Comparisons of Calculations and Measurements

R. H. Ott
L. E. Vogler
G. A. Hufford

U.S. DEPARTMENT OF COMMERCE
Juanita M. Kreps, Secretary

Henry Geller, Assistant Secretary
for Communications and Information

May 1979

TABLE OF CONTENTS

LIST OF FIGURES

LIST OF TABLES

GROUND WAVE PROPAGATION OVER IRREGULAR, INHOMOGENEOUS TERRAIN: COMPARISONS OF CALCULATIONS AND MEASUREMENTS

R. H. Ott, L. E. Vogler, and G. A. Hufford*

An algorithm (PROGRAM WAGNER) that evaluates HF ground-wave attenuation over irregular, inhomogeneous terrain is used to compare calculated field strengths with observed measurements for 9 actual paths and frequencies ranging from 120 kHz to 50 MHz. All comparisons show encouraging agreement between calculations and measurement. The 20 MHz comparisons over the Colorado Mountains provided a challenge for PROGRAM WAGNER.

Key Words: HF-VHF groundwave prediction; integral equation method; irregular terrain; measurement comparisons; radio propagation.

1. INTRODUCTION

A method for calculating the ground-wave field over irregular, inhomogeneous terrain was developed by Ott (1970, 1971a), and comparisons with alternative analytical methods were made for idealized terrain profiles such as concave parabolas, sea-land-sea paths, and single Gaussian ridges (Ott, 1971b, 1974). The excellent agreement between methods like Fock currents for concave surfaces, the classical residue series, and an integral equation developed by Hufford (1952), and Ott's method based upon an elementary function (closely related to the Sommerfeld flat-earth attenuation function) for the parabolic wave equation provided encouragement for the usefulness of Ott's method and the associated algorithm.

The computer program (called PROGRAM WAGNER) implementing the method based upon the parabolic wave equation is described in Ott (1971a). Improvements in the algorithm PROGRAM WAGNER which have been developed are: 1) a linear interpolation to represent the terrain heights between input terrain heights versus distance, and 2) the inclusion of an effective height-gain function to account for the influence of an elevated

*The authors are with the U. S. Department of Commerce, National Telecommunications and Information Administration, Institute for Telecommunication Sciences, Boulder, Colorado 80303.

transmitting and/or receiving antenna. The input terrain height versus distance data can be obtained from existing digitized profiles (Hopkins, 1977).

The purpose of the present paper is to describe certain extensions and modifications of the original program, and also to present a comparison of computed field strength values with actual measurements obtained over nine particular paths and frequencies ranging from 120 kHz to 50 MHz.

A draft new report on propagation over irregular, inhomogeneous terrain based on PROGRAM WAGNER was recommended in the CCIR XIV Plenary Assembly in June 1978 in Kyoto, Japan as a contribution to propagation by diffraction" and will be recommended to the Special Preparatory Meeting for GWARC-79 scheduled for October 1978 in Geneva. In addition, several groups in this country have implemented the computer algorithm at their facility. For example, Hansen (1977) used PROGRAM WAGNER to estimate the effects of a bluff along a path from Point Loma in San Diego, California to Point Mugu near Santa Cruz island. Recently Monteath (1973) pointed out the use of our integral equation program for solving the problem of propagation over irregular, inhomogeneous terrain. Wait (1974) discusses the use of our integral equation for cases where the geometry is not amenable to mode matching.

2. MODIFICATIONS TO PROGRAM WAGNER

In order to compute fields over actual paths using the previous version of PROGRAM WAGNER, the terrain had to be fit with some form of analytic function. Past versions of WAGNER used a series of Gaussian exponential terms to fit the actual terrain data points. A detailed description of this method of terrain fitting is given in an ITS Technical Memorandum of limited distribution, ERLTM-ITS 160, by J. E. Herman and R. H. Ott.

The new version of PROGRAM WAGNER uses a linear fit to the input data points for the terrain elevation versus distance and a 2-point approximation for the derivative or slope of the terrain versus distance.

Another modification of the original WAGNER is the inclusion of an effective height gain function to account for the influence of an elevated receiving antenna. The expression used is the first two terms in the series expansion of the exact height gain function arising from the smooth-earth diffraction residue series, i.e., $1 + ik\Delta h$. Here, k denotes the wave number, Δ is the normalized surface impedance, and h the receiving antenna height. The approximation is valid for heights, h, to about the first maximum in the height-gain pattern.

Finally, the modification to the integral equation for the case of propagation over terrain having up to 2 layers in conductivity and dielectric constant versus depth was derived and is given in Appendix A. This extension would allow the prediction of ground wave field strengths for example in the case of permafrost or a forested and vegetated environment. However, the mathematical results for layered ground have not been included in the latest computer algorithm PROGRAM WAGNER.

3. INTEGRAL EQUATIONS

The derivation of the integral equation used in the algorithm PROGRAM WAGNER is given in Ott (1970, 1971). The final result is

$$f(x) = W(x,0) - \sqrt{\frac{i}{\lambda}} \int_0^x f(\xi) e^{-ik\omega(x,\xi)} \{y'(\xi) W(x,\xi) - \frac{y(x)-y(\xi)}{x-\xi} + (\Delta(\xi) - \Delta_r) W(x,\xi)\} \left[\frac{x}{\xi(x-\xi)}\right]^{1/2} d\xi \ , \qquad (1)$$

where x, ξ, y(x) and y(ξ) are defined in Figure 1 and f(x) is the field normalized to twice the free-space field. The factor $(\Delta-\Delta_r)$ arises in mixed-path problems. The factor Δ_r is constant with distance and is the relative value of the normalized surface impedance. This factor is computed using the values for σ and ε_r for the first section of a mixed path. The factor Δ varies with distance in a mixed path problem. The variation of Δ with x may be continuous or contain abrupt changes. The factor $(\Delta-\Delta_r)$ is zero for a single section path. The remaining factors in (1) are defined as

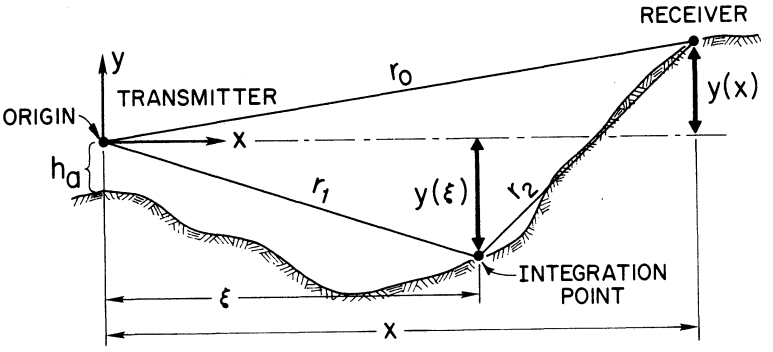

Figure 1. Great circle path geometry for integral equations.

$$\omega(x,\xi) = \frac{[y(x)-y(\xi)]^2}{2(x-\xi)} + \frac{y^2(\xi)}{2\xi} - \frac{y^2(x)}{2x} \quad ;$$

$$W(x,\xi) = 1 - i\sqrt{\pi p}\, w(-\sqrt{u}) \quad ;$$

$$p = -ik\,\Delta^2(x-\xi)/2 \quad ;$$

$$u = p\left\{1 - \frac{y(x)-y(\xi)}{\Delta(x-\xi)}\right\}^2 \quad ;\xi < x$$

$$w(-\sqrt{u}) = e^{-u}\operatorname{erfc}(i\sqrt{u})$$

$$= \frac{1}{i\pi}\int_{-\infty}^{\infty} \frac{e^{-t^2}\,dt}{\sqrt{u}+t} \quad \text{(Abramowitz and Stegun, 1964);}$$

$$\Delta = \begin{cases} \dfrac{\sqrt{\eta-1}}{\eta} & , \text{ vertical polarization} \\ \sqrt{\eta-1} & , \text{ horizontal polarization;} \end{cases}$$

$$\eta = \varepsilon_r - \frac{i\ 18(10^3)\sigma}{f(MHz)} \ ;$$

f = frequency, in MHz;

σ = ground conductivity;

ε_r = dielectric constant.

Equation (1) gives the integral equation for the attenuation function normalized to twice the free-space field

The derivation of the integral equation used in the algorithm PROGRAM INTEQ (given in Appendix B2) is described by Hufford (1952), and the final result is

$$f(x) = 1 \ - \sqrt{\frac{i}{\lambda}} \int_o^x f(\xi)\ [\Delta + y'(\xi) - \frac{y(x)-y(\xi)}{x-\xi}\ ]\ \exp\{ik/2(\rho_1-\rho_2-\rho_0)\}\ [\frac{x}{\xi(x-\xi)}]^{1/2}\ d\xi \tag{2}$$

where

$$\rho_o = \frac{[y(x)-h_a]^2}{x} - \phi(x) \simeq 2(r_o-x)-\phi(x), \tag{3}$$

$$\rho_1 = \frac{[y(\xi)-h_a]^2}{\xi} - \phi(\xi) \simeq 2(r_1-\xi)-\phi(\xi), \tag{4}$$

$$\rho_2 = \frac{[y(x)-y(\xi)]^2}{x-\xi} - \phi(x)+\phi(\xi) \simeq 2[r_2-(x-\xi)]-\phi(x)+\phi(\xi), \tag{5}$$

$$\phi(x) = -\ 2\ y'_o h_a + \int_o^x [y'(\xi)]^2\ d\xi, \tag{6a}$$

$$y'_o = y'(\xi)\Big|_{\xi=o}, \tag{6b}$$

and the distances ρ_o, ρ_1, and ρ_2 correspond to the first two terms in the binomial expansion for the distances r_o, r_1, and r_2 shown in Figure 1 minus the distance the wave travels along the surface of the terrain.

The numerical analysis used to solve (1) and (2) is significantly different, and the form for the integral equation in (1) has the potential of being numerically more efficient because the integral part of the integral equation is subtracted from a function, $W(x,0)$, that decays with distance according to the Sommerfeld flat earth attenuation function. For example, if $\sigma = .01$ S/m, $\varepsilon_r = 10$, frequency = 10 MHz, and $x = 1$ km, then $\Delta \simeq 0.024 + i0.042$, $p \simeq 4.44 - i2.47$, and $W(x,0) \simeq -0.077 + i0.064$. Suppose the exact value for the magnitude normalized attenuation, $|f(x)|$, is 0.11. Then using the form for the integral equation in (1) requires only one significant figure from the integral portion whereas the form in (2) requires two significant figures. However, in the actual examples considered in this study it was not clear that the algorithm PROGRAM WAGNER was more efficient than the algorithm PROGRAM INTEQ. In principle, PROGRAM WAGNER should allow a larger spacing for the observation points, x, to achieve a convergent solution than PROGRAM INTEQ. The present versions of both algorithms indicate that PROGRAM INTEQ is at least a factor of 4 faster in computation time than PROGRAM WAGNER. Obviously, the techniques used to code the integral equation in (2) need to be considered in coding of (1) but this is well beyond the scope of this report.

4. COMPARISONS WITH MEASUREMENT

Table 1 summarizes the comparisons of the integral equation predictions and the measurements, together with the source of the latter. The spacing of points refers to the variable x in (1) or (2) and is the distance projected on a horizontal plane. The computational time is for a CDC 6600 computer. The spacings used were not necessarily optimum and were arrived at by deciding the 100 meter spacing yielded reasonable agreement for the WGR-TV path from Buffalo, New York. When the terrain was relatively flat, spacings as large as 1 km were used.

TABLE I
Predictions/Comparisons for 9 Paths

Path	Frequency	Reference	x-spacing	Time(sec.)	Figure No.
Transmitter (WGR-TV) in Buffalo, NY-over Lake Erie toward Cleveland, Ohio	59.75 MHz (horizontal polarization)	Head, H.T. (1958)	1(1)100m;100(50)1000m 1(1) 47km;47(0.25)155km	1213 (596 pts.)	2
Transmitter (KCBS) north of San Francisco Bay, south through San Francisco, over Santa Cruz Mountains	740 kHz	CBS Radio (1971)	0.5(0.5) 72 km	113 (144 pts.)	3
Transmitter (KBOL) in Boulder, south over Davidson Mesa	1490 kHz	W. A. Kissick, et al., (1978)	0.1(0.1)19.3km;19.31km (σ=0.008 s/m)	116 (194 pts.)	4
			0.1(0.1)19.3km;19.31km (σ=0.015 s/m)	82 (194 pts.)	5
Transmitter (KBLU) in Yuma, AZ, beyond Tinajas Altas Mountains toward Mexico	560 kHz	Heckscher, J. (1977)	0.5(0.5)41km;41(0.1)45km 45(0.5)61km;61(0.1)73km 73(0.5)83km	203 (294 pts.)	6
			0.5(0.5)46km;46(0.1)48.5km; 48.6(0.5)67km	55 (154 pts.)	7
			0.5(0.5)46km;46(0.1)48.5km; 48.5(0.5)67km	56 (154 pts.)	8
Canyonlands, UT adjacent to Canyonlands National Park	2.0 MHz	W. A. Kissick, et al., (1978)	0.1(0.1)48.5km;48.58km	620 (486 pts.)	9
Canyonlands, UT adjacent to Canyonlands National Park	1.619 MHz	Same	0.1(0.1)48.5km;48.58km	609 (486 pts.)	10
Canyonlands, UT adjacent to Canyonlands National Park	518	Same	0.1(0.1)48.5km;48.58km	611 (486 pts.)	11
Canyonlands, UT adjacent to Canyonlands National Park	.419	Same	0.1(0.1)48.5km;48.58km	636 (486 pts.)	12

Table I (Continued)

Path	Frequency	Reference	x-spacing	Time(sec.)	Figure No.
Canyonlands, UT adjacent to Canyonlands National Park	.180	W. A. Kissick, et al., (1978)	0.1(0.1)48.5km;48.58km	632 (486 pts.)	13
Canyonlands, UT adjacent to Canyonlands National Park	.120	Same	0.1(0.1)48.5km;48.58km	625 (486 pts.)	14
Canyonlands, UT adjacent to Canyonlands National Park	2.0	Same	0.1(0 1)48.5km;48.58km (Colorado River σ & ε)	608 (486 pts.)	15
Canyonlands, UT adjacent to Canyonlands National Park	2.0	Same	0.1(0.1)48.5km;48.58km (ECAC profile data)	679 (486 pts.)	16
From Mare Island, Valejo, CA south over San Francisco Bay over Marin Peninsula	2.0 MHz	Same	0.1,0.2km;0.23(0.5)11.23km 11.41(0.1)12.01km;12.07(0.5)18.57km 18.72(0.1)20.22km;20.31(0.5)26.81km; 26.94(0.1)28.44km;28.52(0.5)31.02km; 31.48(0.1)37.28km;37.3km	57 (158 pts.)	17
From Mare Island, Valejo, CA south over San Francisco Bay over Marin Peninsula	1.619 MHz	Same	0.1,0.2km;0.23(0.5)11.23km 11.41(0.1)12.01km;12.07(0.5)18.57km; 18.72(0.1)20.22km;20.31(0.5)26.81km; 26.94(0.1)28.44km 28.52(0.5)31.02km; 31.48(0.1)37.28km;37.3km	57 (158 pts.)	18
Same	0.518 MHz	Same	Same	59 (158 pts.)	19
Same	0.419 MHz	Same	Same	59 (158 pts.)	20
Same	0.161 MHz	Same	Same	58 (158 pts.)	21
Same	0.137 MHz	Same	Same	56 (158 pts.)	22

TABLE I (Continued)

Path	Frequency	Reference	x-spacing	Time(sec.)	Figure No.
Santa Ritas, AZ near Greenvalley, AZ and adjacent to AZ Experimental Range	2.0 MHz	W. A. Kissick, et al., (1978)	0.1(0.1)1km; 1(0.5)7km 7(0.1)20km; 20(0.5)30km (σ change at 16.40 km)	72 (172 pts.)	23
Same	Same	Same	0.1(0.1)30km (σ change at 12.95 km)	210 (300 pts.)	24
Same	Same	Same	Same (measured values for σ)	106 (166 pts.)	25
Same	Same	Same	Same (Two section flat earth)	7 (49 pts.)	26
Same	1.619 MHz	Same	0.1(0.1)km; 1(0.5)7 km 7(0.1)20km; 20(0.5) 30 km (conductivity from geological maps) (σ change at 16.40 km)	70 (172 pts.)	27
Same	Same	Same	0.1(0.1) 1 km; 1(0.5) 7 km 7(0.1) 20 km; 20(0.5) 30 km conductivity from geological maps) (except σ change at 12.95 km)	97 (172 pts.)	28
Same	0.518 MHz	Same	Same (except σ change at 16.40 km)	71 (172 pts.)	29
Same	Same	Same	Same (except σ change at 12.95 km)	97 (172 pts.)	30
Same	0.419 MHz	Same	Same (except σ change at 16.40 km)	70 (172 pts.)	31
Same	Same	Same	Same (except σ change at 12.95 km)	107 (172 pts.)	32
Same	0.160 MHz	Same	Same (except σ change at 16.40 km)	69 (172 pts.)	33
Same	Same	Same	Same (except σ change at 12.95 km)	106 (172 pts.)	34
Same	0.137 MHz	Same	Same (except σ change at 16.40 km)	69 (172 pts.)	35
Same	Same	Same	Same (except σ change at 12.95 km)	108 (172 pts.)	36

TABLE I (Continued

Path	Frequency	Reference	x-spacing	Time(sec.)	Figure No.
Dry Lake, NE, Transmitter on east slope of Highland Peak to Dry Lake Valley	2.0 MHz	W. A. Kissick, et al. (1978)	0.1(0.1) 15km;15(0.5)21 km; 21(0.1)23km;23(0.5)42km 42(0.1)44.5km;44.5(0.5)52km; 52.46 km (PROGRAM INTEQ)	8 (147 pts.)	37
Same	Same	Same	Same (PROGRAM WAGNER)	263 (261 pts.)	38
Same	1.619 MHz	Same	Same	263 (261 pts.)	39
Same	0.518 MHz	Same	Same	254 (261 pts.)	40
Same	0.419 MHz	Same	Same	259 (261 pts.)	41
Same	0.160 MHz	Same	Same	267 (261 pts.)	42
Same	0.137 MHz	Same	Same	262 (261 pts.)	43
Colorado Mountain Data toward Berthoud Pass Campground	20.084 MHz	M. E. Johnson, et al. (1967)	0.1(0.1)50.4km;50.46km	599 (505 pts.)	44
Same	Same	Same	0.05(0.05)30km	677 (600 pts.)	45
Same	Same	Same	0.01 (0.01) 6 km	913 (600 pts.)	46
Same	Same	Same	0.46(0.1)30.76km; (PROGRAM INTEQ)	59 (304 pts.)	47
Same	Same	Same	0.26 (0.05) 29.96 km (PROGRAM INTEQ)	186 (595 pts.)	48
Same	Same	Same	0.05 (0.01) 10 km (PROGRAM INTEQ)	445 (996 pts.)	49

The algorithm, PROGRAM WAGNER, is best suited to propagation frequencies below VHF. Also, because of problems in maintaining numerical accuracy during the integration process, predicting attenuation for vertical polarization is usually more successful than for horizontal polarization.

In the upcoming comparisons, the ordinate scales are in the familiar dBμ/kW, which is to say the field intensity measured in dB above 1μV/m and normalized to the case of 1 kW radiated from a (vertical) half-wave dipole.

To test what might be considered an extreme case for the applicability of WAGNER, a path near Buffalo, New York, was chosen (Head, 1958). Field strength measurements were available along a radial from WGR-TV over a path that extended out to about 155 km. The station transmitted horizontally polarized waves at a frequency of 59.75 MHz. The initial portion of the path (about 47 km) was over Lake Erie, with the remaining portion over land containing variable terrain features. A plot of the path profile is shown in the lower part of Figure 2; it should be noted that the irregularity of the terrain is greatly exaggerated because of the expanded height scale.

The predicted effective radiated power in Figure 2 was obtained using a version of PROGRAM WAGNER which used a series of Gaussian terms to fit the terrain profile, using PROGRAM TERMAP. Fifty-eight terms were used in the terrain fit, with the difference between fit and actual terrain data points being everywhere less than about 27 m. The predicted field, represented by the solid line, is shown in the upper part of Figure 2. The abrupt change at about 47 km is caused by the passage of the wave from the smooth surface of Lake Erie (with assumed dielectric constant = 81 and conductivity = 0.01 S/m) to the land (with dielectric constant = 15 and conductivity = 0.03 S/m).

Measured values are represented by X's that start near the shore of the lake and are plotted at various distances over the land portion of the path. The upper end of the vertical line

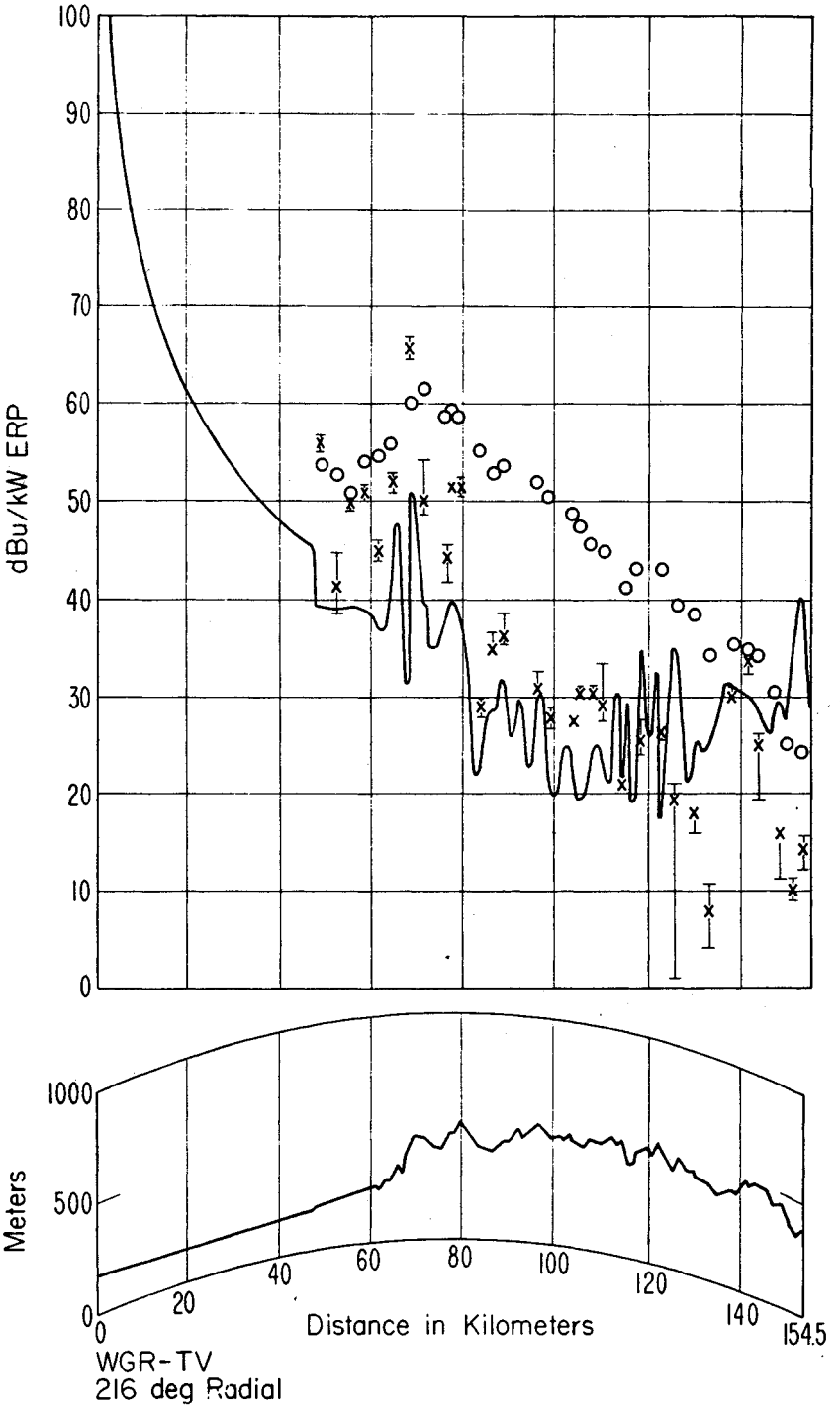

Figure 2. Path profile (lower portion) and received signal in dB above 1 μV/m for 1 kW Effective Radiated Power) for WGR-TV. Crosses denote measured spatial averages taken on 100 ft. mobile runs; circles denote "residue-height gain" predictions (see text). WGR antenna: 133 m above ground, 320 m above sea level.

through each X is the maximum field that was measured during a 100-ft. mobile run at each receiving site; the lower end is the minimum observed field and the X's are plotted at the median values.

The calculated field appears to follow the general trend of the observed values although individual points are not predicted. One reason for this, of course, could be that local terrain effects at the measurement sites (e.g., buildings, telephone wires, etc.) greatly influence the received field. There is also some indication, especially in the first few measurements near Lake Erie, that complex interference effects not accounted for by the simple ground-wave model are operating.

Figure 2 also shows a set of points, denoted by circles, that give a predicted field obtained by multiplying the classical residue series over a smooth sphere (with $\varepsilon = 15$ and $\sigma = 0.03$ S/m) by a "terrain-height gain" function, $1 + ik\Delta y$, where y is the terrain height above the sphere. This was included, not as a recommended prediction model, but merely as a matter of interest to show an attempt at a simple approach to the problem of irregular terrain propagation. It is apparent that the received fields depend significantly on the intervening terrain and not just the terrain height at the receiving point.

A second comparison of calculations and observations was made on a path in the San Francisco region (CBS Radio, 1971). Measurements were available on a radial from KCBS, a station transmitting vertically polarized waves at a frequency of 740 kHz. Figure 3 shows the path profile, measured field strength values, and prediction curve over a path of about 73 km. The terrain function deviated from the actual terrain data by about 40 m at the most using PROGRAM TERMAP. As can be seen, the prediction is well in accord with the observed data except for the end of the path. Whether the disagreement in this region is because of inaccurate values of electrical ground constants or, perhaps, the wrong assumption for the effect of atmospheric refraction is not known. The following table shows the ground constants used over various portions of the path.

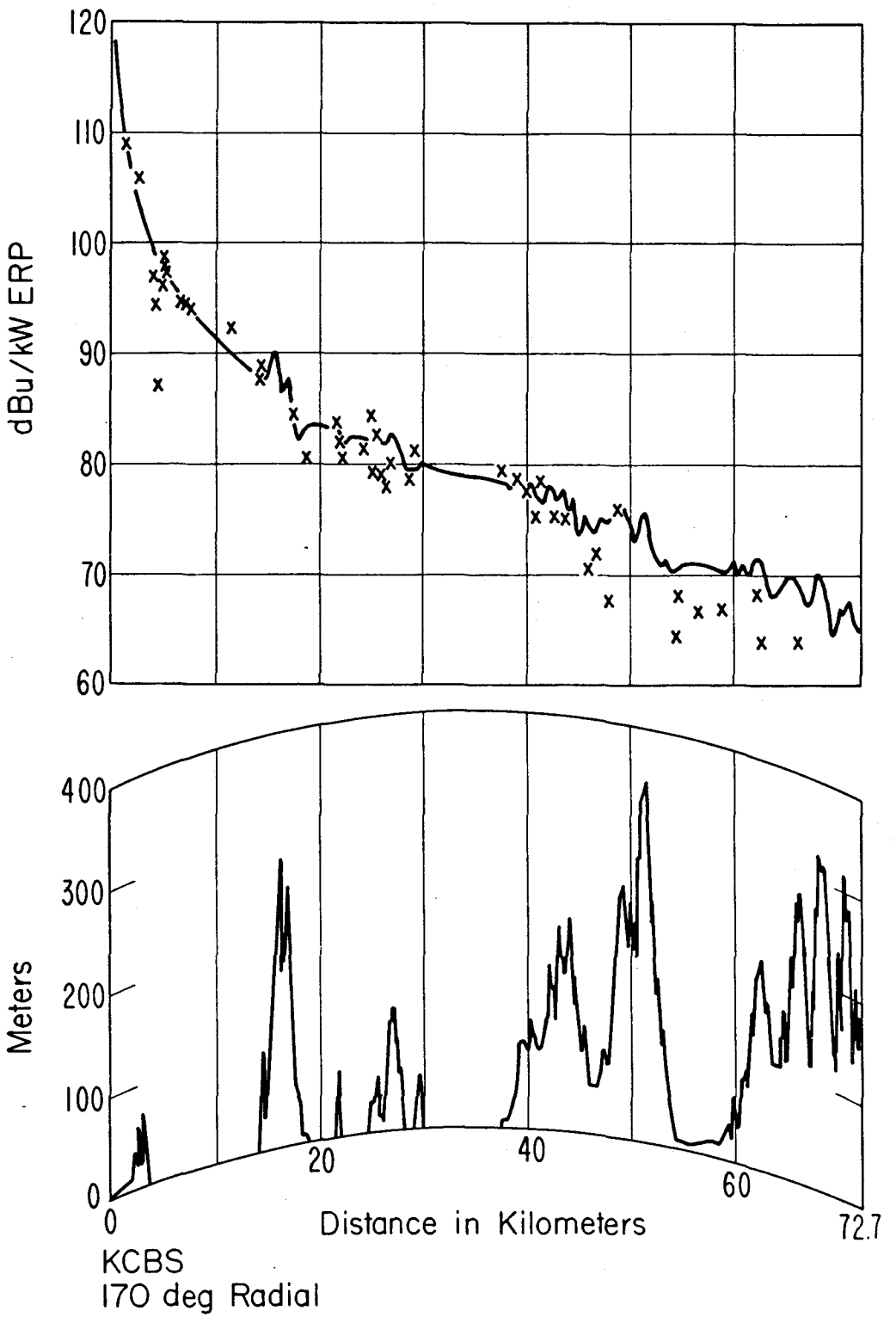

Figure 3. Path profile (lower portion) and received signal (in dB above 1 μV/m for 1 kW Effective Radiated Power) for KCBS. Crosses denote measured medians.

Distance (km)		ε	σ (S/m)
to	19.19	15	0.01
	21.98	81	5
	22.50	15	0.03
	25.05	81	5
	30.41	15	0.03
	37.72	81	5
	72.73	15	0.008

In both of the examples presented here, a standard "4/3-earth" atmosphere was assumed. The computer program is capable of including other values of constant atmospheric ray bending through the use of the effective earth's radius concept.

It should again be noted that the first few measurements near the transmitting end of the path indicate a more complex interference mechanism than is assumed in the present model.

4.1 KBOL - Davidson Mesa Path

Two sets of field strength measurements were taken along a radial running from station KBOL in Boulder, Colorado (f = 1490 kHz, vertical polarization), southeast towards the Davidson Mesa area. The terrain profile is shown in the lower portions of Figures 4 and 5. The measurements P_m, in terms of received power in dBm, were taken on Dec. 9 and Dec. 15, 1977.

d(km)	P_m(12/9)	P_m(12/15)	d(km)	P_m(12/9)	P_m(12/15)
1.75	-43 8	-47.4	9.92	-62.5	-64.0
3.63	-58.3	-59.1	10.81	-65.5	-66.0
5.42	-56.5	-57.4	14.57	-68.0	-68.7
6.53	-56.4	-58.1	15.02	-68.2	-69.7
8.61	-61.4	-62.6	19.31	-70.2	-74.1

Because the absolute level of the radiated power from the transmitter, P_t, was not known, the data were adjusted so that the first measured point (at d = 1.75 km) agreed with the WAGNER calculated value at this distance.

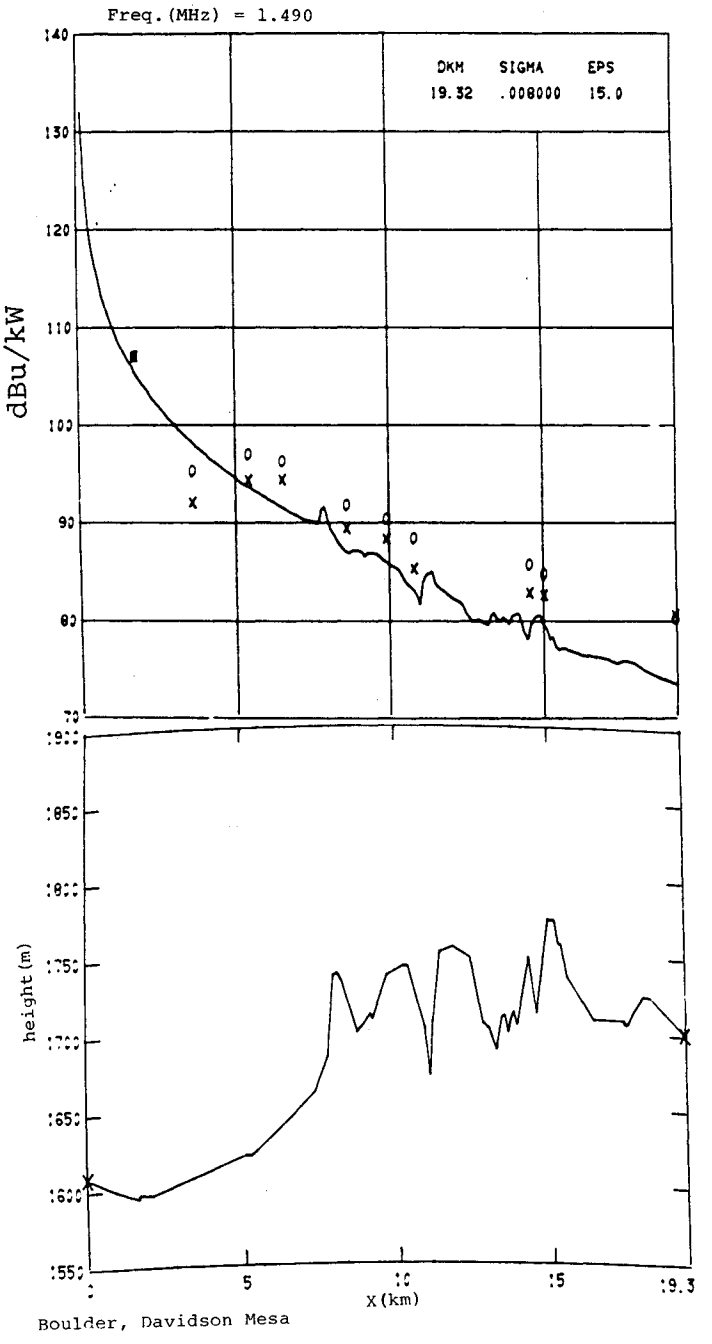

Figure 4. Path profile (lower portion) and received signal (in dB above 1 μV/m for 1 kW effective radiated power) for KBOL. Crosses denote measured 2.5 min. averages on Dec. 9 and the circles those of Dec. 15.

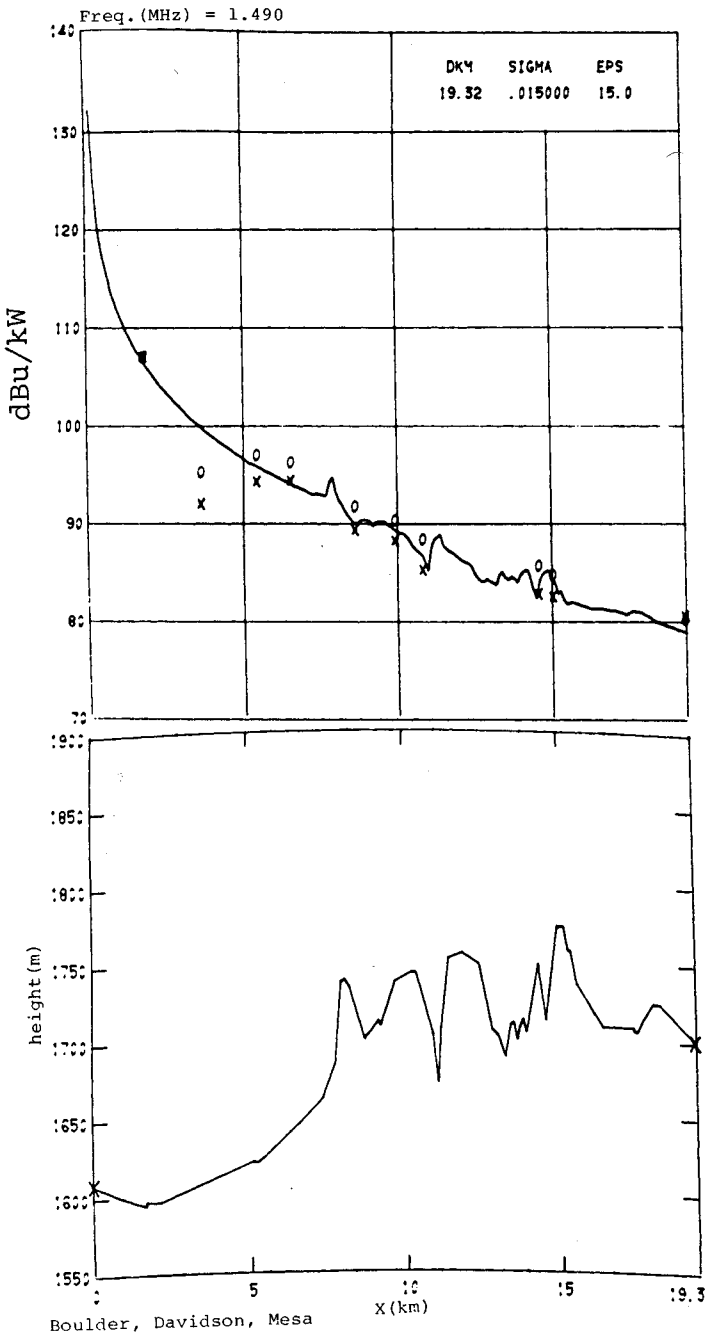

Figure 5. Path profile (lower portion) and received signal (in dB above 1 μV/m for 1 kW effective radiated power) for KBOL. Crosses and circles denote measured 2.5 min. averages.

	σ = 0.008, ε = 15		σ = 0.015, ε = 15	
d(km)	DBU (12/9)	DBU (12/15)	DBU (12/9)	DBU (12/15)
1.75	105.9	105.9	107.0	107.0
3.63	91.4	94.2	92.0	95.3
5.42	93.2	95.9	94.3	97.0
6.53	93.3	95.2	94.4	96.3
8.61	88.3	90.7	89.4	91.8
9.92	87.2	89.3	88.3	90.4
10.81	84.2	87.3	95.3	88.4
14.57	81.7	84.6	82.8	85.7
15.02	81.5	83.6	82.6	84.7
19.31	79.5	79.2	80.6	80.3

Figures 4 and 5 show the plots of predictions and measurements, the X's representing the measurements of Dec. 9 and the circles those of Dec. 15. The measurements compare favorably with calculations when a conductivity of σ = 0.015 S/m is assumed (Fig. 5). This is understandable since the Boulder path is more over a "plains type" region (corresponding to σ = 0.015) rather than the adjacent foothills (σ = 0.008).

The measurements at the 3.6 km site are some 5 to 8 dB away from prediction, but this is believed due to the fact that this site (and only this site) was located in the midst of high buildings and considerable traffic congestion.

4.2 RADC Paths: KBLU to Junction and Water

Rome Air Development Center (Heckscher, 1979) has made a number of field strength measurements in an area southeast of Yuma, Arizona using as a source the Yuma commercial broadcast station KBLU (560 kHz). The measurement sites are along jeep roads that run in various directions throughout the area. Although no series of measurements are strictly along a radial from KBLU, some are approximately so. Two series were found in the southern-most sector, and path profiles were determined from USGS maps along two radials from KBLU. The profiles are shown in the lower portions of Figures 6, 7, and 8. Path #1 (Fig. 6) crosses a minor ridge (Vopoki Ridge) at about 45 km and, later on, a higher ridge (Tinajas Altas Mtns.) at about 65 km. Path #2 (Figs. 7 and 8) crosses Vopoki Ridge also at about 45 km but nearer the southern end.

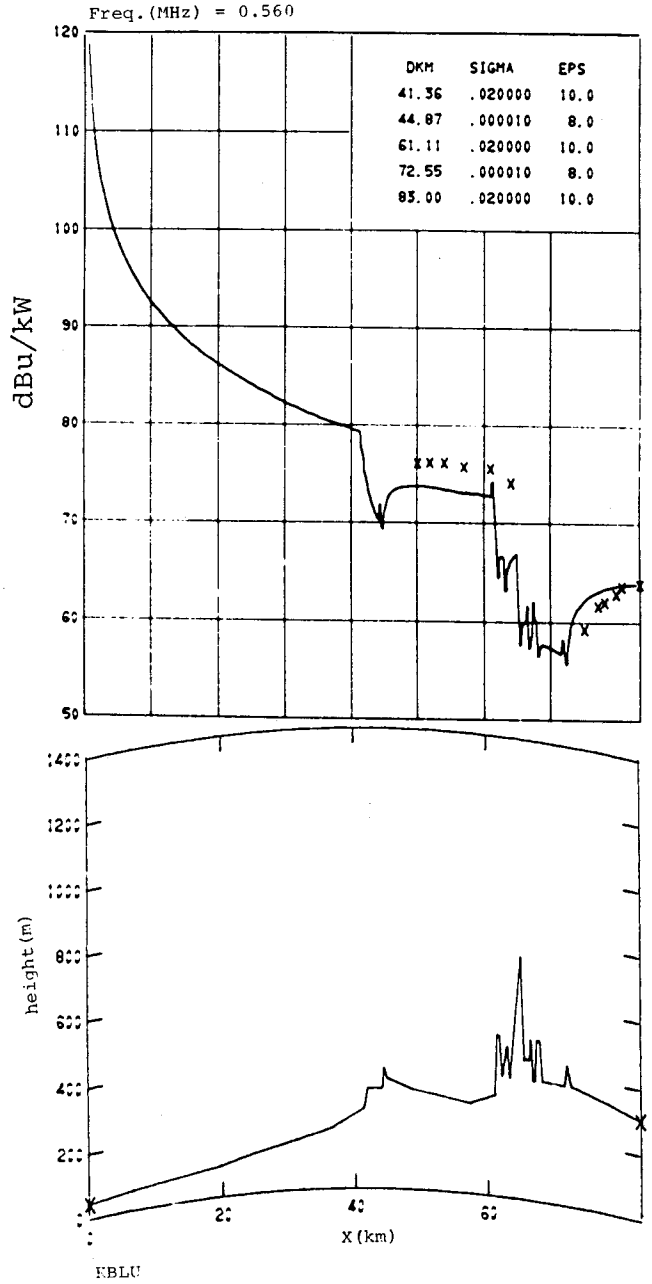

Figure 6. Path profile (lower portion) and received signal (in dB above 1 μV/m for 1 kW effective radiated power) for KBLU. Crosses denote measured averages.

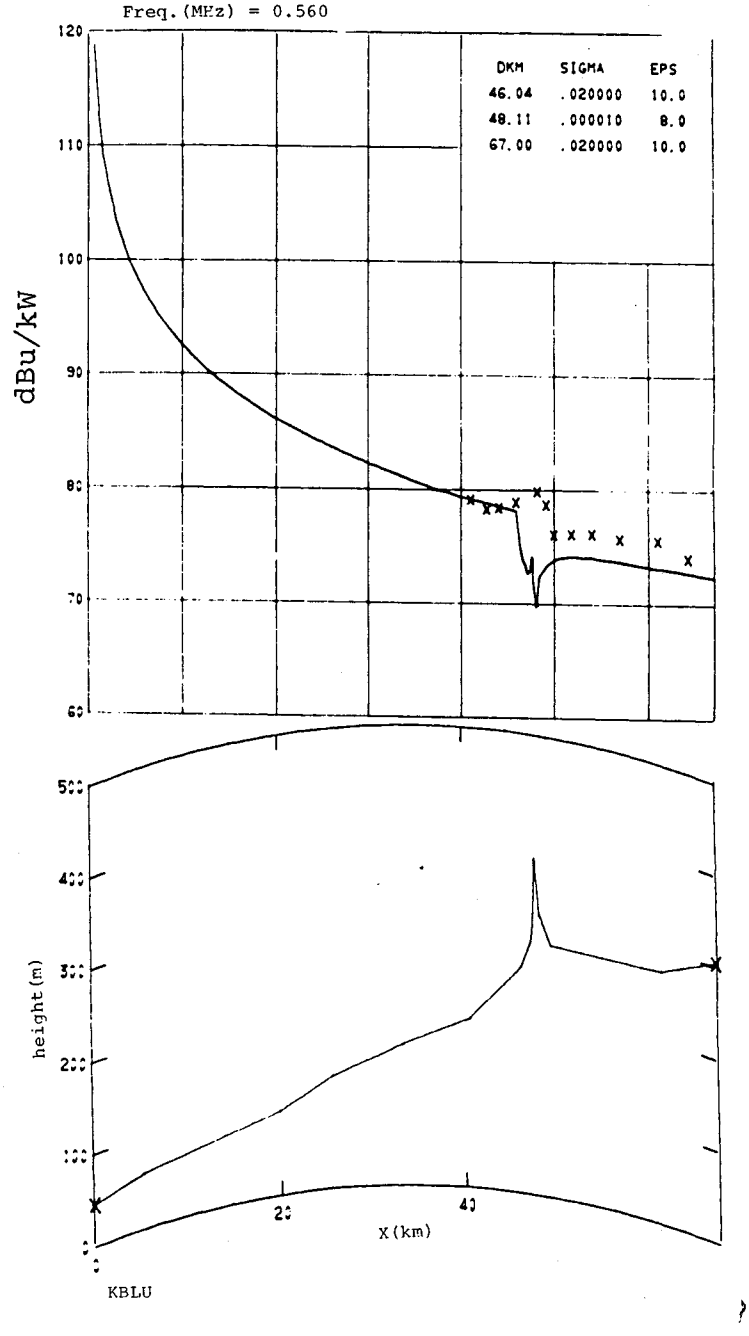

Figure 7. Path profile (lower portion) and received signal (in dB above 1 μV/m for 1 kW effective radiated power) for KBLU. Crosses denote measured averages.

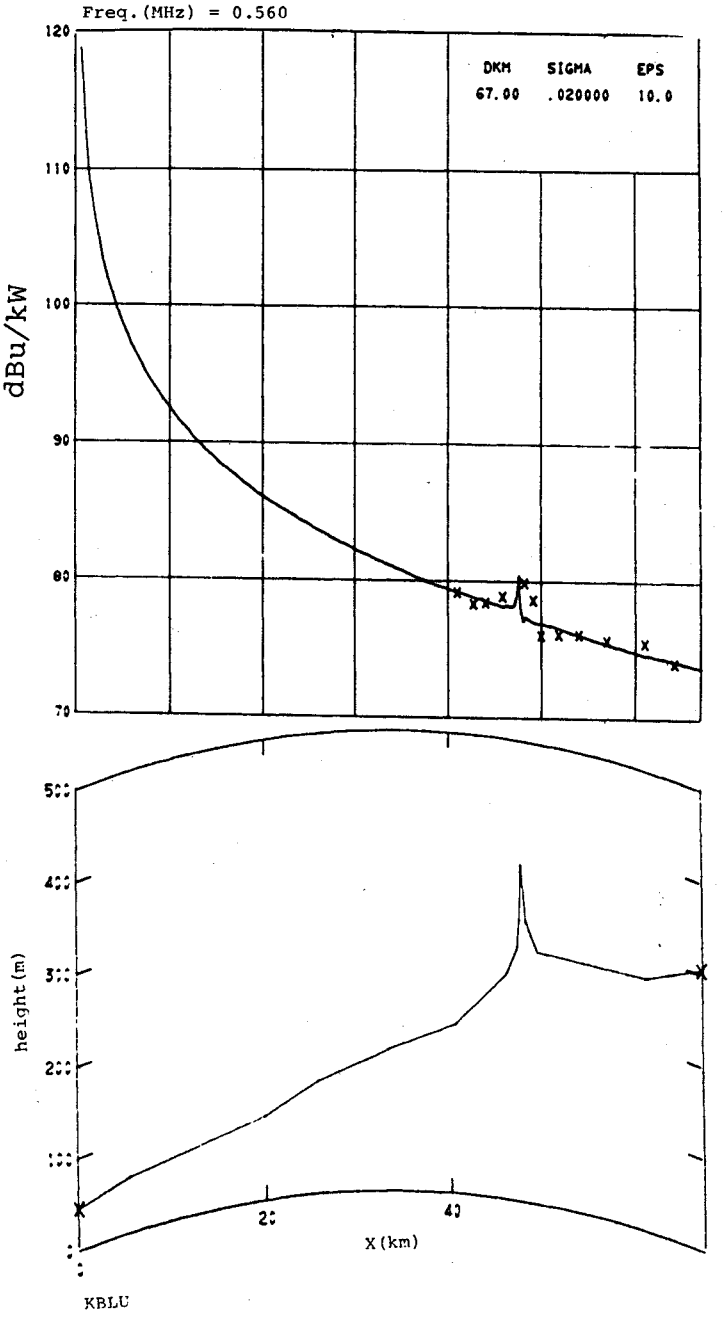

Figure 8. Path profile (lower portion) and received signal (in dB above 1 μV/m for 1 kW effective radiated power) for KBLU. Crosses denote measured averages.

The measurements corresponding to these two radials are tabulated below in terms of the field intensity, E(mV/m), measured at each location times the distance, d(km), from the transmitter.

Path #1		Path #2			
d(km)	E·d(V)	d(km)	E·d(V)	d(km)	E·d(V)
75	38	41	205	50	178
77	52	43	196	52	185
78	55	44	204	54	192
80	62	46	223	57	193
81	68	48	267	61	204
83	72	49	243	64	180

From other measurements nearer the transmitter, E·d was found to approach a value of about 250. Thus, in order to compare with the WAGNER predictions in DBU, the measurements obey the relationship

$$DBU = E_o + 20 \log a_m = 112.94 - 20 \log d(km) + 20 \log a_m, \quad (3)$$

where E_o is the reference field used in WAGNER and $a_m = (E \cdot d)/250$ is the attenuation at each receiving site. The values of measured DBU for each path are given in the following table:

Path #1		Path #2			
d(km)	DBU	d(km)	DBU	d(km)	DBU
75	61.6	43	78.2	52	76.0
78	61.9	44	78.3	54	76.0
80	62.8	46	78.7	57	75.6
81	63.5	48	79.9	61	75.5
83	63.7	49	78.9	64	74.0

PROGRAM WAGNER was run for Path #1 using the following electrical ground constants:

d(km)	ε	σ(S/m)
0-41.4	10	0.02
41.4-44.9	8	10^{-5}
44.9-61.1	10	0.02
61.1-72.5	8	10^{-5}
72.5-83.0	10	0.02.

The conductivity value of $\sigma = 0.02$ represents the nearly level, sandy portions of the area and was obtained from RADC on-site measurements. The values of $\sigma = 10^{-5}$ and $\varepsilon_r = 8$ represent the conductivity and dielectric constant of the rock composing the mountains and ridges of the area. The type of rock was determined from a geological map of Arizona, and σ and ε_r were obtained from tables in a paper discussing ground constants of various rock materials (Ring, 1958).

Figure 6 is a plot of predicted DBU from WAGNER (the solid curve) for Path #1, together with measured DBU represented by crosses. The last six measurements, which were taken along this profile, appear to agree very well with prediction. The first six crosses are measurements taken along Path #2 but plotted here because of the near proximity and similarity of terrain for the two paths in this area. These measurements do not agree as well because of slight differences between the two profiles.

Path #2 was run on WAGNER with the following values for electrical ground constants:

d(km)	ε_r	σ(S/m)
0-46.0	10	0.02
46.0-48.1	8	10^{-5}
48.1-67.0	10	0.02 .

Figure 7 shows the WAGNER prediction together with the measurements taken along this radial. The abrupt drop in predicted field at about 46 km is due to the change in ground constants at this point. Because this radial crosses Vopoki Ridge at its southern-most end where the ridge merges into the surrounding plain, it was decided to run WAGNER again for this same profile using the values $\varepsilon = 10$ and $\sigma = 0.02$, throughout the length of the path. The result is shown in Figure 8. The better agreement between prediction and measurements would indicate that the received signal was travelling mostly over terrain characterized by a conductivity of $\sigma = 0.02$.

4.3 ITS Measurements

In the first half of 1978, signal strength measurements were made by ITS (Kissick et al., 1978) along four different paths located in the western part of the U.S. An attempt was made to locate the paths in areas where access roads provided numerous sites along the radial at which measurements could be taken. The four paths and their location designations are:

(1) Canyonlands: Canyonlands National Park in southern Utah;

(2) San Francisco: a path in the bay area of San Francisco, California;

(3) Santa Rita: located near the Santa Rita Mountains of southern Arizona;

(4) Nevada: a path west of Pioche, Nevada.

Measurements of received power at six different nominal frequencies (2000, 1600, 500, 400, 200, 100 kHz) were recorded at each site along the four paths. In figures 4 through 43 the measured values denote the average of about 256 samples taken over a period of about 2.5 minutes. In order to compare the measurements with the output of WAGNER in terms of field-strength in decibels above 1 μV/m (designated DBU), the following relationship is used:

$$DBU = 139.37 + 20 \log f_{MHz} - P_t + P_m , \qquad (4)$$

where P_m is the measured received power in dB above 1 mW and P_t is an unknown constant (for each frequency run). To adjust the DBU such that the first measured point (or some chosen one) equals the WAGNER DBU prediction at that distance, d, solve (20) for P_t:

$$P_t = 139.37 + 20 \log f_{MHz} + P_m(d=d_1) - DBU(\text{WAGNER at } d=d_1) = \text{const.} \qquad (5)$$

The remaining DBU are then calculated from (4).

In general, values of electromagnetic ground constants were determined from geological maps of the areas involved in conjunction with tables of conductivity and dielectric constant contained in a paper by Lytle (1974). Estimates of σ and ε for various types of rocks are given in the tables, which values were then used for the appropriate segments of the radio path as determined by the geological maps. The one exception to this procedure was in the case of San Francisco where much of the path was over water. For this path, sea water values were used over water and FCC suggested values were used for the portion over land. We felt the FCC maps were more appropriate for portions of this path which went over swampy regions where the soil type was difficult to identify.

Canyonlands

Measurements were taken at 31 sites along a 45 km radial. At some of the sites, signal records for particular frequencies are missing; however, in general it was possible to obtain measurements for all 6 frequencies at each site. A tabulation of the site distances (from the transmitter), the received power levels (at the 6 frequencies), and the values of DBU used to compare with WAGNER calculations are shown in Table II. The constant values, P_t, for each frequency were determined from the first site at d = 1.16 km.

Figures 9 through 14 show comparisons of measurements (denoted by crosses) with WAGNER predictions for the 6 frequencies. The lower portion of each figure shows the terrain profile of the Canyonlands path with the terrain height above mean sea level in meters versus the distance in kilometers. Since the geological formations appear to consist almost entirely of various types of sandstone, a constant σ = 0.004 S/m and ε = 5 was assumed throughout the path.

Table II. Measured received power in dBm, P_m (upper number), and field strength in dB above 1 μV/m, DBU (lower number), for the designated frequencies and distances from the transmitter along the Canyonlands path.

d(km) \ f(MHz)	2.00	1.618	0.520	0.412	0.182	0.121
1.16	-28.6 108.8	-25.9 109.9	-41.2 111.7	-44.9 111.8	-53.9 111.8	-60.3 111.8
1.44	-31.4 106.0	-28.8 107.0	-43.9 109.0	-48.3 108.4	-57.4 108.3	-64.1 108.0
2.00	-38.1 99.3	-33.0 102.8	-50.0 102.9	-54.2 102.5	-62.5 103.2	--
3.19	--	-39.1 96.7	-49.4 103.5	-55.1 101.6	-65.2 100.5	-72.7 99.4
4.69	-50.2 87.2	-44.8 91.0	-52.7 100.2	-57.2 99.5	-62.2 103.5	-72.5 99.6
6.75	-52.5 84.9	-48.3 87.5	-58.1 94.8	-60.5 96.2	-70.8 94.9	-78.3 93.8
7.22	-50.8 86.6	--	-56.3 96.6	-60.0 96.7	-65.8 99.9	-72.7 99.4
9.75	-56.5 80.9	-51.9 83.9	-60.8 92.1	-62.8 93.9	-70.7 95.0	75.4 96.7
13.75	--	-64.5 71.3	-67.9 85.0	-71.0 85.7	-78.9 86.8	-80.8 91.3
14.06	-73.2 64.2	-65.4 70.4	-71.8 81.1	-71.8 84.9	-79.3 86.4	-81.3 90.8
14.72	-71.0 66.4	-65.7 70.1	-68.5 84.4	-69.1 87.6	-74.5 91.2	-79.5 92.6
19.62	-69.4 68.0	-67.0 68.8	-69.8 83.1	72.2 84.5	-74.7 91.0	-79.1 93.0
21.56	-72.3 65.1	-70.0 65.8	-75.3 77.6	-74.9 81.8	-81.1 84.6	-85.3 86.8
22.03	-77.1 60.3	--	-70.6 82.3	--	--	-86.5 85.6
22.97	-71.6 65.8	-65.4 70.4	-77.8 75.1	-75.8 80.9	-79.6 86.1	-84.6 87.5
24.37	-83.5 53.9	-80.4 55.4	-79.1 73.8	-76.9 79.8	-83.3 82.4	-89.5 82.6
24.44	--	-79.5 56.3	-86.9 66.0	-88.1 68.6	-85.7 80.0	-92.0 80.1
25.25	79.0 58.4	-75.8 60.0	-80.4 72.5	-79.7 77.0	-84.7 81.0	-90.8 81.3

Table II continued

d(km) \ f(MHz)	2.00	1.618	0.520	0.412	0.182	0.121
25.31	-81.5 55.9	-74.7 61.1	-84.4 68.5	-79.8 76.9	-82.7 83.0	--
30.81	-82.5 54.9	-78.8 57.0	-80.7 72.2	-81.7 75.0	-82.2 83.5	-87.8 84.3
31.94	-76.0 61.4	-74.0 61.8	-80.3 72.6	-82.2 74.5	-81.7 84.0	-84.7 87.4
32.75	-87.4 50.0	-83.1 52.7	-88.6 64.3	-90.2 66.5	-89.5 76.2	-94.7 77.4
35.03	-73.9 63.5	-72.5 63.3	-88.9 64.0	-82.8 73.9	-82.9 82.8	-89.1 83.0
37.19	-78.2 59.2	-76.4 59.4	-91.6 61.3	-83.0 73.7	-82.9 82.8	-91.4 80.7
38 41	-77.7 59.7	-75.0 60.8	-87.3 65.6	-86.8 69.9	-89.4 76.3	-89.9 82.2
39.50	-80.6 56.8	-77.2 58.6	-91.1 61.8	--	-88.1 77.6	-91.8 80.3
40.87	-83.9 53.5	-81.0 54.8	-89.3 63.6	-91.1 65.6	-86.9 78 8	-87.3 84.8
43.16	-94.1 43.3	-85.4 50.4	-98.5 54.4	-90.8 65.9	-89.8 75.9	-94.2 77.9
43.69	-93.0 44.4	-88.3 47.5	-94.7 58.2	-91.4 65.3	-92.1 73.6	-97.3 74.8
44.31	-90.2 47.2	-85.2 50.6	-93.2 59.7	-92.9 63.8	-92.3 73.4	-93.7 78.4
44.78	--	-85.0 50.8	-94.0 58.9	-90.5 66.2	-90.5 75.2	-92.4 79.7

The figures show fairly good agreement between measurements and WAGNER predictions at the two higher frequencies, f = 2.00 and 1.618 MHz. At the lower frequencies, the agreement is less satisfactory; however, many of the measurements still fall on or very near the WAGNER curve.

Since the Canyonlands path crosses the Colorado River at about 28 km, another run of WAGNER was made for f = 2 MHz assuming σ = 0.1 S/m, ε = 80 over this small portion of the path. Figure 15 presents the comparison and shows only a very slight improvement over the corresponding plot of Figure 9:

WAGNER was also run for f = 2 MHz using a fairly coarse file of digitized topographic data we happen to have. Figure 16 shows the "ECAC" profile and measurement/WAGNER comparisons for this run; the agreement is less satisfactory as can be seen by comparing with Figure 9.

San Francisco

The San Francisco path was 37 km along and provided 10 sites at which measurements were taken. All frequencies except f = 2 MHz were recorded at every site. A tabulation of the data is presented in Table III. The constants used to evaluate the DBU were determined from the measured power levels recorded at the site at d = 27.04 km.

Table III. Measured received power in dB_m, P_m (upper number), and field strength in dB above 1 $\mu V/m$, DBU (lower number), for the designated frequencies and distances from the transmitter along the San Francisco path.

d(km) \ f(MHz)	2.00	1.619	0.518	0.419	0.161	0.137
11.45	-46.85 96.0	-42.97 98.1	-72.45 93.0	-77.08 97.1	-72.74 95.8	-74.54 97.0
18.98	-51.97 90.9	-47.90 93.2	-77.66 87.8	-83.81 90.4	-81.75 86.8	-83.93 87.6
20.31	--	-44.48 96.6	-91.03 74.4	-97.68 76.5	-90.24 78.3	-91.49 80.0
27.04	-55.97 86.9	-54.33 86.7	-79.62 85.8	-88.66 85.6	-83.39 85.1	-86.40 85.1
28.49	-63.01 79.9	-61.78 79.3	-90.87 74.6	-94.20 80.0	-100.93 67.6	-104.25 67.3
31.50	-55.42 87.5	-52.36 88.7	-86.51 78.9	-90.50 83.7	-93.68 74.8	-97.41 74.1
32.87	--	-61.97 79.1	-78.80 86.7	-86.72 87.5	-104.16 64.3	-106.07 65.4
34.69	-67.09 75.8	-62.24 78.8	-84.99 80.5	-90.63 83.6	-88.92 79.6	-90.80 80.7
35.83	-71.74 71.2	-67.15 73.9	-87.52 77.9	-92.52 81.7	-86.63 81.9	-91.05 80.5
37.10	--	-66.74 74.3	-83.91 81.5	-89.23 85.0	-88.76 79.7	-91.29 80.2

Figures 17 through 22 show the measurements (X's)/WAGNER comparison for the 6 frequencies, the lower portion of each figure representing the terrain profile for the San Francisco path. The box in the upper right corner of the field strength plot indicates the ground constants used over the various segments of the path.

The comparisons show better agreement, again, at 2 MHz, with the lower frequencies having more spread between measurement and prediction. Most of the measurement sites for this path were necessarily located in heavily congested areas, and the recorded signals may have been affected by interference from nearby structures.

Santa Rita

On the Santa Rita Mountains path, measurements were taken at 16 sites along a 23 km radial, with data at all 6 frequencies being obtained at every site. The recorded data are shown in Table IV. The constants used to adjust the DBU were determined from the first site at d = 2.48 km.

Table IV. Measured received power in dBm, P_m (upper number), and field strength in dB above 1 μV/m, DBU(lower number), for the designated frequencies and distances from the transmitter along the Santa Rita path.

d(km) \ f(MHz)	2.00	1.619	0.518	0.419	0.160	0.137
2.48	-37.65 104.0	-33.51 104.4	-61.92 105.1	-65.35 105.1	-58.62 105.1	-61.17 105.1
5.81	-50.05 91.6	44.65 93.3	-69.41 97.6	-71.60 98.8	-65.77 98.0	-67.67 98.6
6.92	-55.59 86.1	-49.54 88.4	-70.86 96.2	-74.65 95.8	-68.63 95.1	-69.86 96.4
8.39	-63.69 78.0	-58.93 79.0	-79.25 87.8	-79.66 90.8	-74.68 89.1	-75.64 90.7
9.46	-67.70 74.0	-61.91 76.0	79.99 87.1	-83.19 87.2	-77.77 86.0	-79.49 86.8
9.85	-61.09 80.6	-57.14 80.8	-72.13 94.9	-75.15 95.3	-69.13 94.6	-71.26 95.0

Table IV. Continued

d(km) \ f(MHz)	2.00	1.619	0.518	0.419	0.160	0.137
10.19	-64.45 77.2	-59.54 78.4	-75.18 91.9	-76.52 93.9	-72.19 91.6	-75.35 91.0
11.41	-67.59 74.1	-62.54 75.4	-74.63 92.4	-77.91 92.5	-72.56 91.2	-73.59 92.7
12.30	-69.91 71.8	-66.47 71.5	-79.54 87.5	-81.04 89.4	-77.15 86.6	-79.92 86.4
13 02	-76.97 64.7	-71.54 66.4	-89.58 77.5	-92.29 78.1	-86.20 77.6	-87.24 79.1
13.35	-76.09 65.6	-70.07 67.9	-89.09 78 0	-89.76 80.7	-87.46 76.3	-89.73 76.6
13.70	-73.48 68.2	-66.72 71.2	-84.60 82.5	-87.07 83.3	-79.10 84.7	-84.17 82.1
14.77	-74.23 67.5	-68.41 69.5	-83.08 84.0	-88.44 82.0	-81.16 82.6	-82.16 84.1
16.82	-74.02 67.7	-68.16 69.8	-81.28 85.8	-82.02 88.4	-74.47 89.3	-76.78 89.5
22.42	-77.56 64.1	-71.19 66.8	-85.40 81.7	-86.78 83.6	-81.10 82.7	-81.45 84.9
22.84	-79.78 61 9	-71.80 66.2	-86.36 80.7	-87.37 83.0	-81.12 82.6	-81.90 84.4

WAGNER runs were made for two different sets of ground constants, the only difference being in the length of the "mountain" segment of the profile. One set assumed the "mountain" constants, $\sigma = 10^{-5}$ S/m and $\varepsilon = 5$, to extend from 7.2 km to 16.4 km; the other set had this segment extending from 7.2 km to 12.95 km (see ground constant tables in the figures).

Figures 23 to 36 show comparisons at the 6 frequencies for the Santa Rita path; again, the terrain profile is shown in the lower portion of the figures. From comparisons of figures 23 and 24 it would appear that better agreement between measurements and prediction is obtained if the low conductivity of the mountainous material ends at about 13 km rather than 16 km. As with the other paths, the higher frequencies show better measurement/prediction agreement than the lower frequencies. Figure 25

shows comparison of measurement prediction using measured values for the conductivity (Kissick et al., 1978). The measured conductivity for the peak near 10 km is much higher than that given by Lytle (1974) for this type of granite rock. However, Lytle's value corresponds to rock with all moisture absent and the observed values by Kissick were under wet conditions. Kissick may also have been observing the effect of the top or surface soil. The values for the conductivity on either side of the peak of the ridge observed by Kissick are larger than the sedimentary values shown by Lytle, perhaps because the alluvial deposits observed by Kissick were a result of erosion and not part of actual strata. The results in Figure 25 motivated a simple two section flat-earth model for the predictions shown in Figure 26. The predictions show a "recovery effect" at about 16 km corresponding to the assumed jump in conductivity from .0005 s/m to .005 s/m. Although the agreement between predictions/measurement is reasonable out to about 10 km, the agreement thereafter breaks down, indicating in part the diffraction loss over the ridge needs to be included in the predictions.

Nevada

Data were recorded at 22 sites for all 6 frequencies on the Nevada path. The data are tabulated in Table V with the constants used to adjust the DBU determined from the first site at d = 1.90 km.

Table V. Measured received power in dBm, P_m (upper number), and field strength in dB above 1 μV/m, ^{m}DBU (lower number), for the designated frequencies and distances from the transmitter along the Nevada path.

d(km) \ f(MHz)	2.000	1.619	0.518	0.419	0.160	0.137
1.90	-39.27	-33.52	-58.31	-62.87	-58.38	-60.38
	106.0	106.4	107.1	107.2	107.3	107.3
2.38	-41.13	-35.55	-58.44	-63.04	-57.72	-58.95
	104.2	104.4	107.0	107.1	107.9	108.8
3.56	-45.77	-40.14	-63.47	-69.36	-63.67	-67.75
	99.5	99.8	102.0	100.8	102.0	100.0
5.55	-65.0	-55.0	-71.0	-77.0	-75.5	-79.0
	80.3	85.0	94.5	93.1	90.2	88.7
10.38	-88.5	-82.0	-93.0	-92.5	-82.0	-85.0
	56.8	58.0	72.5	77.6	83.7	82.7
10.82	-81.0	-76.0	-84.0	-86.0	-75.5	-77.5
	64.3	64.0	81.5	84.1	90.2	90.2
14.06	-79.0	-71.0	-84.0	-85.0	-75.0	-78.0
	66.3	69.0	81.5	85.1	90.7	89.7
17.78	-80.0	-73.5	-83.5	-87.0	-77.0	-78.5
	65.3	66.5	82.0	83.1	88.7	89.2
18.67	-80.5	-74.5	-87.0	-89.0	-78.5	-82.0
	64.8	65.5	78.5	81.1	87.2	85.7
20.15	-80.0	-74.0	-87.0	-89.5	-79.5	-82.0
	65.3	66.0	78.5	80.6	86.2	85.7
21.36	-81.0	-75.0	-87.0	-89.0	-81.0	-84.0
	64.3	65.0	78.5	81.1	84.7	83.7
22.46	-83.0	-77.0	-87.0	-91.0	-80.0	-83.0
	62.3	63.0	78.5	79.1	85.7	84.7
24.33	-84.0	-77.5	-91.0	-93.0	-81.0	-84.0
	61.3	62.5	74.5	77.1	84.7	83.7
26.94	-84.0	-77.0	-89.0	-92.0	-81.0	-83.0
	61.3	63.0	76.5	78.1	84.7	84.7
28.53	-85.68	-79.39	-91.28	-94.98	-82.22	-85.47
	59.6	60.6	74.2	75.1	83.4	82.2
36.00	-83.75	-78.14	-91.38	-96.08	-85.40	-88.81
	61.5	61.8	74.1	74.0	80.3	78.9

Table V. Continued

d(km) \ f(MHz)	2.000	1.619	0.518	0.419	0.160	0.137
36.32	-84.28 61.0	-78.44 61.5	-91.32 74.1	-96.42 73.7	-86.09 79.6	-89.50 78.2
39.53	-87.12 58.2	-80.38 59.6	-93.69 71.8	-97.07 73.0	-86.12 79.5	-90.53 77.2
45.22	-96.45 48.8	-88.21 51.7	-96.08 69.4	-98.52 71.6	-87.05 78.6	-90.98 76.7
47.75	-91.89 53.4	-85.96 54.0	-97.02 68.4	-99.40 70.7	-89.28 76.4	-90.71 77.0
50.36	-92.26 53.0	-85.41 54.5	-95.89 69.6	-98.42 71.7	-87.10 78.6	-90.45 77.3
52.46	-94.34 51.0	-87.72 52.2	-98.76 66.7	-99.40 70.7	-88.09 77.6	-91.57 76.1

WAGNER predictions for the 6 frequencies, together with the measured data (X's), are shown in Figures 38 through 43. Figure 37 is a comparison of the data at f = 2 MHz with the field strength as calculated by Program INTEQ. In general, the data lie somewhat above the WAGNER predictions, but the trend of the measurements and calculations are similar. It would appear that σ = 0.02 S/m is not the correct value for the conductivity over the "plains" portions of the profile. A higher value of σ would raise the prediction curves and give much better agreement with measurements.

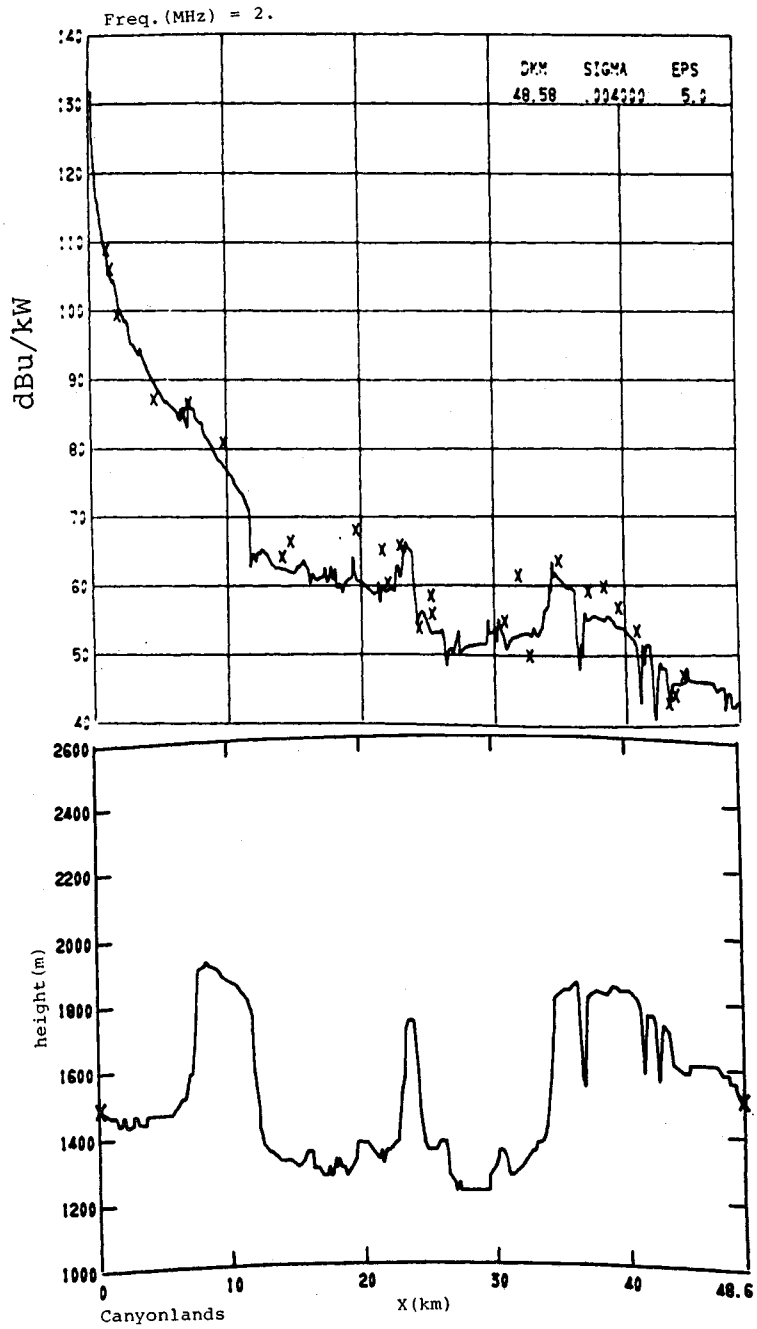

Figure 9. Path profile (lower portion) and received signal (in dB above 1 μV/m for 1 kW effective radiated power) for Canyonlands, Utah, path. Crosses denote measured 2.5 min. averages. Frequency = 2 MHz.

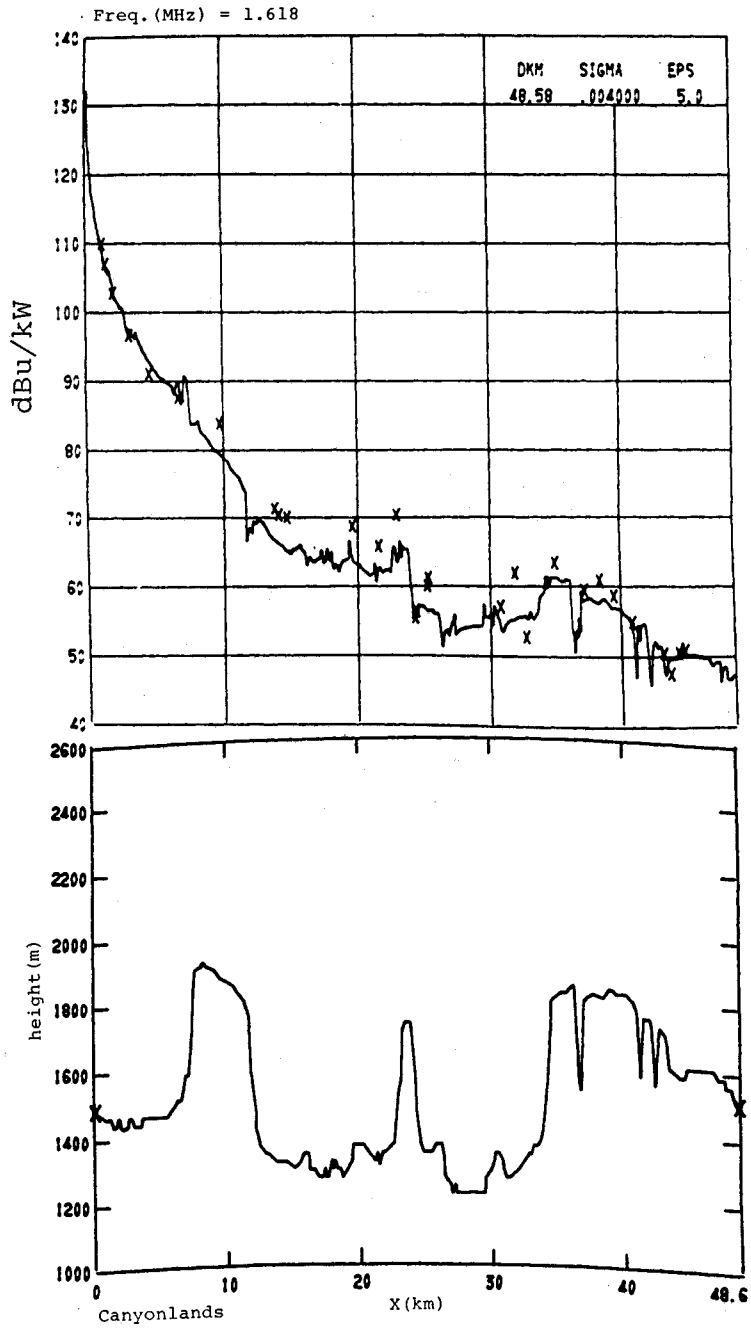

Figure 10. Path profile (lower portion) and received signal (in dB above 1 μV/m for 1 kW effective radiated power) for Canyonlands, Utah, path. Crosses denote measured 2.5 min. averages. Frequency = 1.618 MHz.

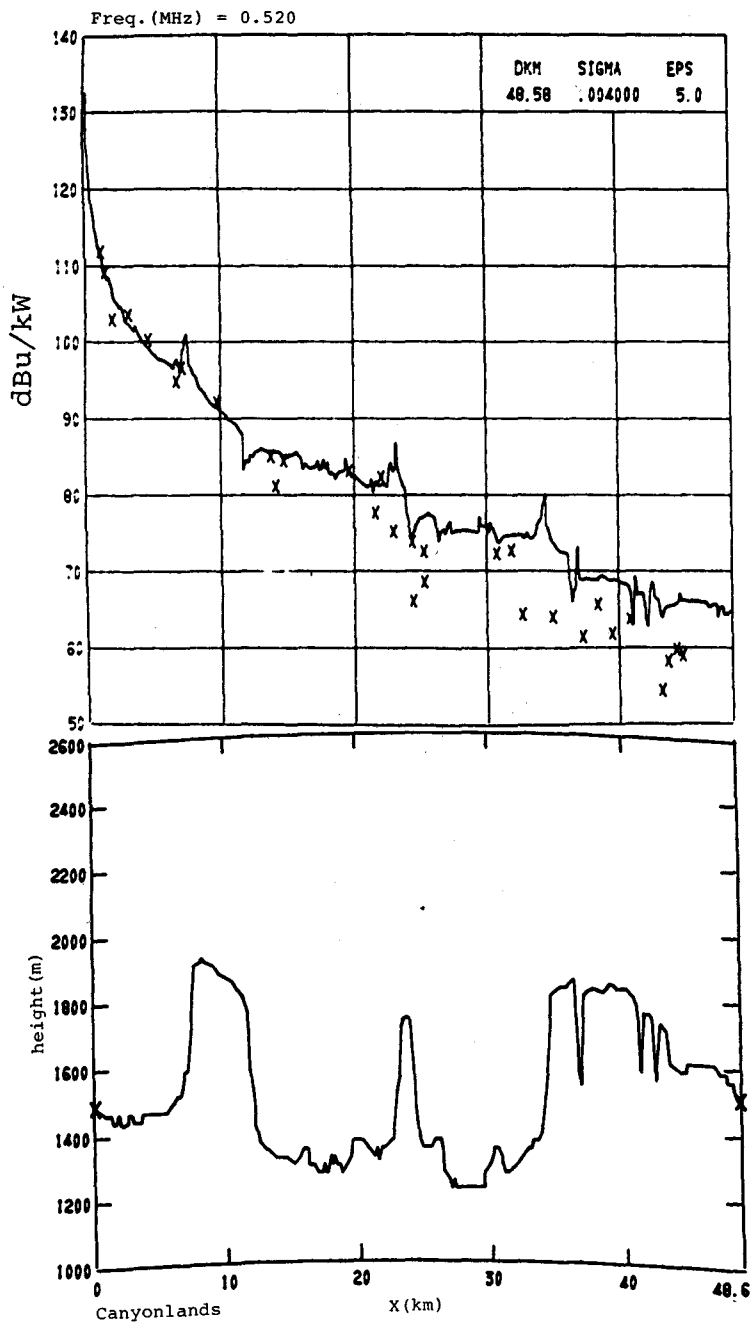

Figure 11. Path profile (lower portion) and received signal (in dB above 1 μV/m for 1 kW effective radiated power) for Canyonlands, Utah, path. Crosses denote measured 2.5 min. averages. Frequency = 0.520 MHz.

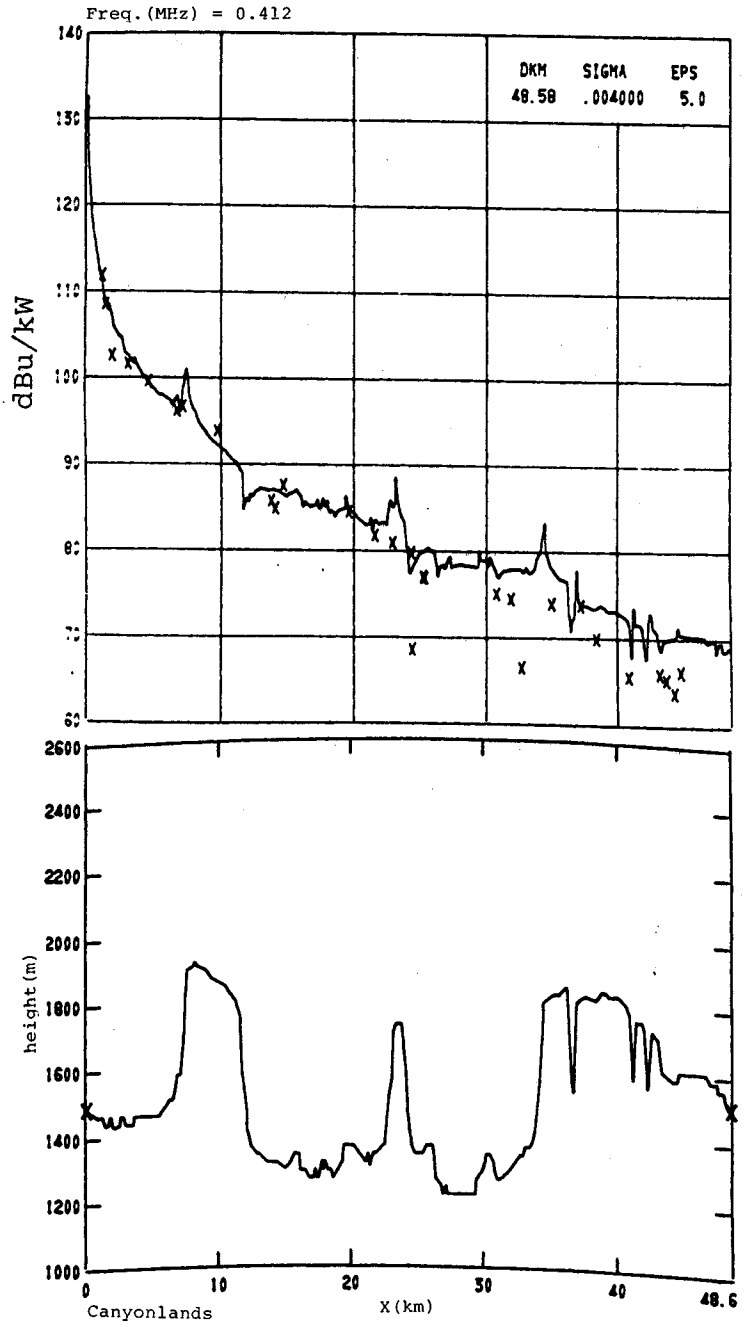

Figure 12. Path profile (lower portion) and received signal (in dB above 1 μV/m for 1 kW effective radiated power) for Canyonlands, Utah, path. Crosses denote measured 2.5 min. averages. Frequency = 0.412 MHz.

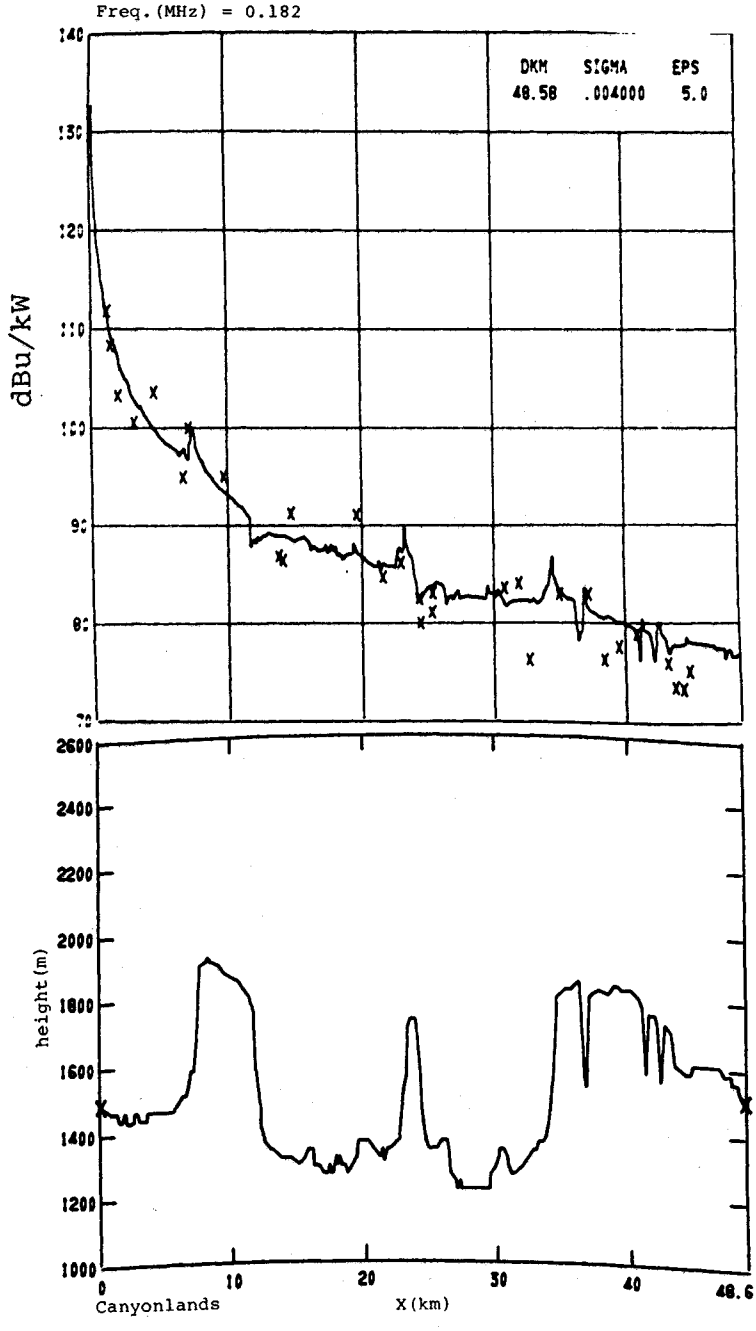

Figure 13. Path profile (lower portion) and received signal (in dB above 1 μV/m for 1 kW effective radiated power) for Canyonlands, Utah, path. Crosses denote measured 2.5 min. averages. Frequency = 0.182 MHz.

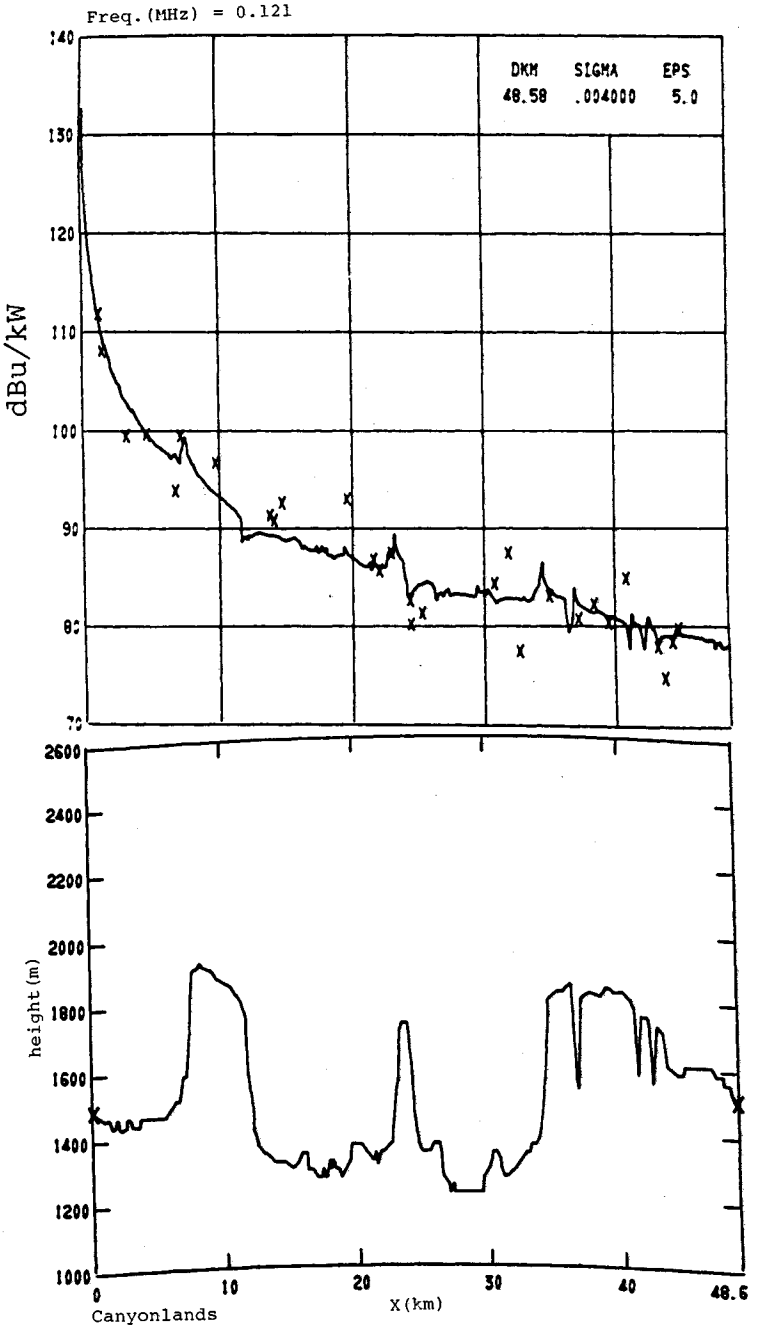

Figure 14. Path profile (lower portion) and received signal (in dB above 1 μV/m for 1 kW effective radiated power) for Canyonlands, Utah, path. Crosses denote measured 2.5 min. averages. Frequency = 0.121 MHz.

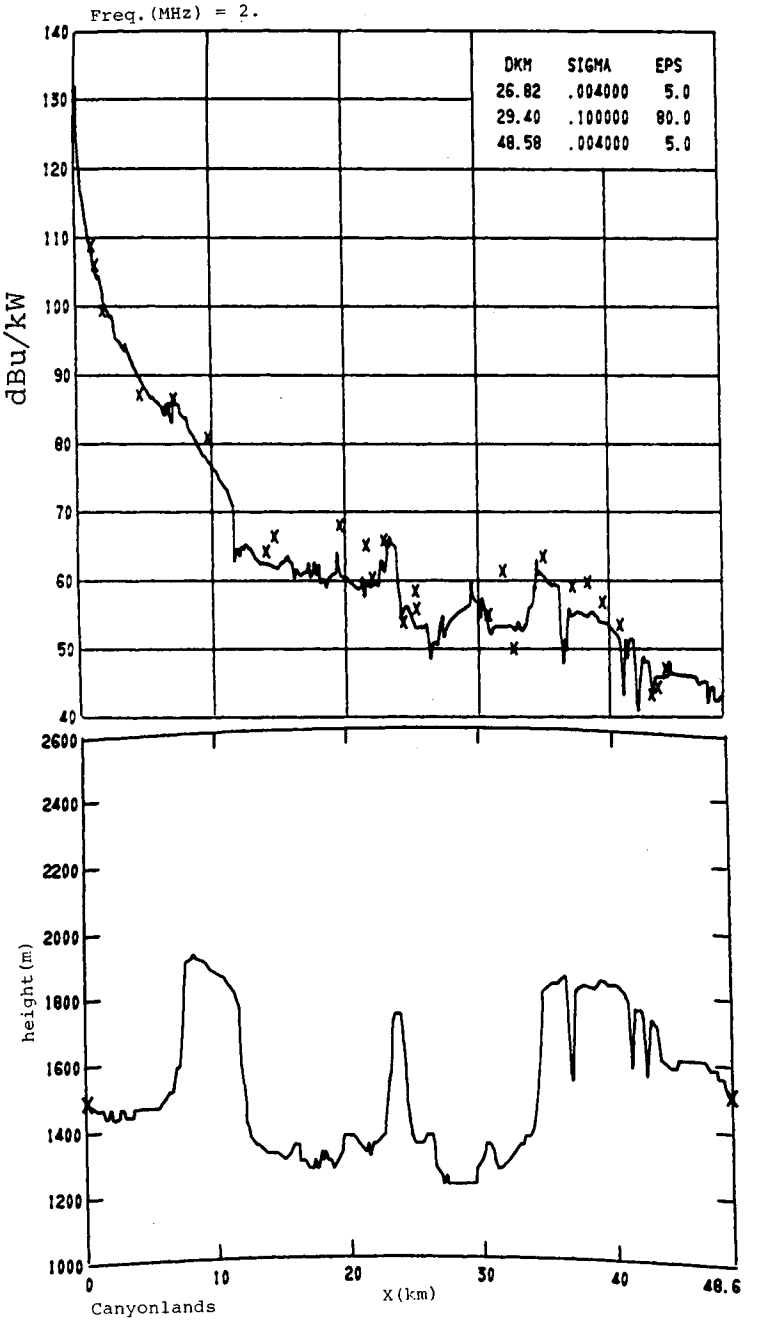

Figure 15. Path profile (lower portion) and received signal (in dB above 1 μV/m for 1 kW effective radiated power) for Canyonlands, Utah, path. Crosses denote measured 2.5 min. averages. Frequency = 2 MHz.

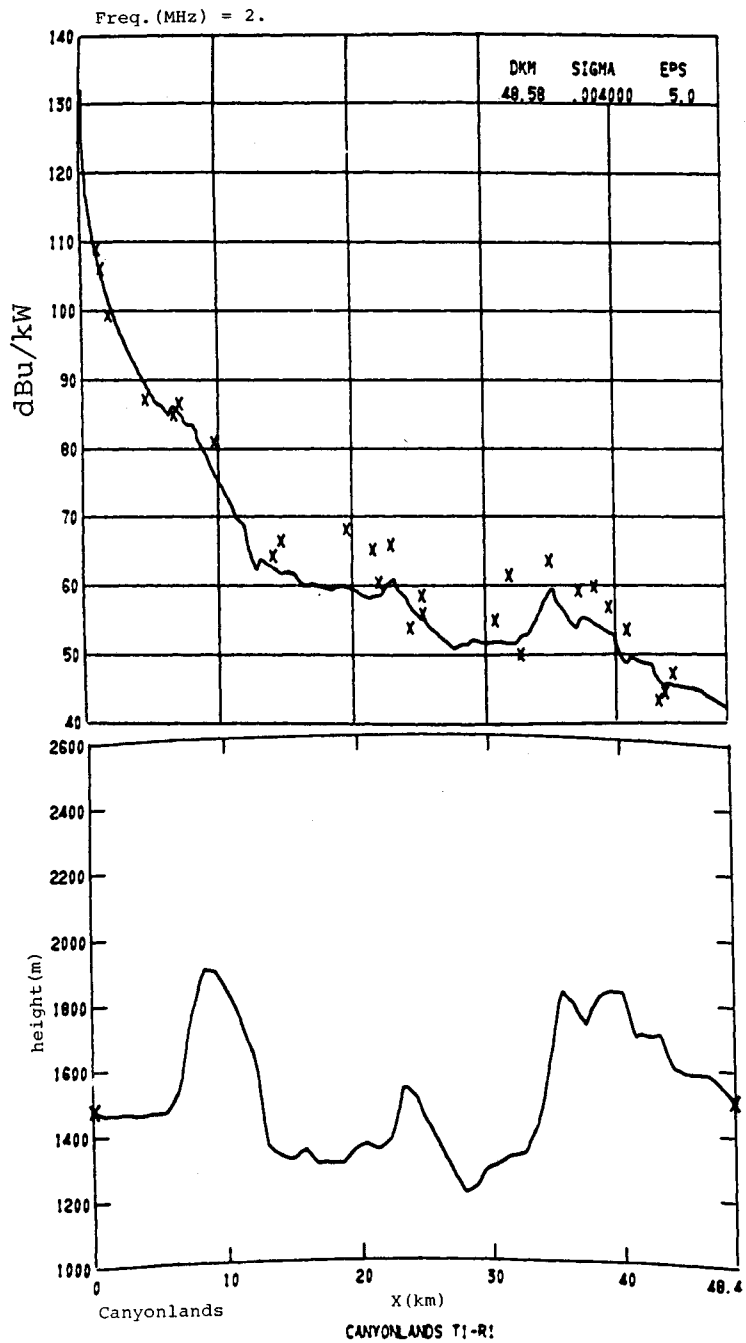

Figure 16. Path profile (lower portion) and received signal (in dB above 1 μV/m for 1 kW effective radiated power) for Canyonlands, Utah, path. Crosses denote measured 2.5 min. averages. Frequency = 2 MHz.

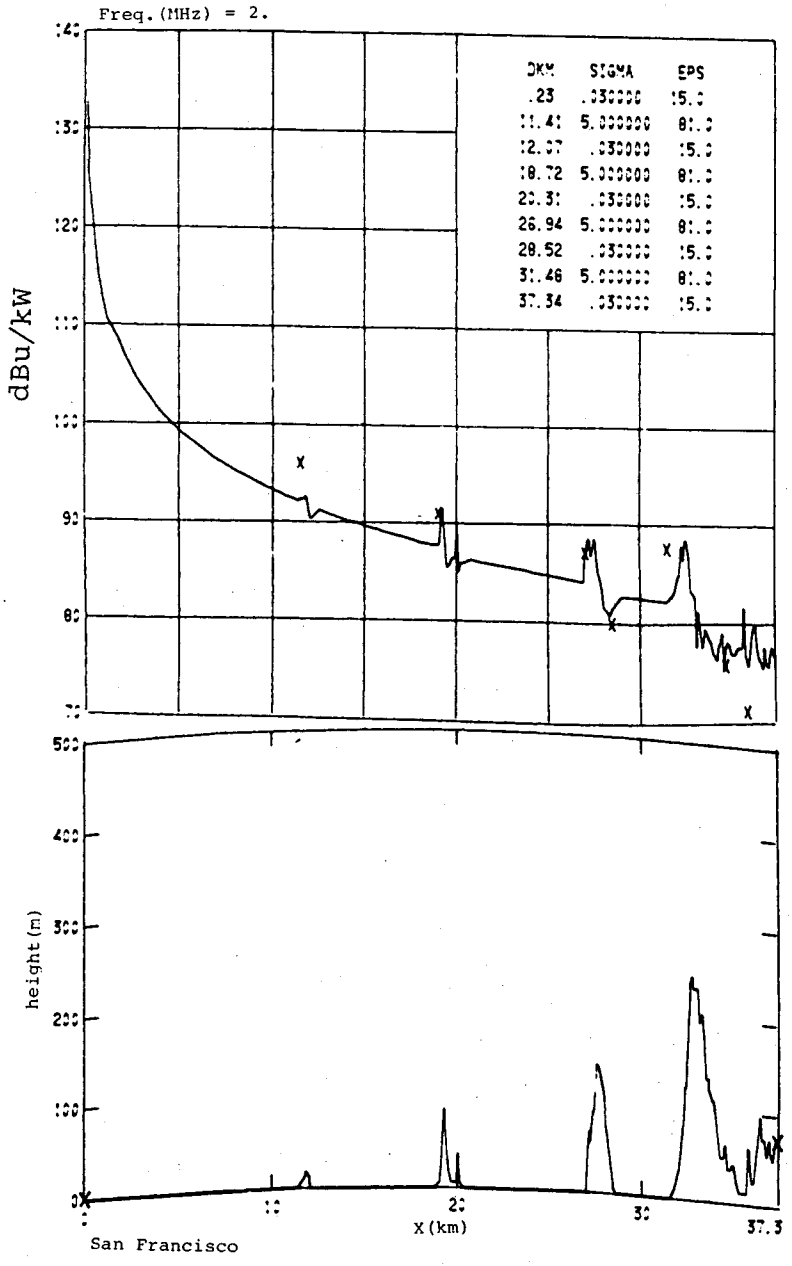

Figure 17. Path profile (lower portion) and received signal (in dB above 1 μV/m for 1 kW effective radiated power) for San Francisco, California, path. Crosses denote measured 2.5 min. averages. Frequency = 2 MHz

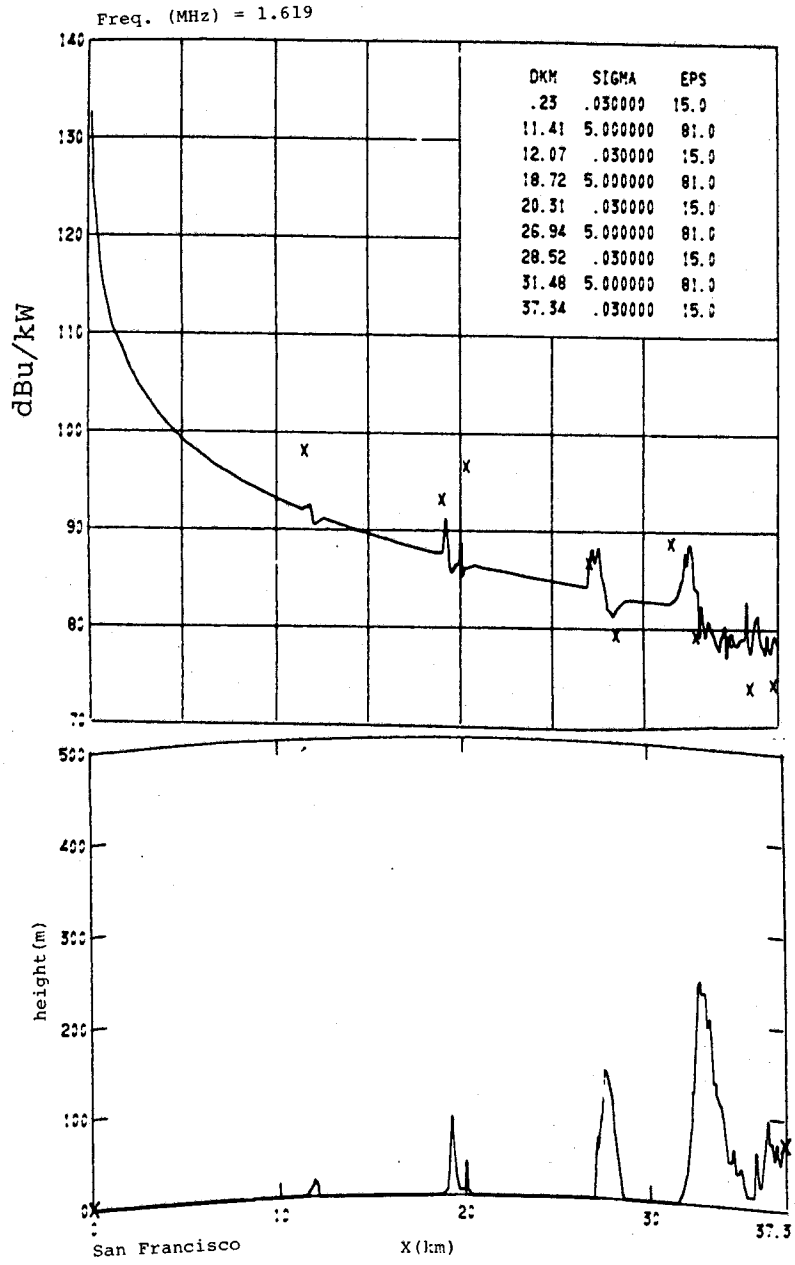

Figure 18. Path profile (lower portion) and received signal (in dB above 1 μV/m for 1 kW effective radiated power) for San Francisco, California, path. Crosses denote measured 2.5 min. averages. Frequency = 1.619 MHz.

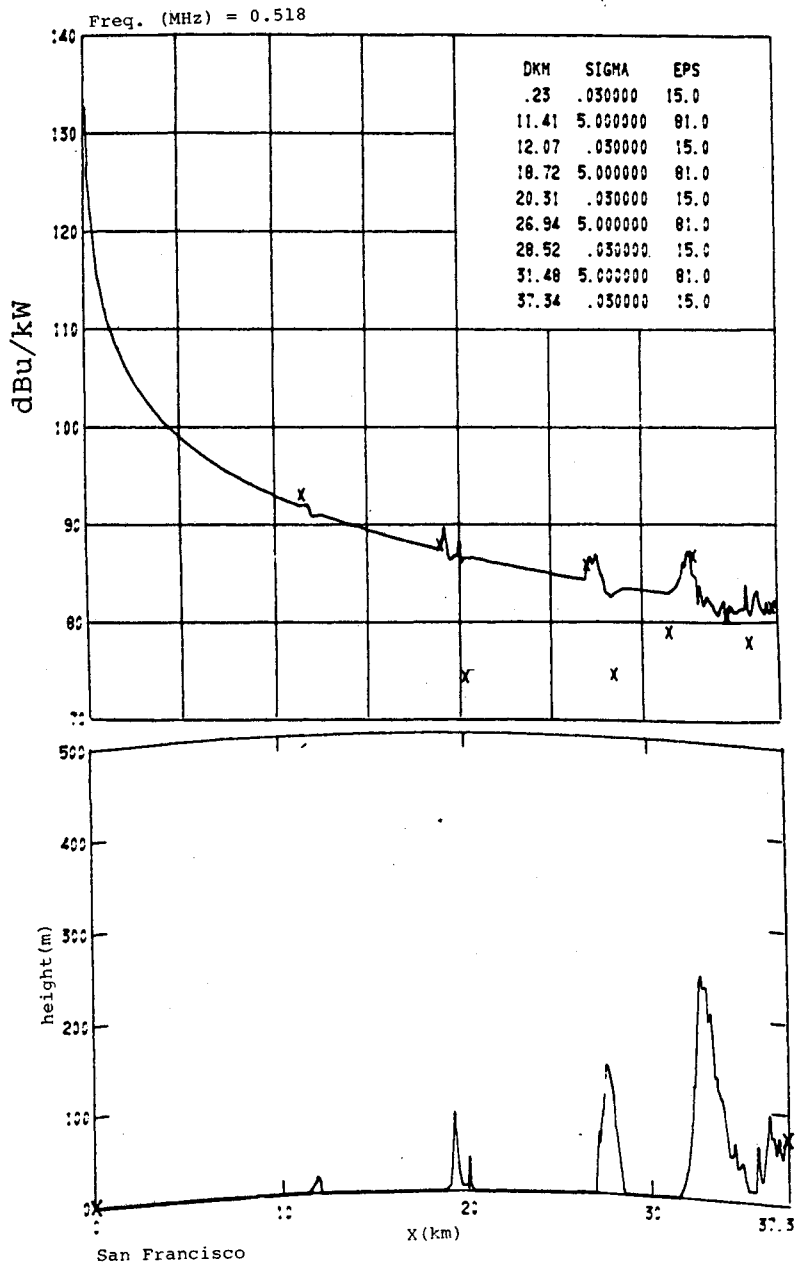

Figure 19. Path profile (lower portion) and received signal (in dB above 1 μV/m for 1 kW effective radiated power) for San Francisco, California, path. Crosses denote measured 2.5 min. averages. Frequency = 0.518 MHz.

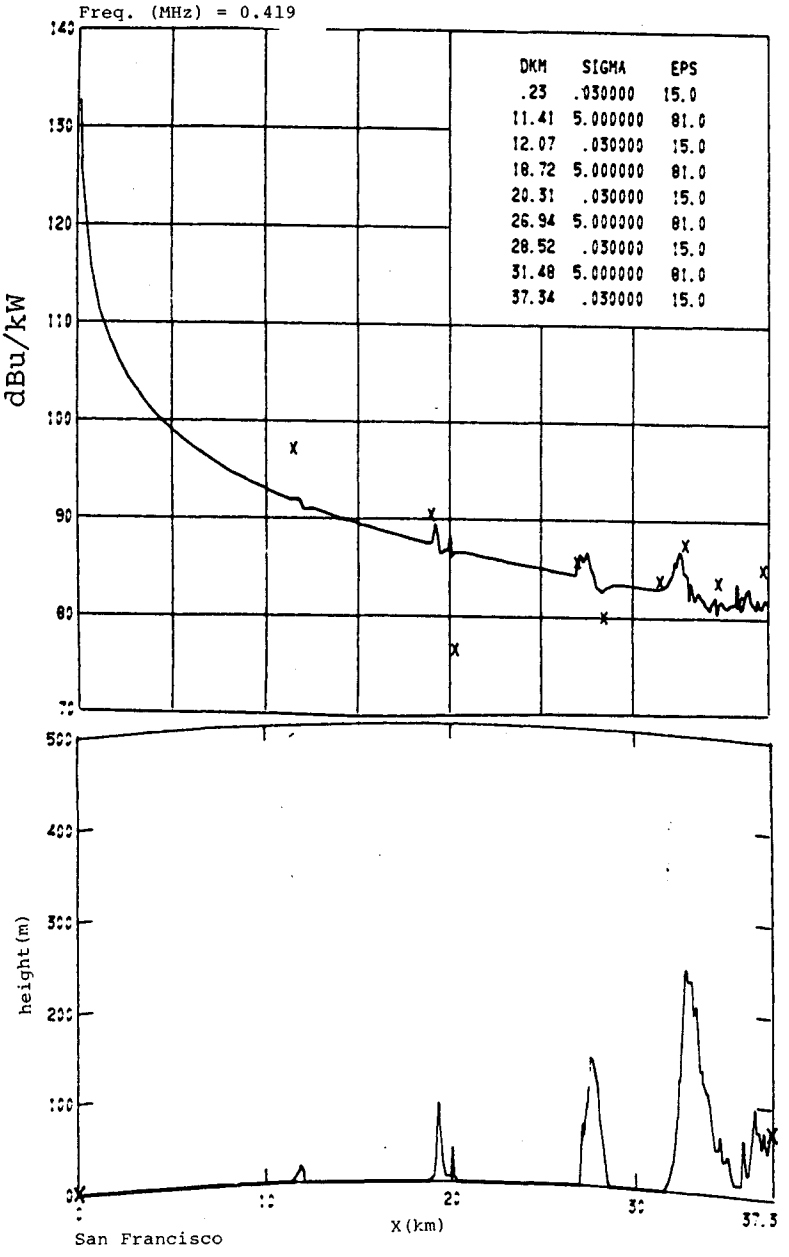

Figure 20. Path profile (lower portion) and received signal (in dB above 1 μV/m for 1 kW effective radiated power) for San Francisco, California, path. Crosses denote measured 2.5 min. averages. Frequency = 0.419 MHz.

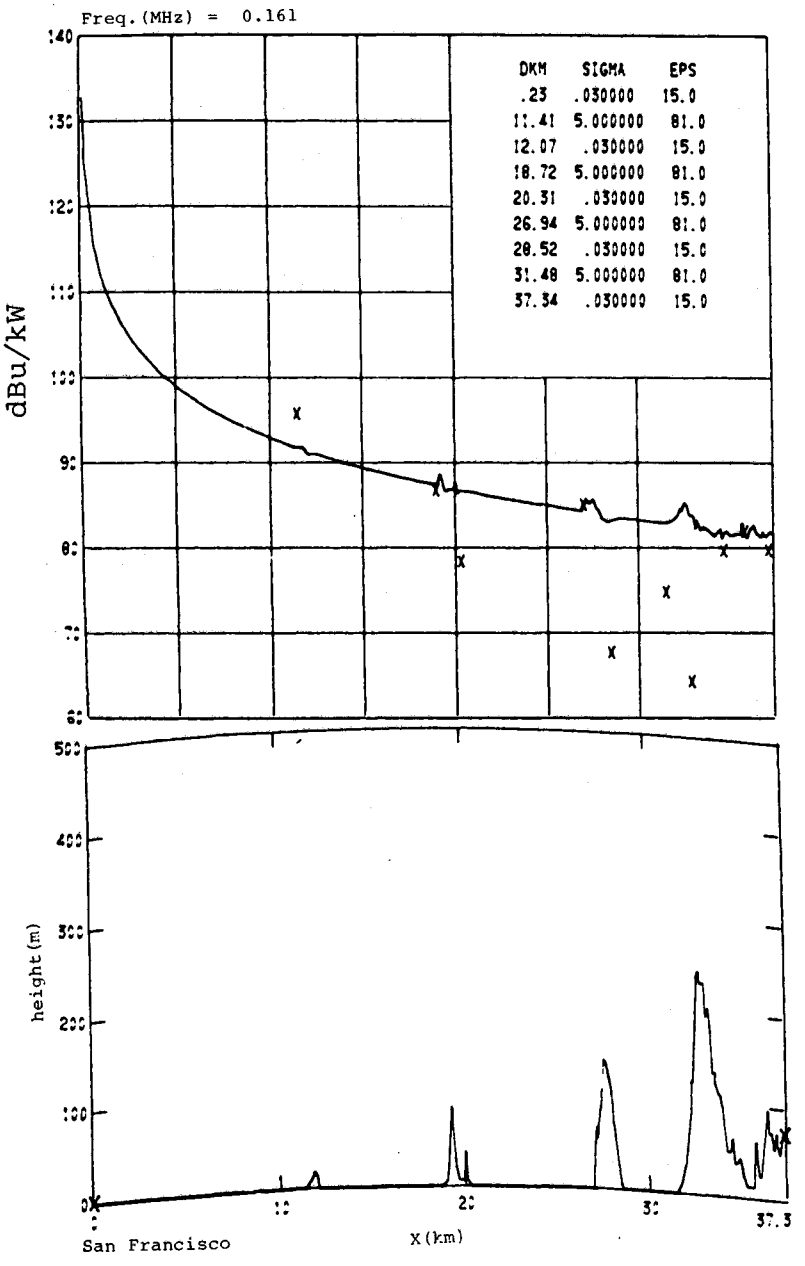

Figure 21. Path profile (lower portion) and received signal (in dB above 1 μV/m for 1 kW effective radiated power) for San Francisco, California, path. Crosses denote measured 2.5 min. averages. Frequency = 0.161 MHz.

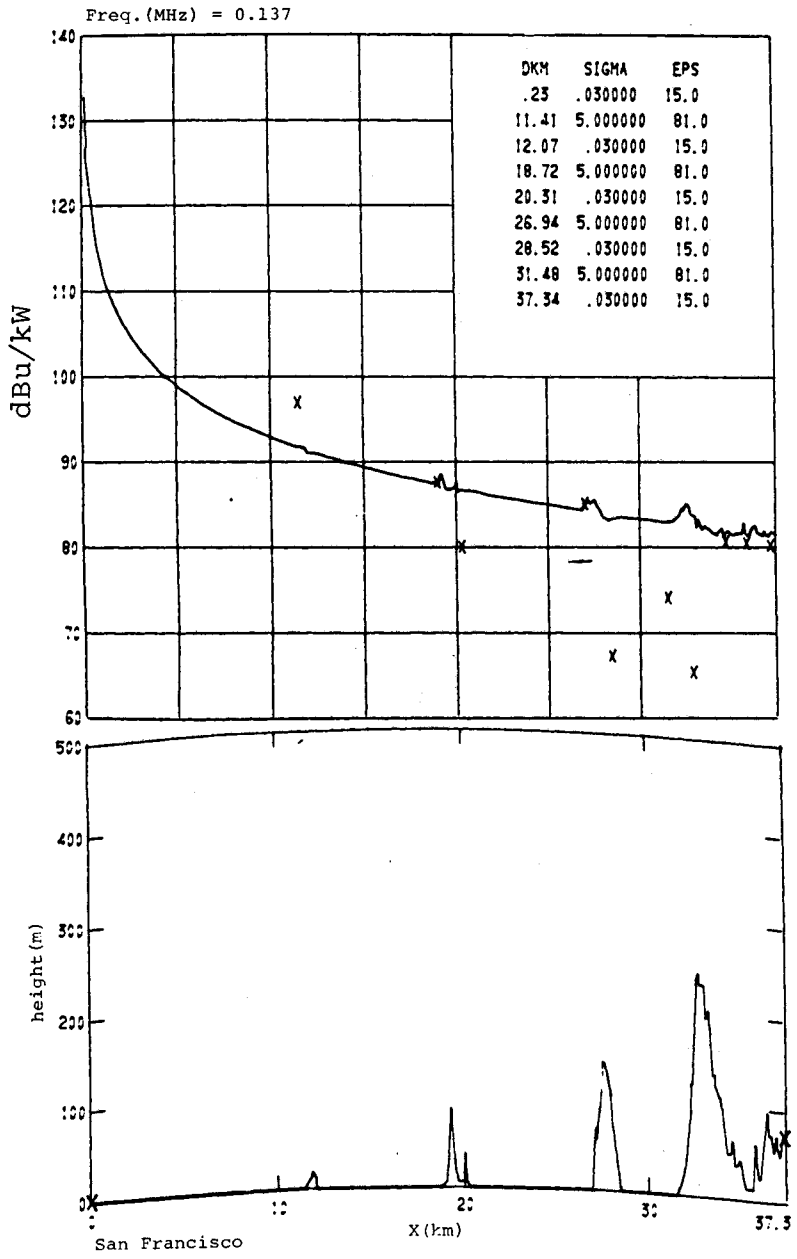

Figure 22. Path profile (lower portion) and received signal (in dB above 1 μV/m for 1 kW effective radiated power) for San Francisco, California, path. Crosses denote measured 2.5 min. averages. Frequency = 0.137 MHz.

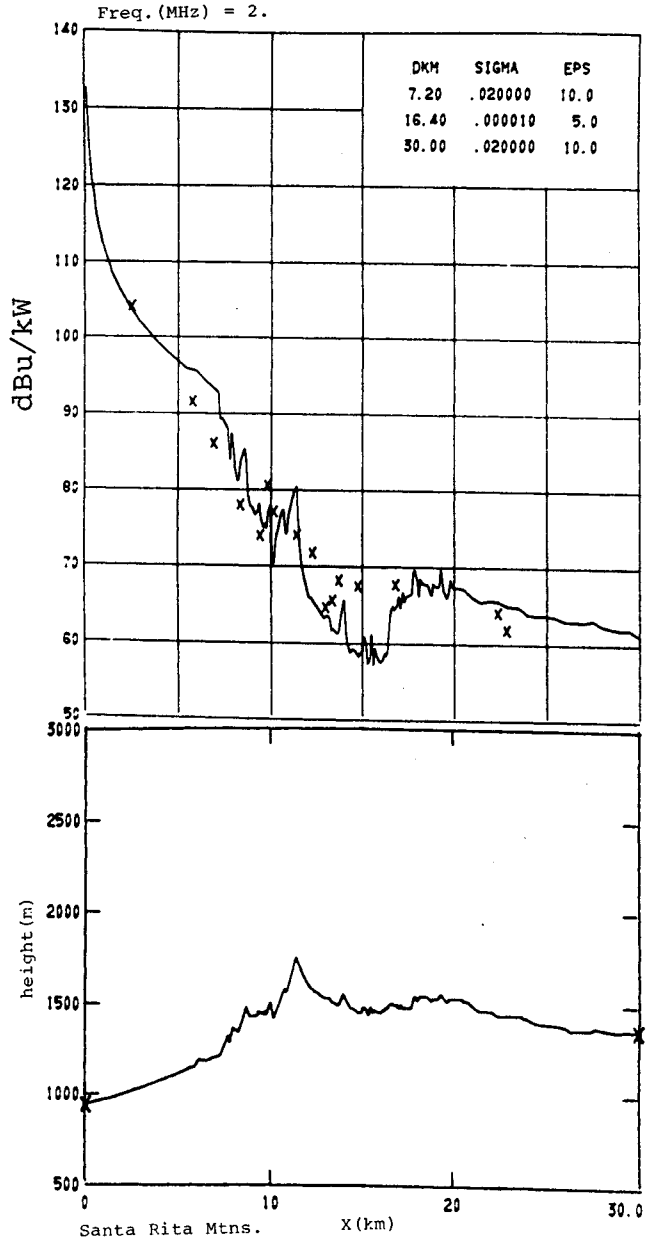

Figure 23. Path profile (lower portion) and received signal (in dB above 1 μV/m for 1 kW effective radiated power) for Santa Ritas, Arizona, path. Crosses denote measured 2.5 min. averages. Frequency = 2 MHz.

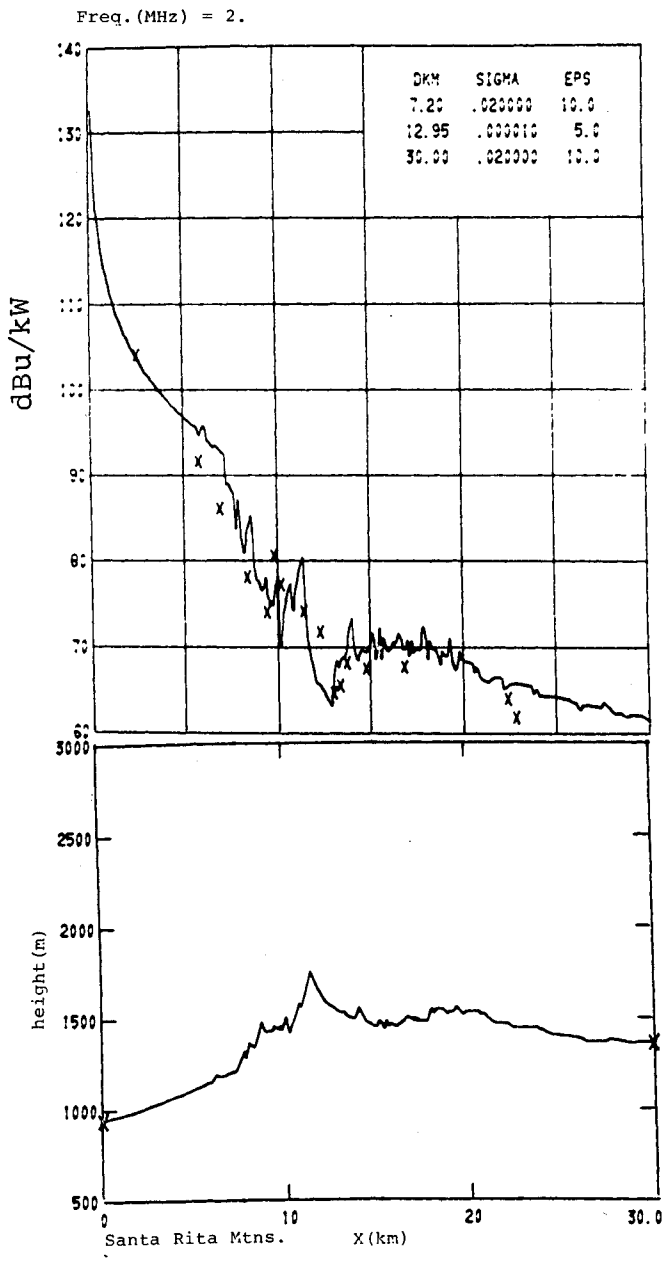

Figure 24. Path profile (lower portion) and received signal (in dB above 1 μV/m for 1 kW effective radiated power) for Santa Ritas, Arizona, path. Crosses denote measured 2.5 min. averages. Frequency = 2 MHz.

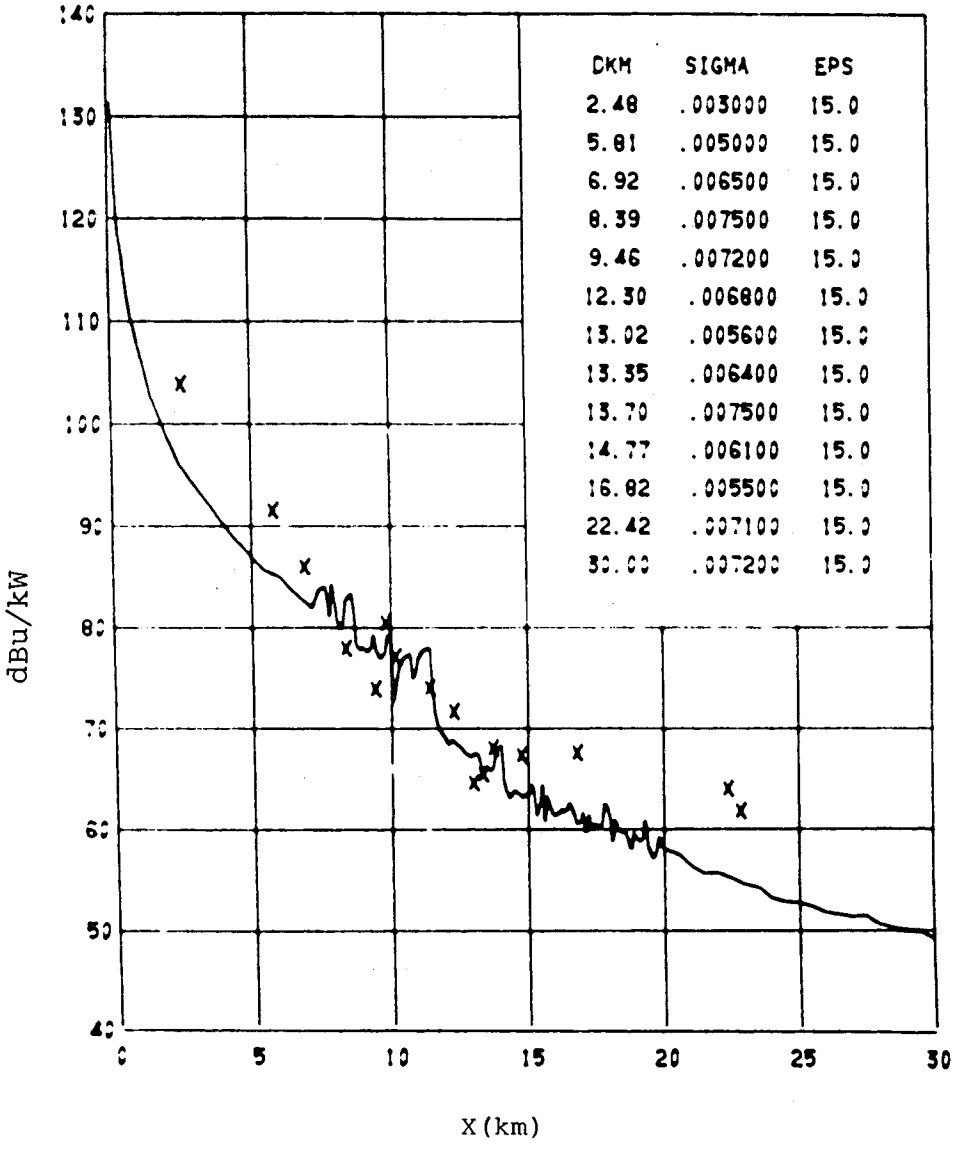

Figure 25. Path profile (lower portion) and received signal (in dB above 1 μV/m for 1 kW effective radiated power) for Santa Ritas, Arizona, path. Crosses denote measured 2.5 min. averages. Frequency = 2 MHz.

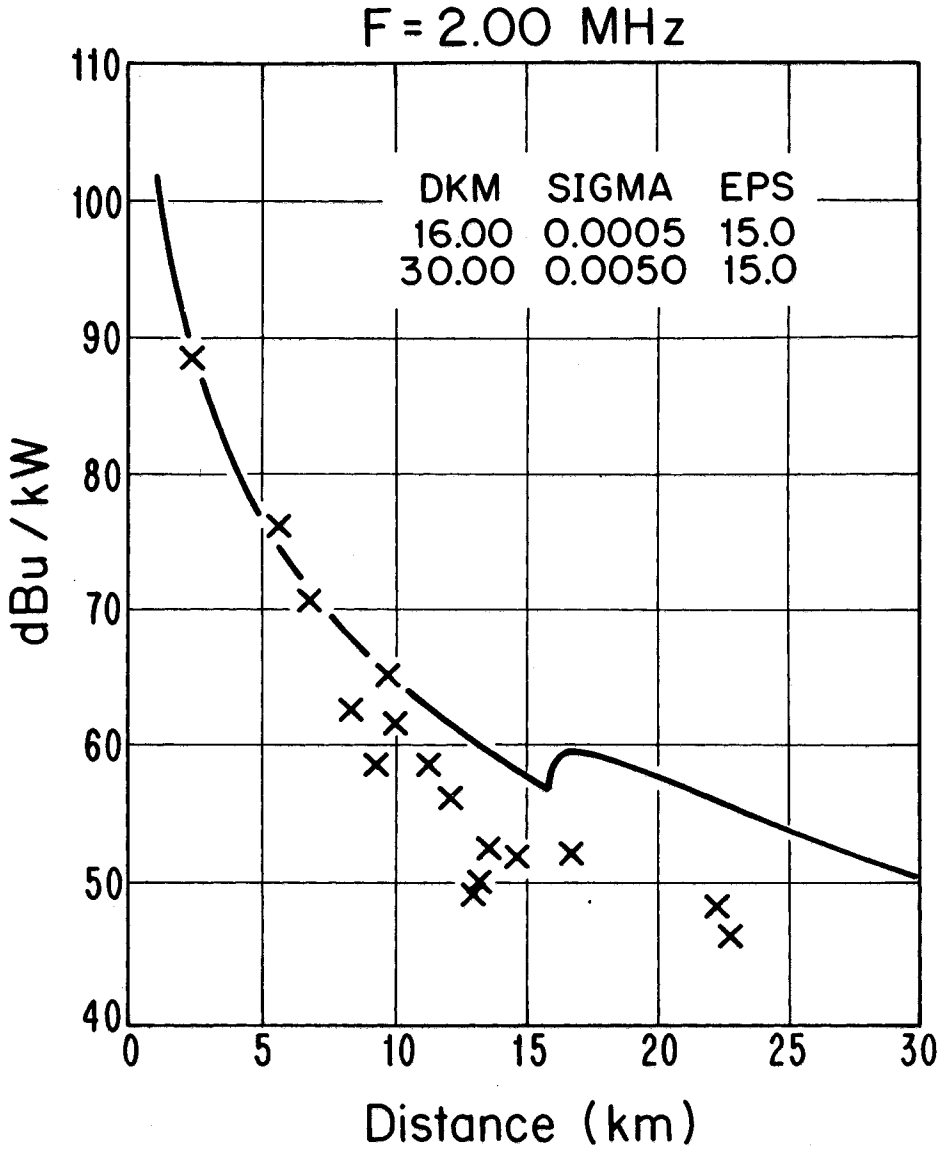

Figure 26. Path profile (lower portion) and received signal (in dB above 1 μV/m for 1 kW effective radiated power) for Santa Ritas, Arizona, path. Crosses denote measured 2.5 min. averages. Frequency = 2 MHz.

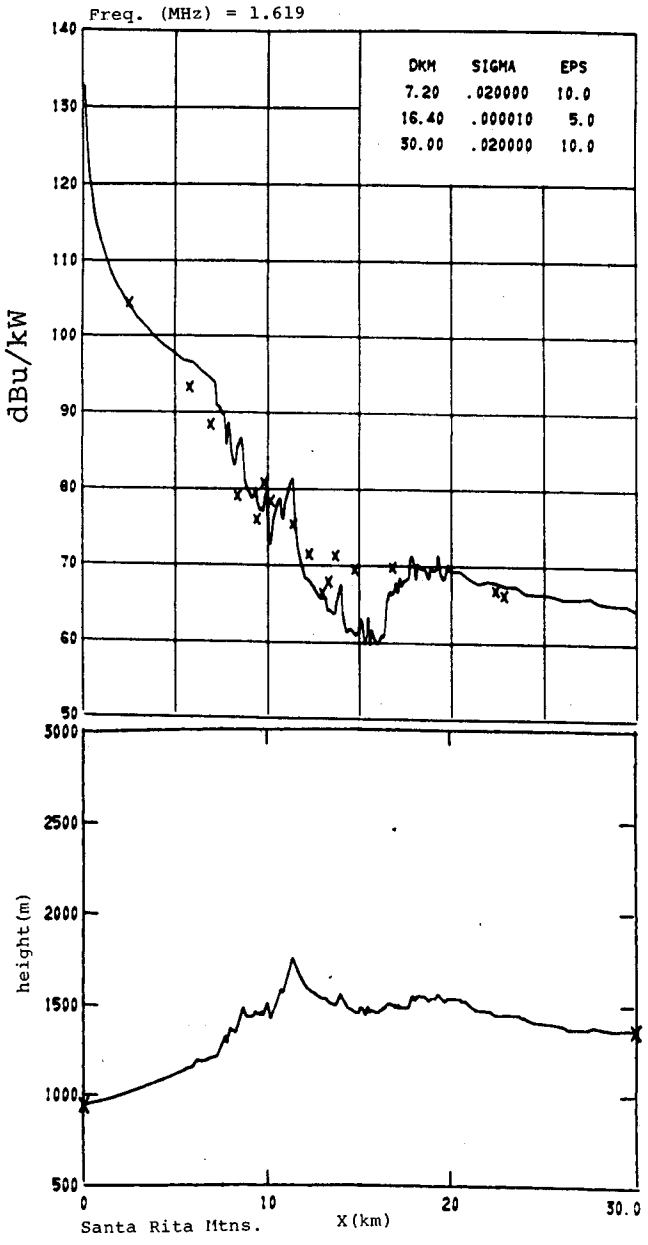

Figure 27. Path profile (lower portion) and received signal (in dB above 1 μV/m for 1 kW effective radiated power) for Santa Ritas, Arizona, path. Crosses denote measured 2.5 min. averages. Frequency = 1.619 MHz.

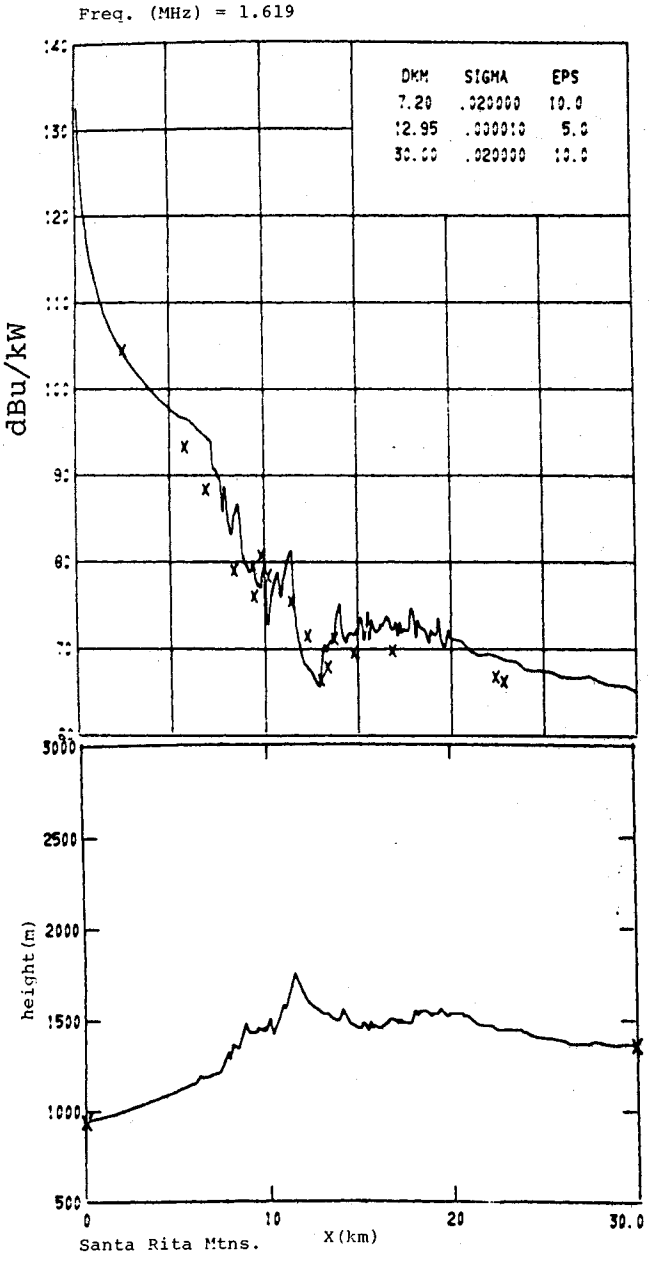

Figure 28. Path profile (lower portion) and received signal (in dB above 1 μV/m for 1 kW effective radiated power) for Santa Ritas, Arizona, path. Crosses denote measured 2.5 min. averages. Frequency = 1.619 MHz.

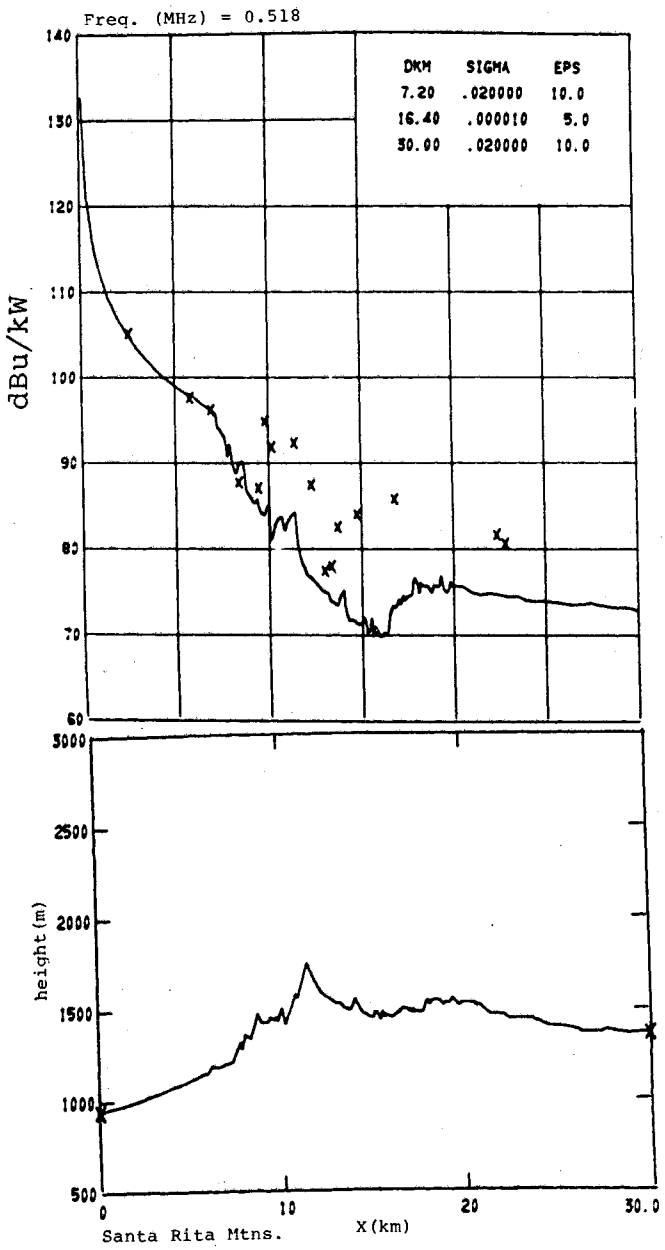

Figure 29. Path profile (lower portion) and received signal (in dB above 1 μV/m for 1 kW effective radiated power) for Santa Ritas, Arizona, path. Crosses denote measured 2.5 min. averages. Frequency = 0.518 MHz.

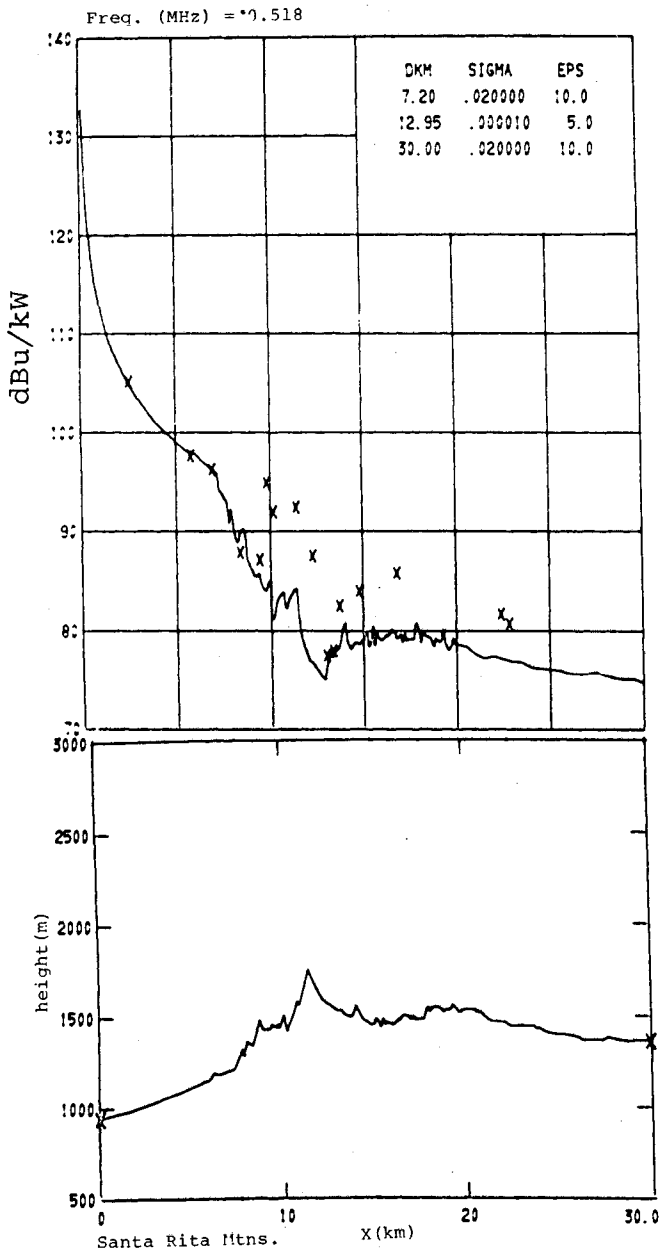

Figure 30. Path profile (lower portion) and received signal (in dB above 1 μV/m for 1 kW effective radiated power) for Santa Ritas, Arizona, path. Crosses denote measured 2.5 min. averages. Frequency = 0.518 MHz.

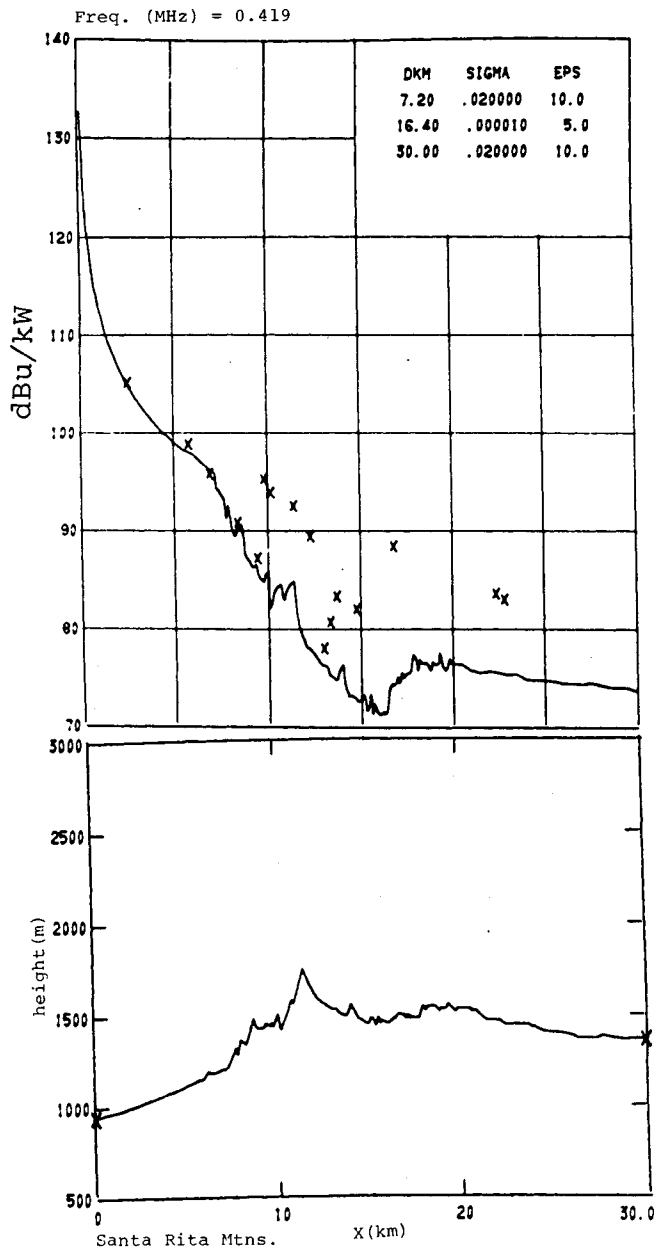

Figure 31. Path profile (lower portion) and received signal (in dB above 1 μV/m for 1 kW effective radiated power) for Santa Ritas, Arizona, path. Crosses denote measured 2.5 min. averages. Frequency = 0.419 MHz.

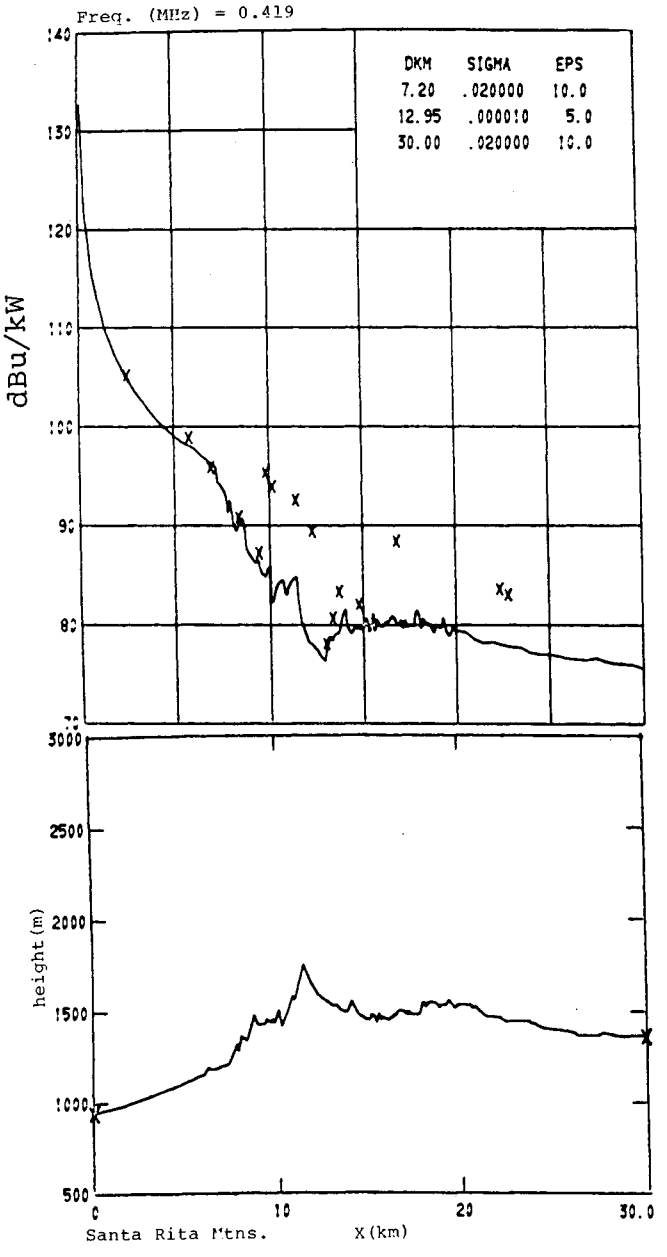

Figure 32. Path profile (lower portion) and received signal (in dB above 1 μV/m for 1 kW effective radiated power) for Santa Ritas, Arizona, path Crosses denote measured 2.5 min. averages. Frequency = 0.419 MHz.

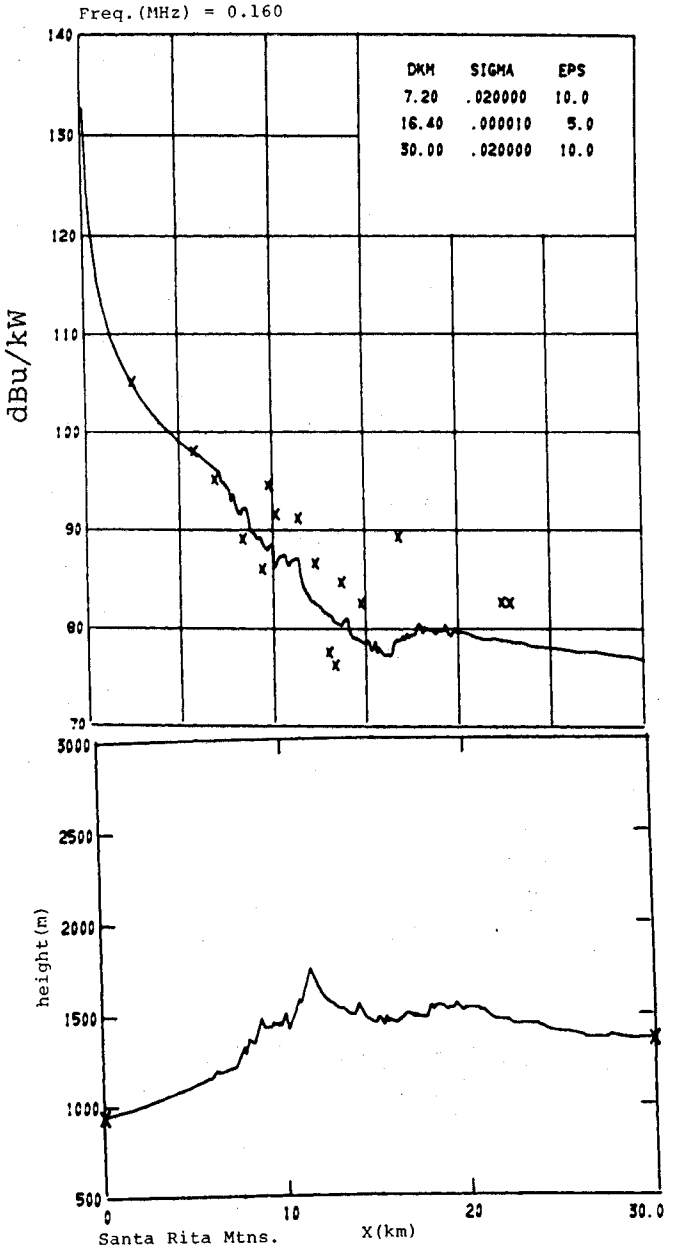

Figure 33. Path profile (lower portion) and received signal (in dB above 1 μV/m for 1 kW effective radiated power) for Santa Ritas, Arizona, path. Crosses denote measured 2.5 min. averages. Frequency = 0.160 MHz.

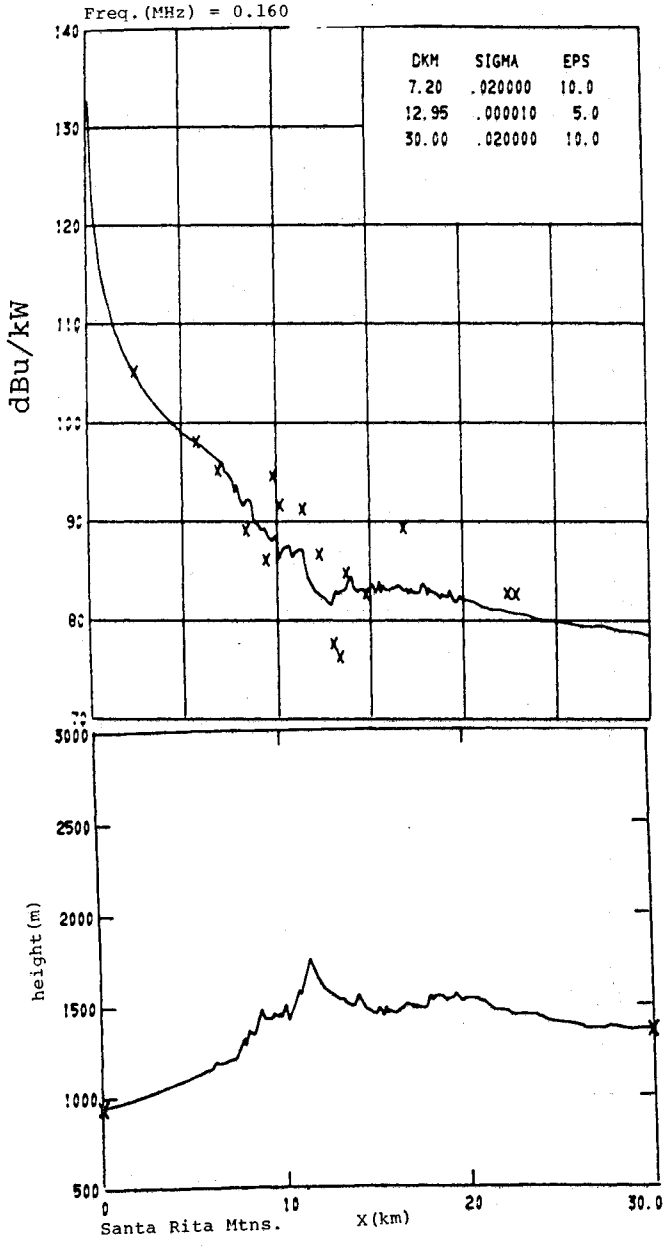

Figure 34. Path profile (lower portion) and received signal (in dB above 1 μV/m for 1 kW effective radiated power) for Santa Ritas, Arizona, path. Crosses denote measured 2.5 min. averages. Frequency = 0.160 MHz.

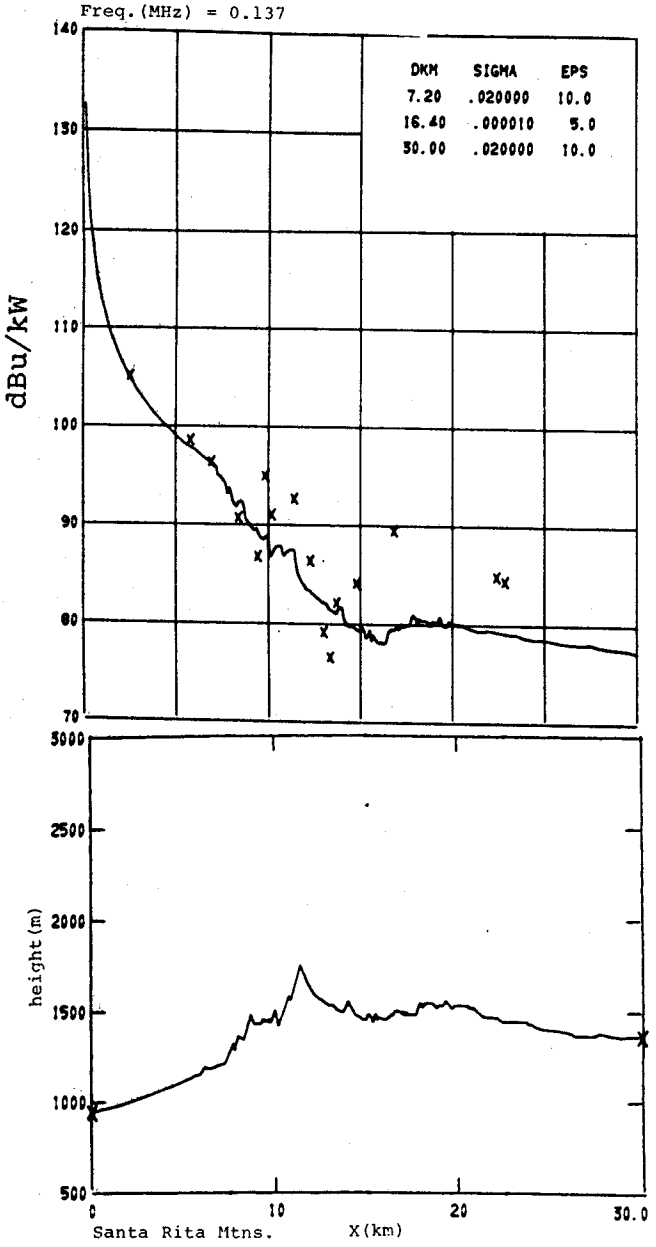

Figure 35. Path profile (lower portion) and received signal (in dB above 1 μV/m for 1 kW effective radiated power) for Santa Ritas, Arizona, path. Crosses denote measured 2.5 min. averages. Frequency = 0.137 MHz.

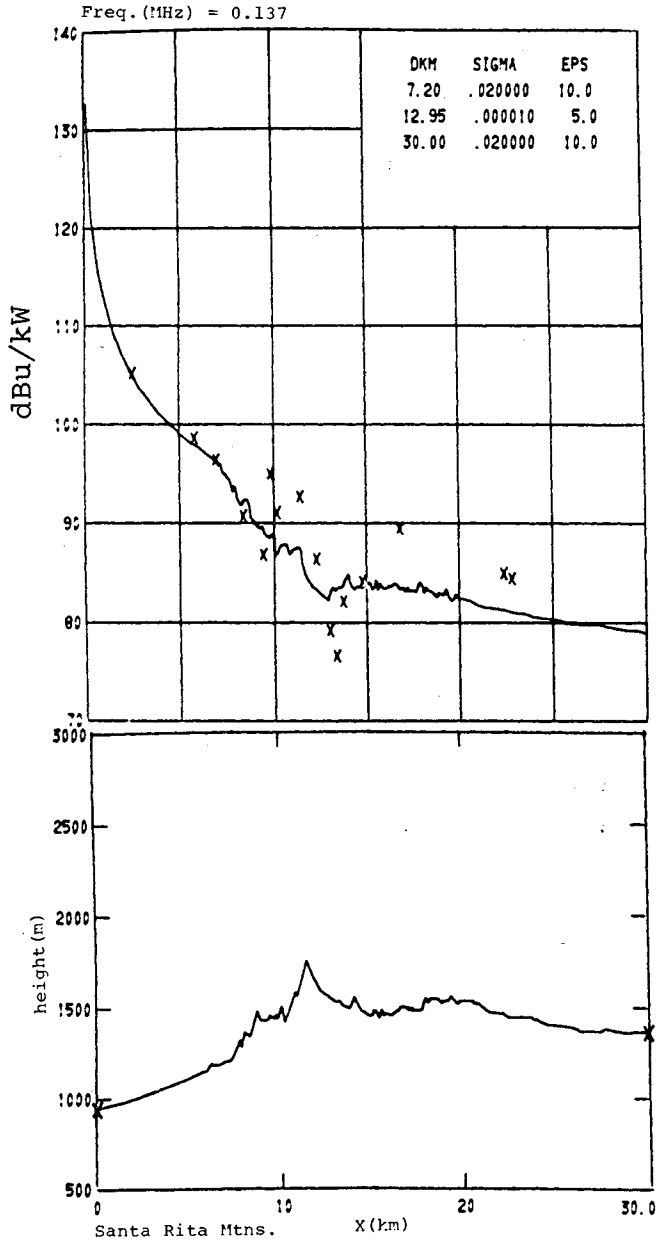

Figure 36. Path profile (lower portion) and received signal (in dB above 1 μV/m for 1 kW effective radiated power) for Santa Ritas, Arizona, path. Crosses denote measured 2.5 min. averages. Frequency = 0.137 MHz.

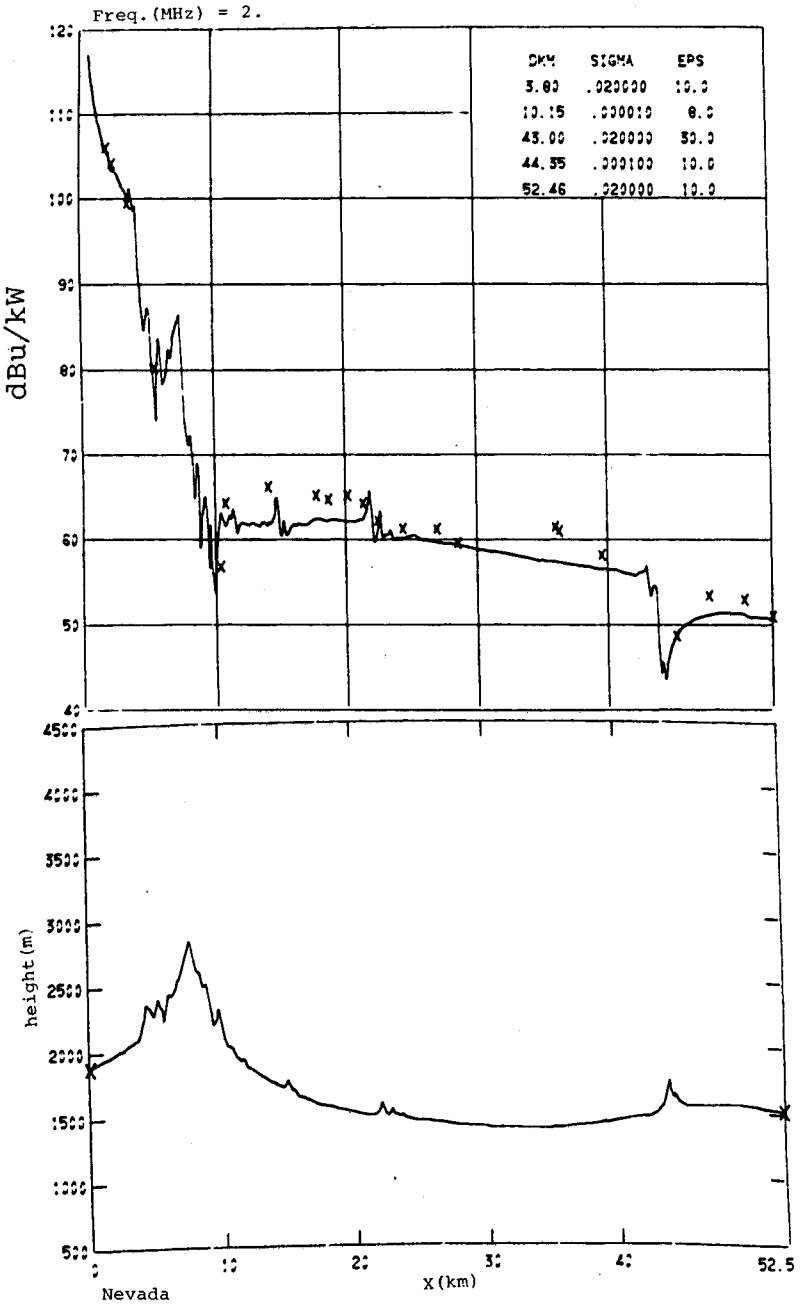

Figure 37. Path profile (lower portion) and received signal (in dB above 1 μV/m for 1 kW effective radiated power) for Dry Lake, Nevada, path. Crosses denote measured 2.5 min. averages. Frequency = 2 MHz. Predictions made using PROGRAM INTEQ.

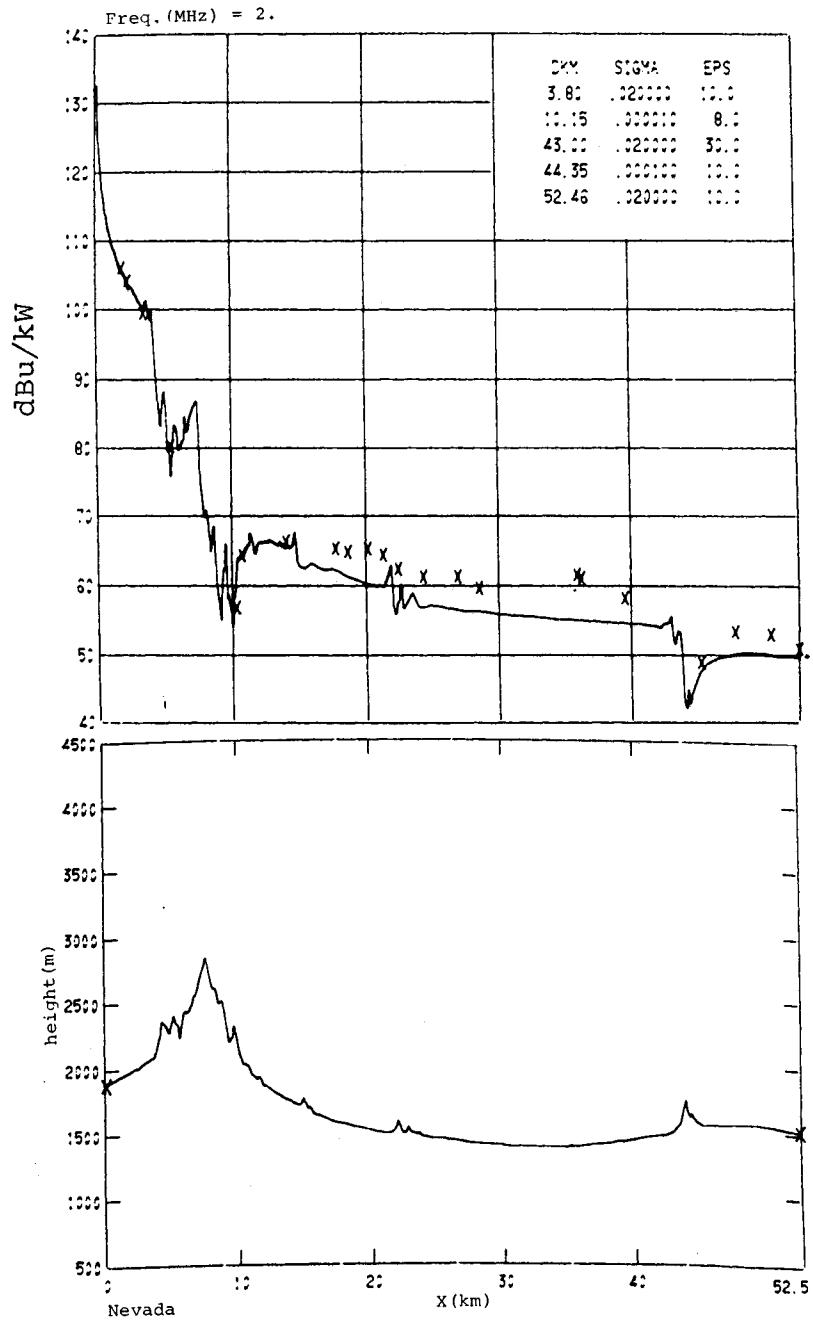

Figure 38. Path profile (lower portion) and received signal (in dB above 1 μV/m for 1 kW effective radiated power) for Dry Lake, Nevada, path. Crosses denote measured 2.5 min. averages. Frequency = 2 MHz.

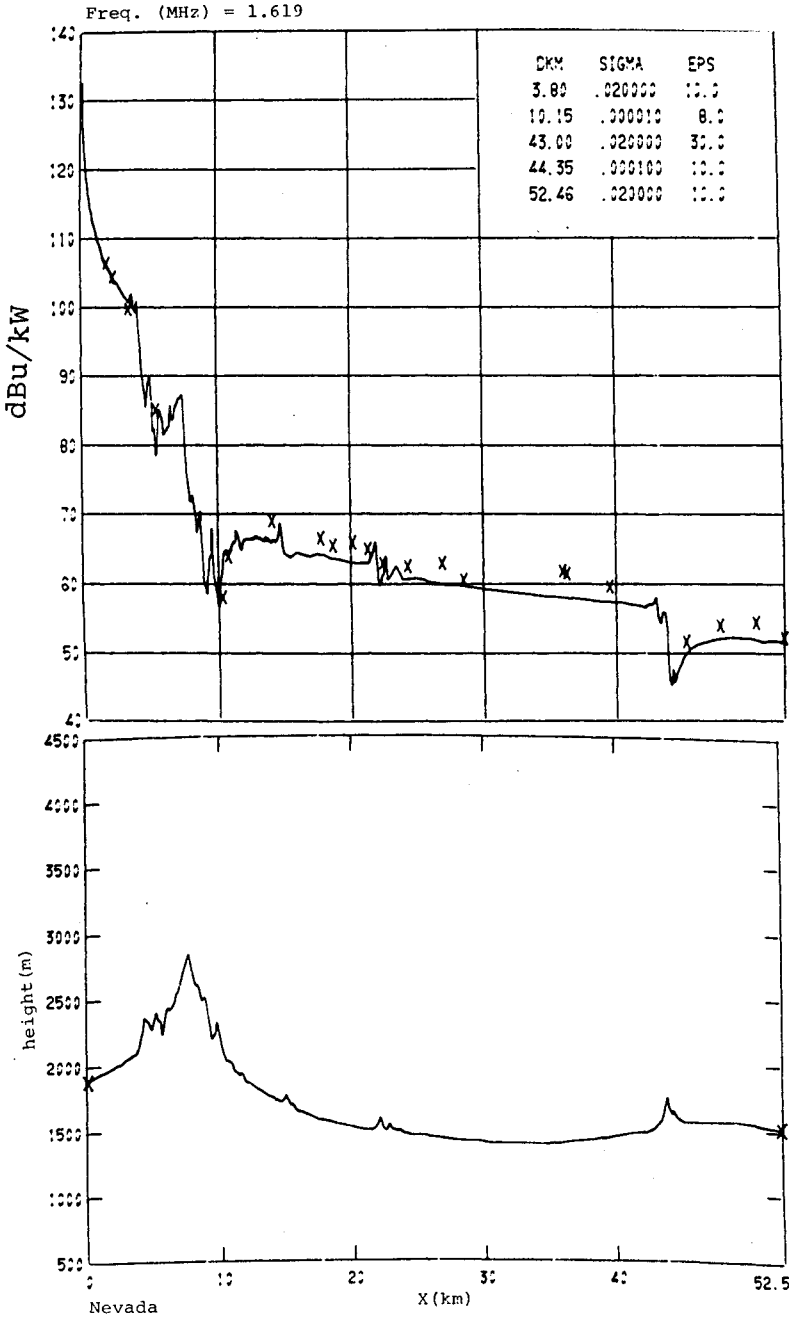

Figure 39. Path profile (lower portion) and received signal (in dB above 1 μV/m for 1 kW effective radiated power) for Dry Lake, Nevada, path. Crosses denote measured 2.5 min. averages. Frequency = 1.619 MHz.

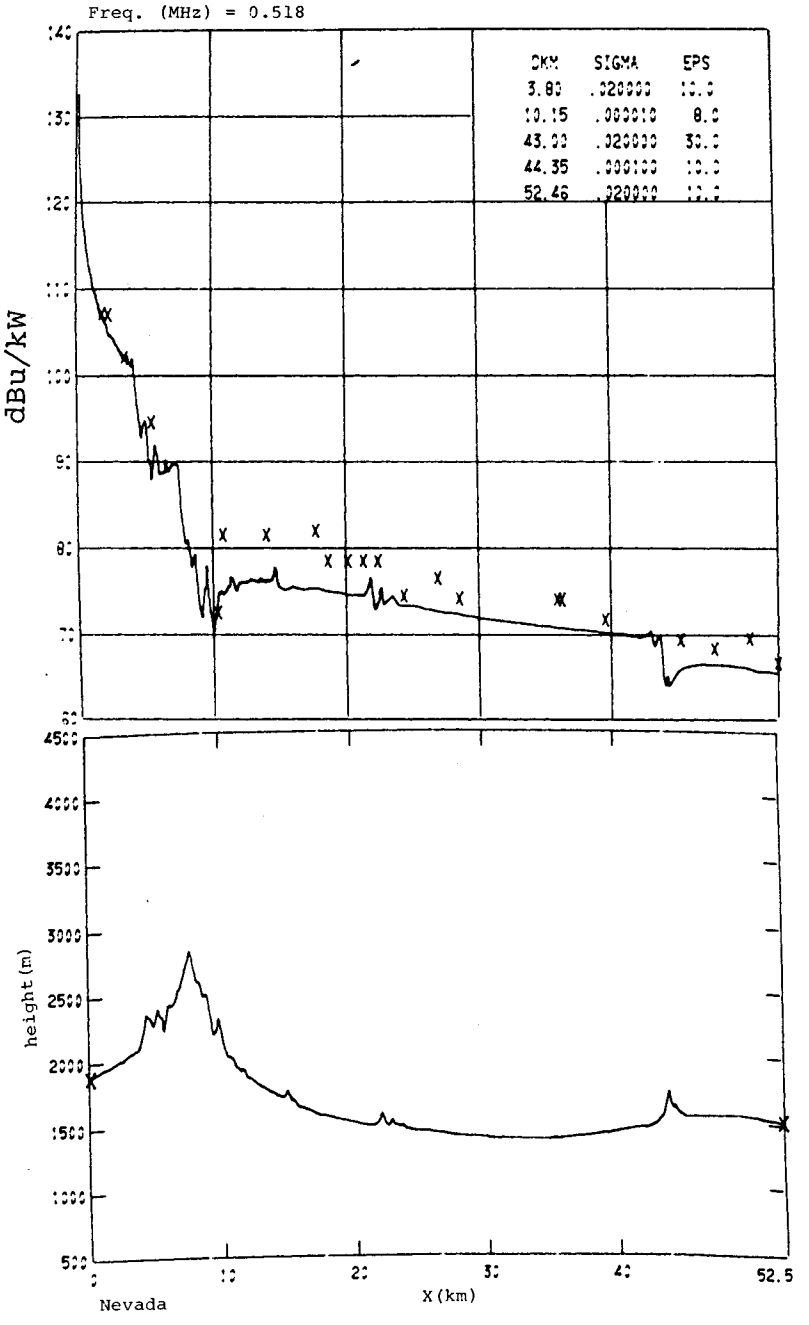

Figure 40. Path profile (lower portion) and received signal (in dB above 1 μV/m for 1 kW effective radiated power) for Dry Lake, Nevada, path. Crosses denote measured 2.5 min. averages. Frequency = 0.518 MHz.

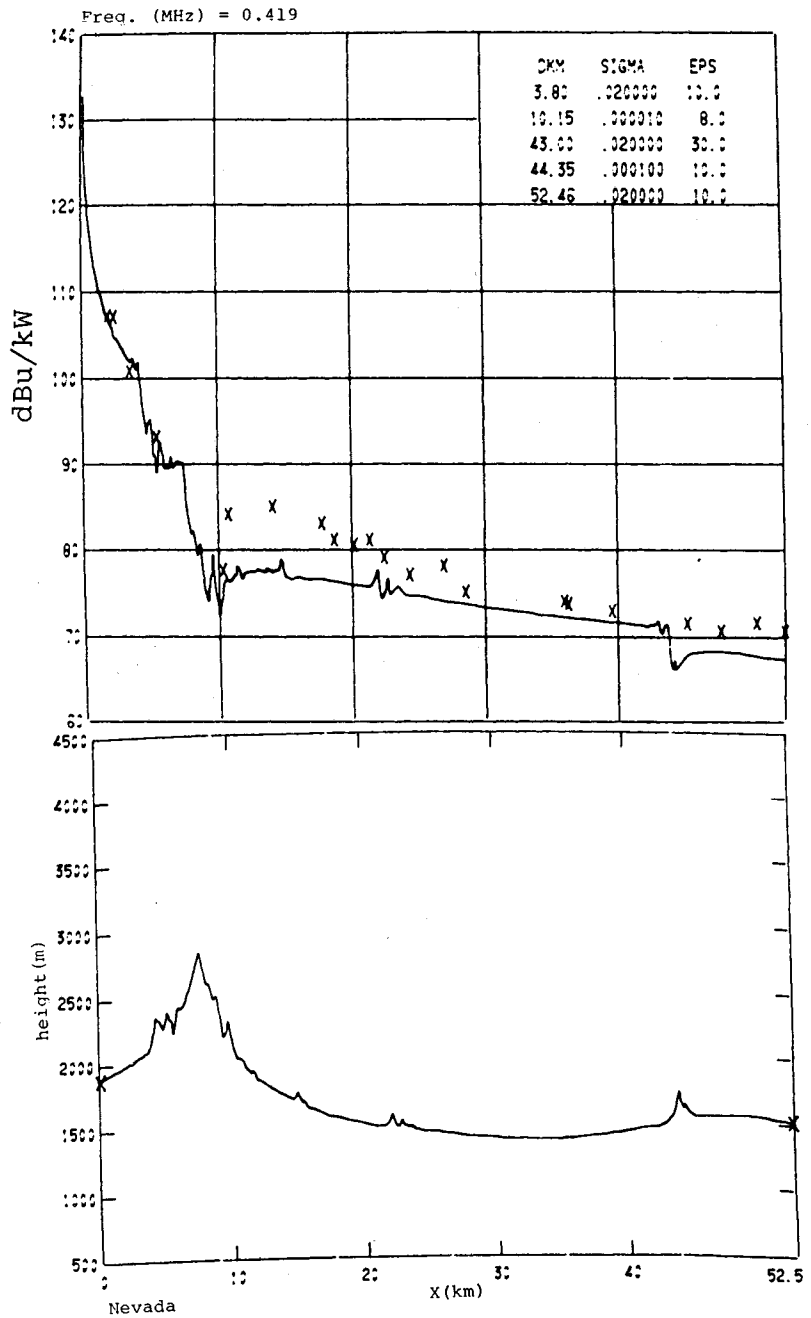

Figure 41. Path profile (lower portion) and received signal (in dB above 1 μV/m for 1 kW effective radiated power) for Dry Lake, Nevada, path. Crosses denote measured 2.5 min. averages. Frequency = 0.419 MHz.

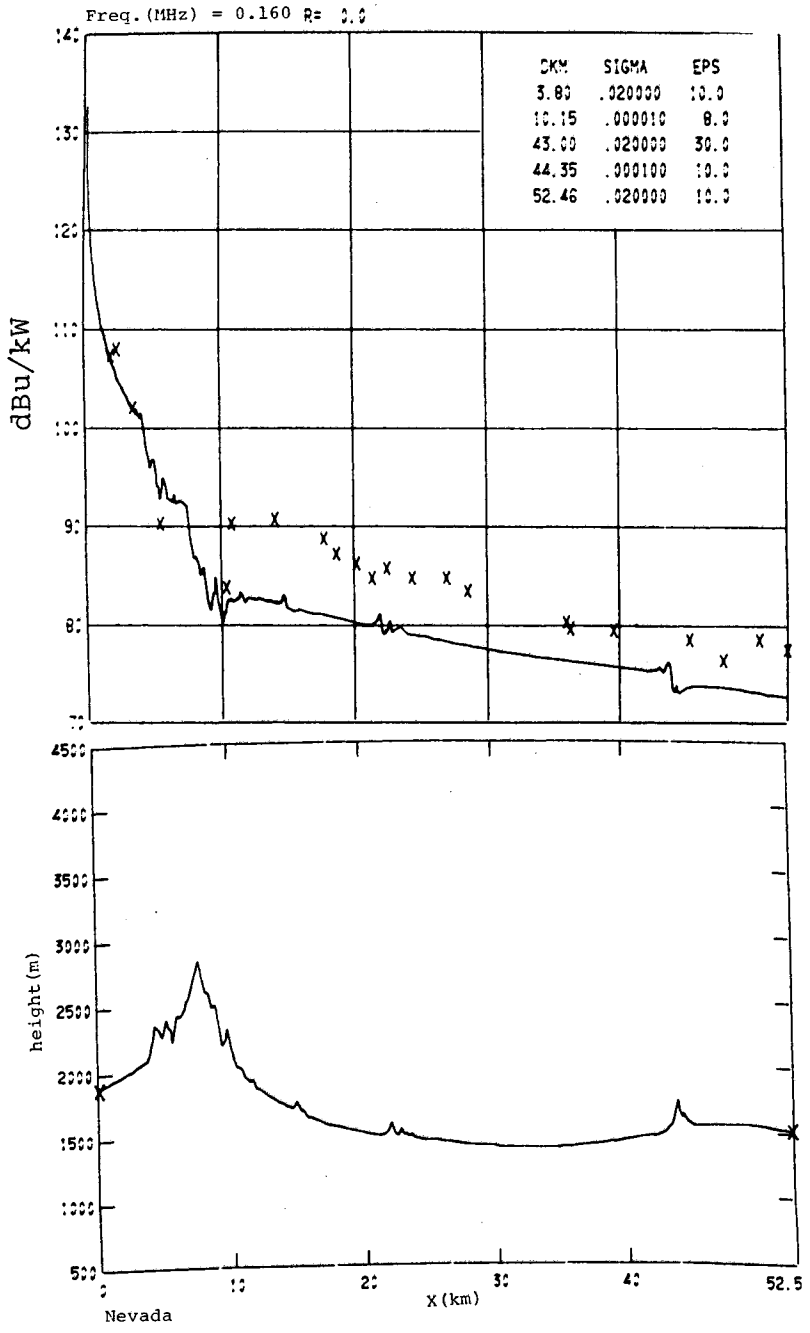

Figure 42. Path profile (lower portion) and received signal (in dB above 1 μV/m for 1 kW effective radiated power) for Dry Lake, Nevada, path. Crosses denote measured 2.5 min. averages. Frequency = 0.160 MHz.

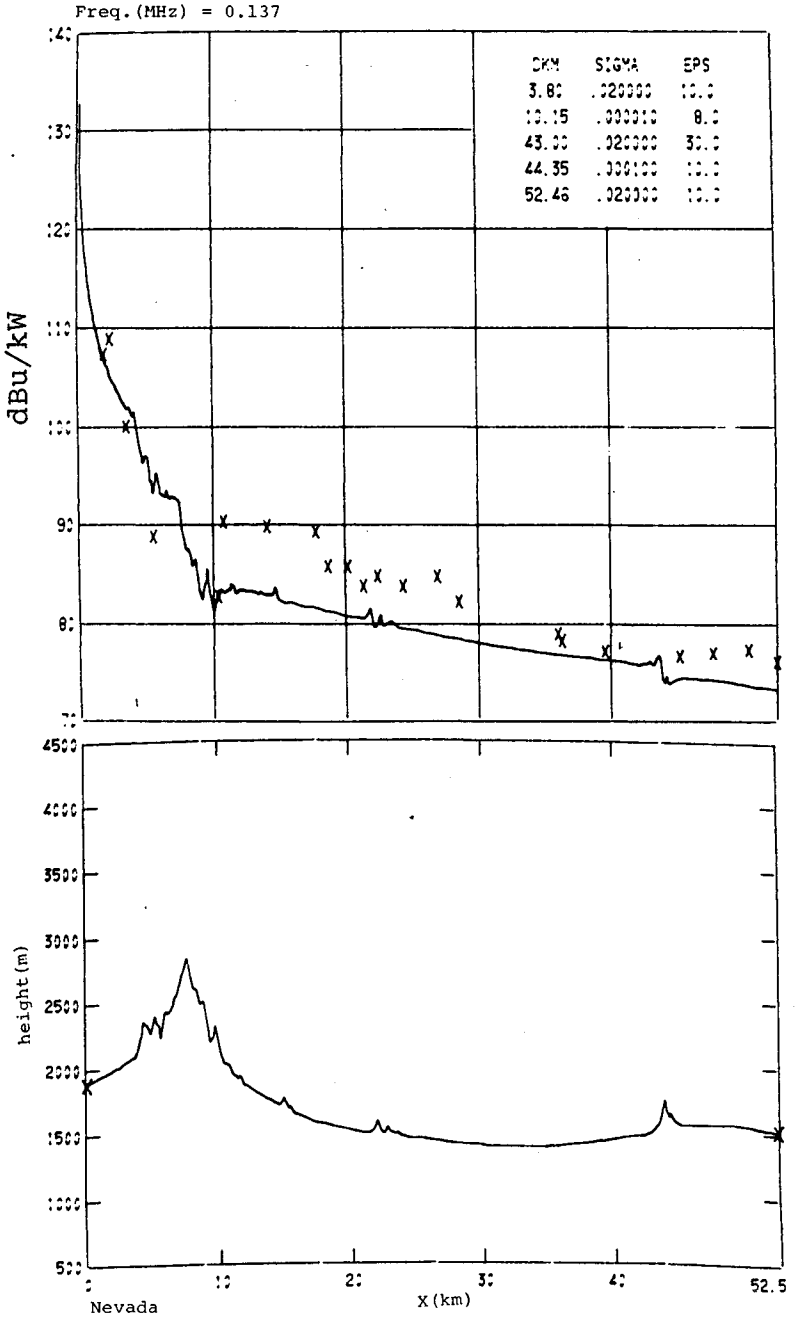

Figure 43. Path profile (lower portion) and received signal (in dB above 1 μV/m for 1 kW effective radiated power) for Dry Lake, Nevada, path. Crosses denote measured 2.5 min. averages. Frequency = 0.137 MHz.

Colorado Mountains

A study of the Colorado Mountain Data report (Johnson et al., 1967) was made to find paths for measurement/prediction comparison purposes. Only one radial has been found for which data at all frequencies (f = 20, 50, and 100 MHz) and all five sites are available. The sites (at 5, 10, 20, 30, and 50 km from the transmitter) fall more-or-less along the radial, and this is probably the best path for study. Other paths will have much fewer comparison points.

The predictions/comparisons for one radial using both PROGRAM WAGNER and PROGRAM INTEQ (Hufford's (1952) integral equation) are shown in Figures 44 through 49. Both integral solutions failed to yield convergent solutions at spacing intervals of 100 m and 50 m, as shown in Figures 44, 45, 47, and 48. This particular terrain profile probably represents an extreme in terms of roughness; however, the large amount of computer time required (913 sec in the case of WAGNER) to go just 6 km suggests more research on the problem is required.

5. SPACING/TIMING COMPARISON FOR PROGRAMS WAGNER AND INTEQ.

Four spacings (100 m, 200 m, 500 m, and 1 km) and 2 frequencies (137 kHz and 2 MHz) were evaluated using WAGNER and INTEQ for the Nevada path previously discussed. The results at 2 MHz using WAGNER are shown in figures 50, 51, 52, and 53, and using INTEQ in Figures 54, 55, 56, and 57. The results seem to indicate that at the 100 m spacing WAGNER came close to the measured values than INTEQ. There was also a smaller change going from the 200 m spacing to the 100 m spacing using WAGNER than for the corresponding spacing using INTEQ. However, INTEQ was much faster; i.e., 100 m spacing using INTEQ took 7.60 sec while the 100 m spacing using WAGNER took 76 sec. A 100 m spacing at 2 MHz is 3 points every 2 radio wavelengths.

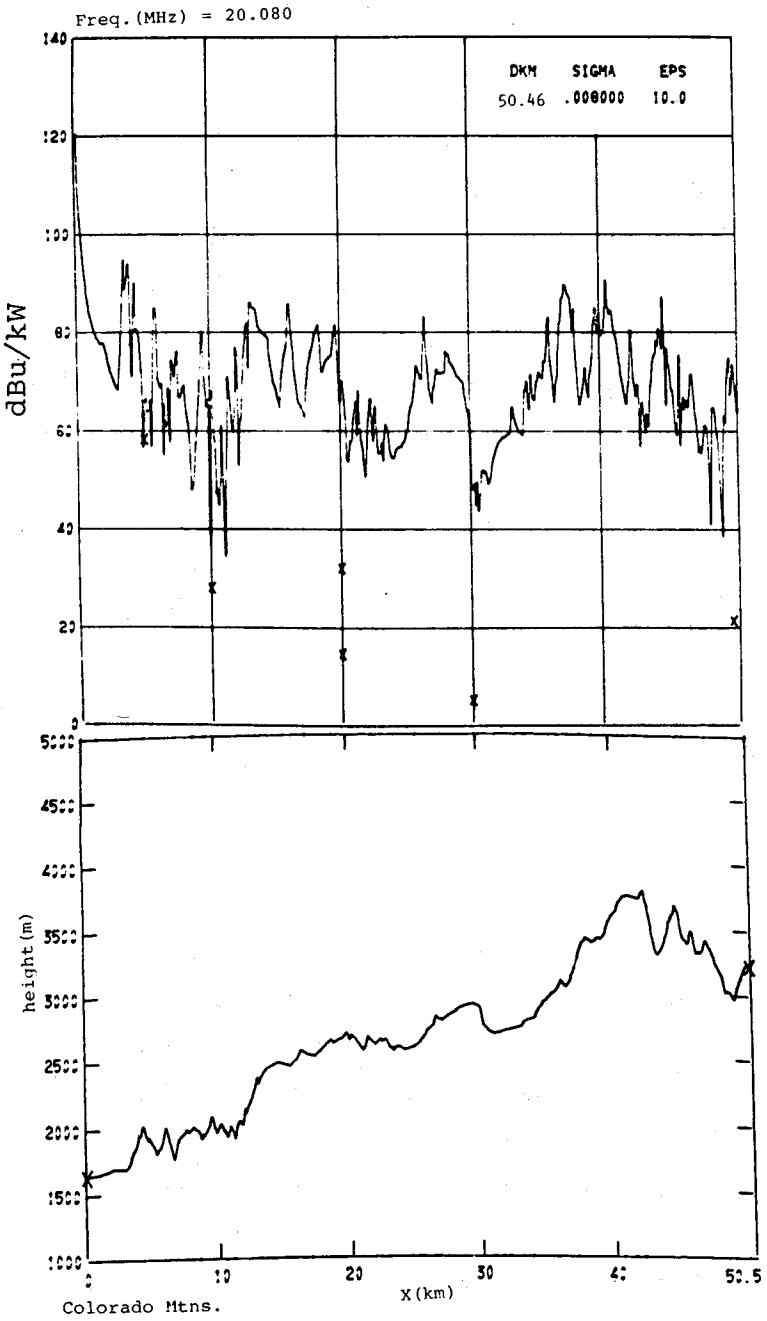

Figure 44. Path profile (lower portion) and received signal (in dB above 1 μV/m for 1 kW effective radiated power) for Colorado Mountain path. Crosses denote measured median. Predictions using PROGRAM WAGNER, 100 m spacing intervals. At 20 km, the two measured values correspond to two sites close to the radial selected for comparisons.

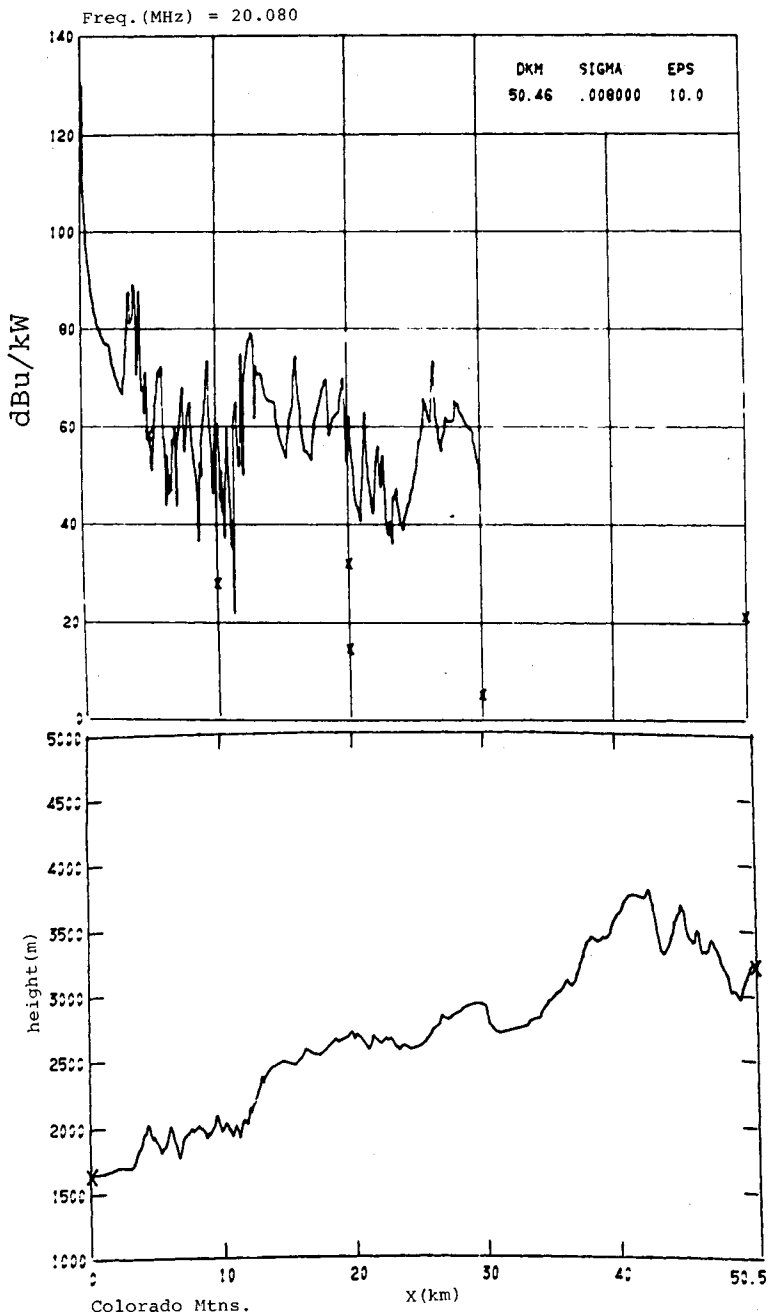

Figure 45. Path profile (lower portion) and received signal (in dB above 1 μV/m for 1 kW effective radiated power) for Colorado Mountain path. Crosses denote measured median. Predictions using PROGRAM WAGNER.

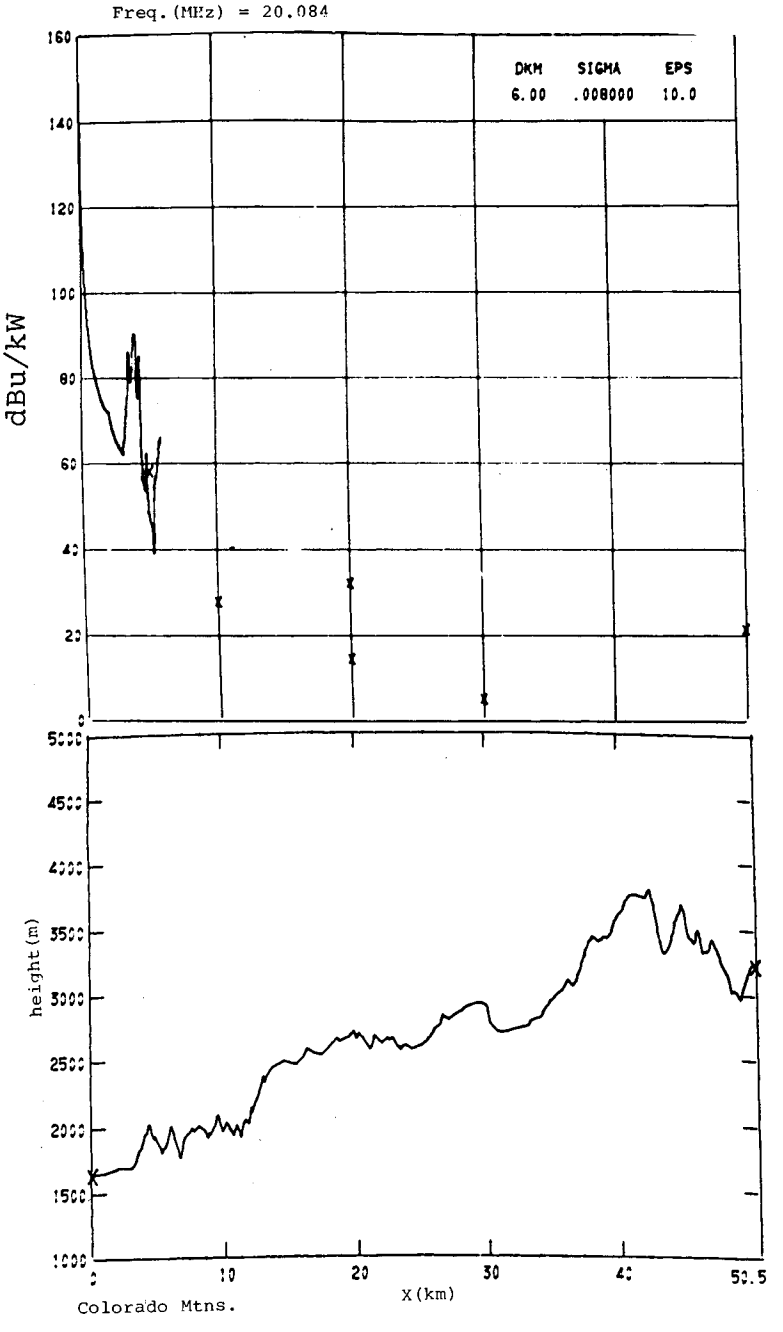

Figure 46. Path profile (lower portion) and received signal (in dB above 1 μV/m for 1 kW effective radiated power) for Colorado Mountain path. Crosses denote measured median. Predictions using PROGRAM WAGNER.

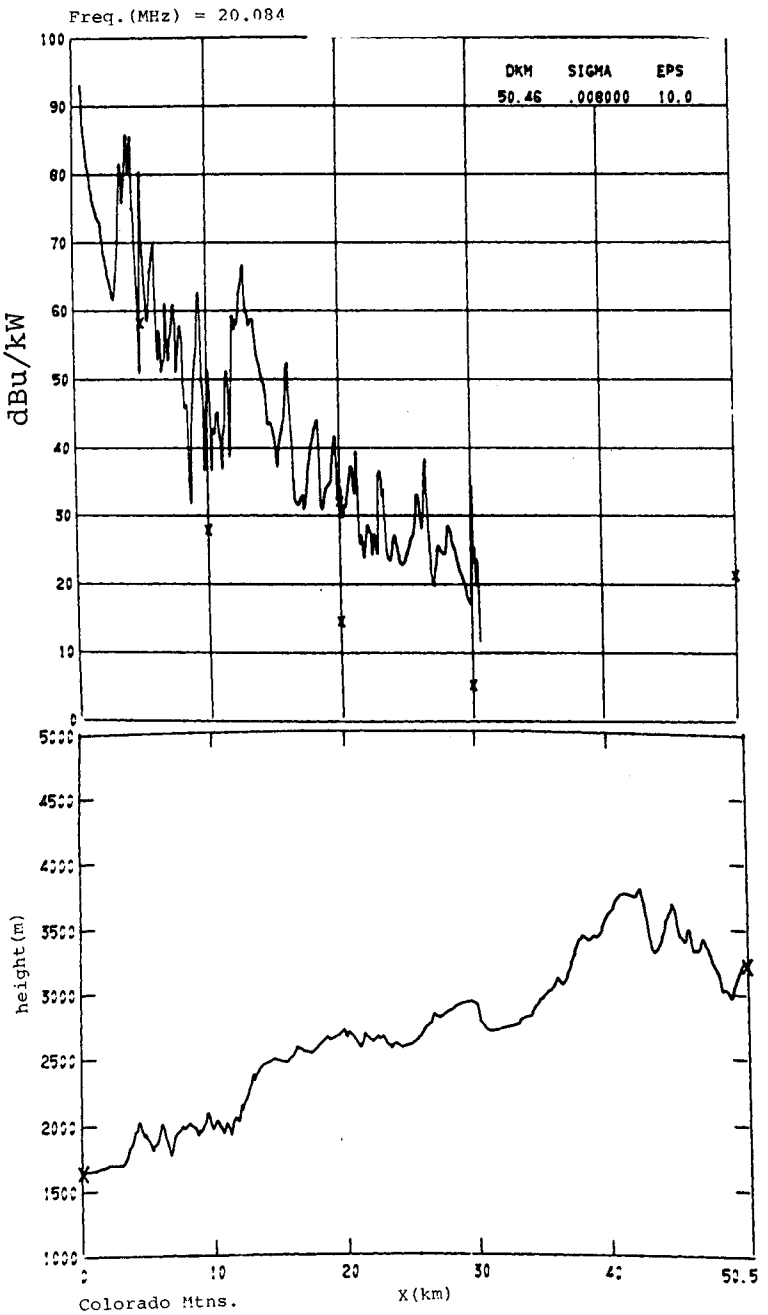

Figure 47. Path profile (lower portion) and received signal (in dB above 1 μV/m for 1 kW effective radiated power) for Colorado Mountain path. Crosses denote measured median. Predictions using PROGRAM INTEQ.

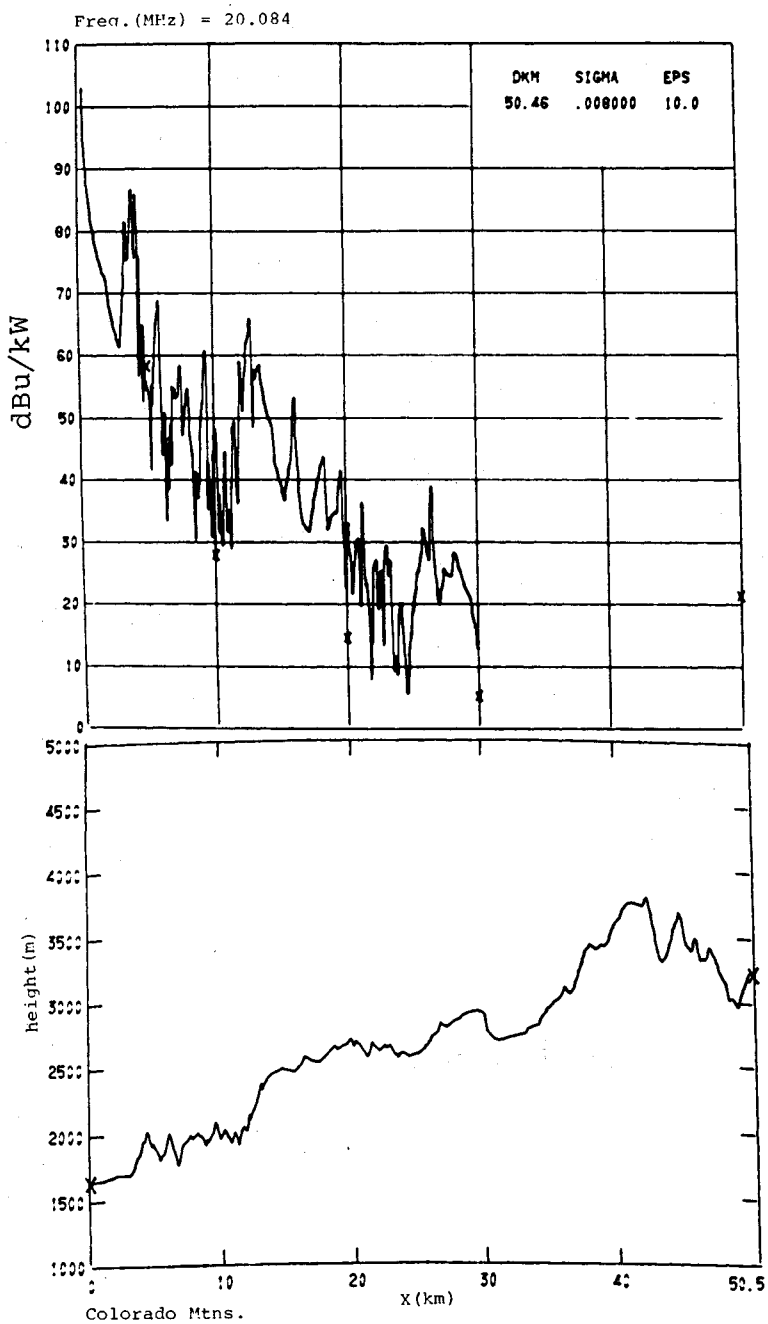

Figure 48. Path profile (lower portion) and received signal (in dB above 1 μV/m for 1 kW effective radiated power) for Colorado Mountain path. Crosses denote measured median. Predictions using PROGRAM INTEQ.

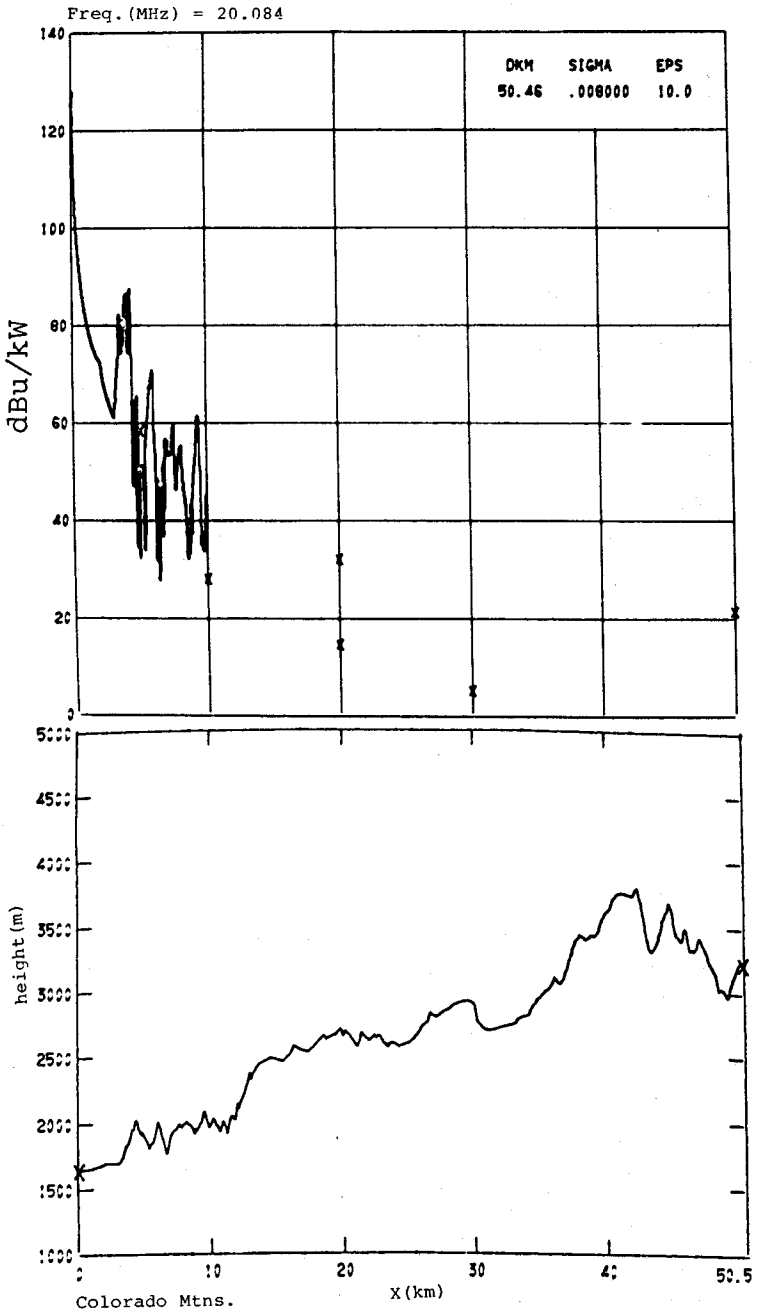

Figure 49. Path profile (lower portion) and received signal (in dB above 1 μV/m for 1 kW effective radiated power) for Colorado Mountain path. Crosses denote measured median. Predictions using PROGRAM INTEQ.

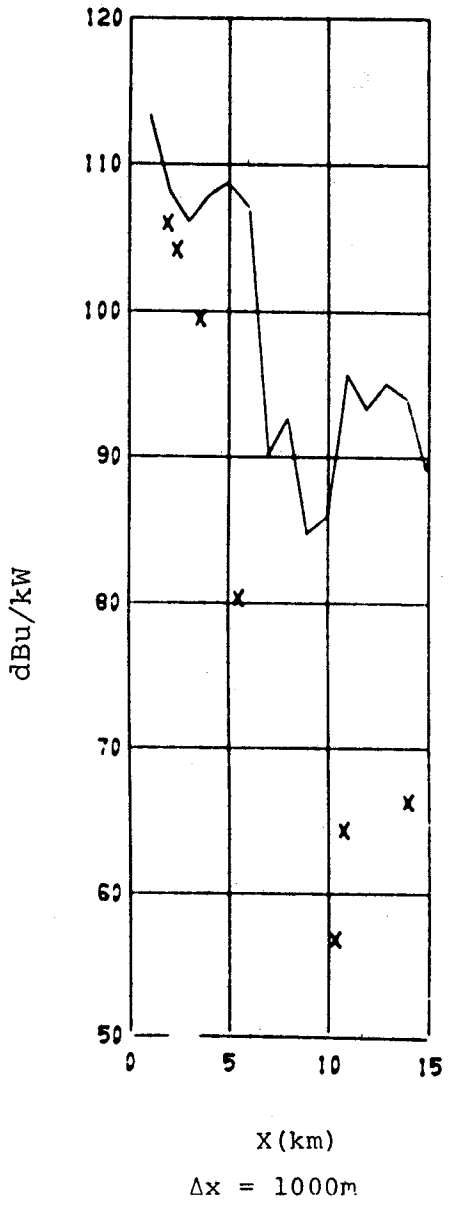

Figure 50. Nevada path at 2 MHz using PROGRAM WAGNER with 1 km spacing of observation points.

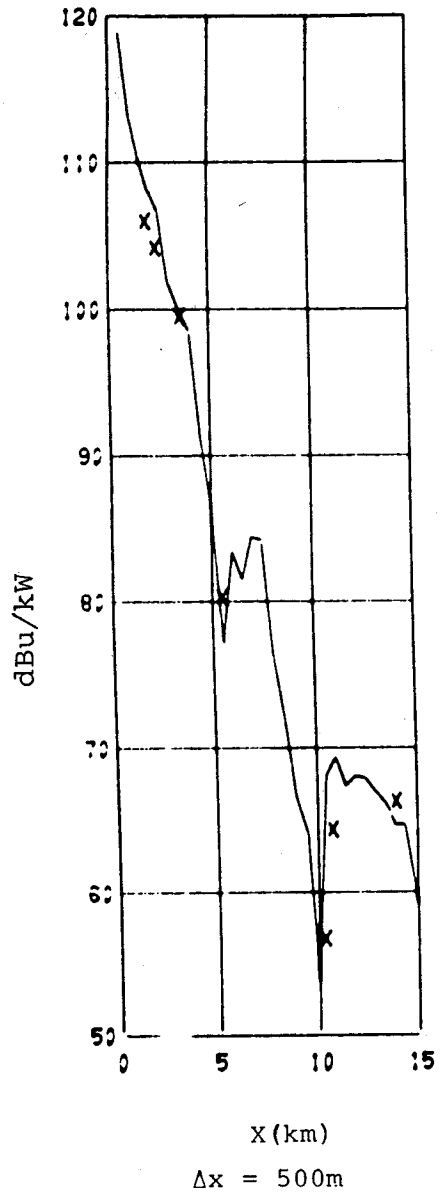

Figure 51. Nevada path at 2 MHz using PROGRAM WAGNER with 500 m spacing of observation points.

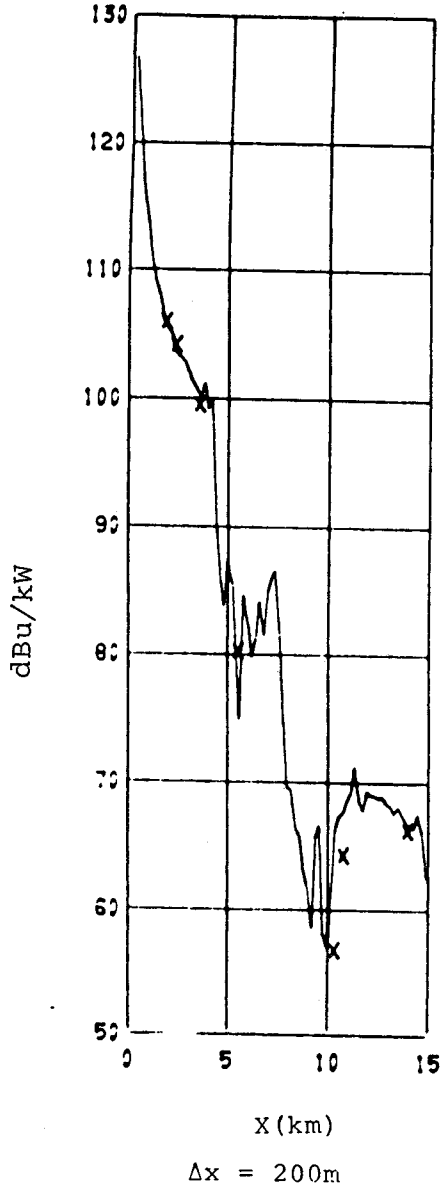

Figure 52. Nevada path at 2 MHz using PROGRAM WAGNER with 200 m spacing of observation points.

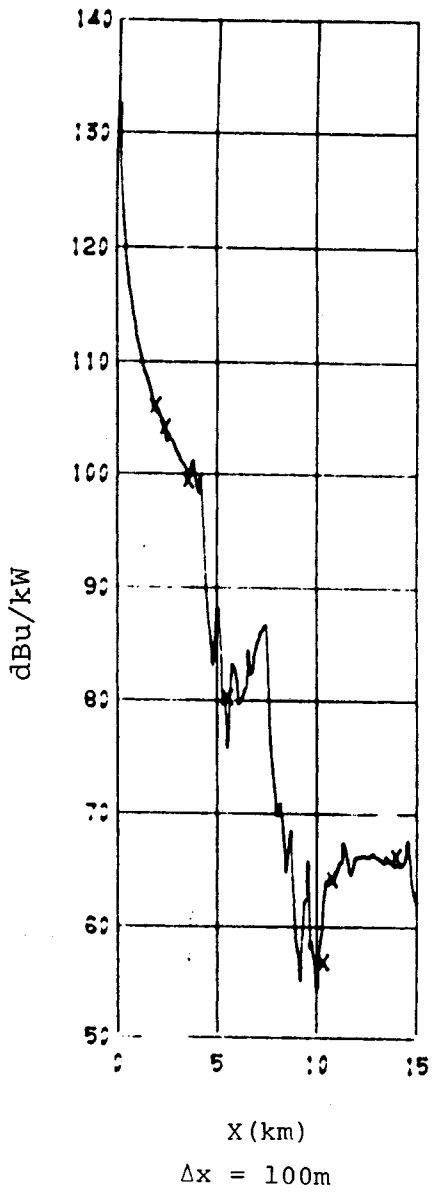

Figure 53. Nevada path at 2 MHz using PROGRAM WAGNER with 100 m spacing of observation points.

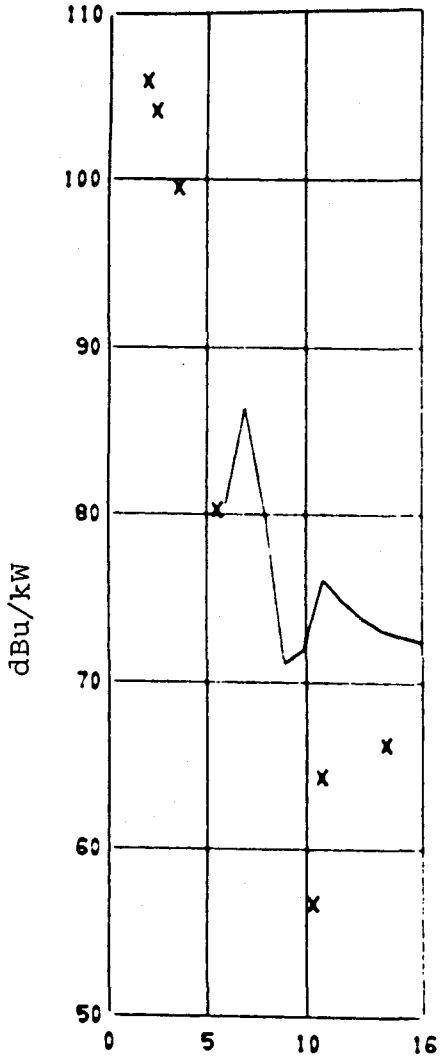

Figure 54. Nevada path at 2 MHz using PROGRAM INTEQ with 1 km spacing of observation points.

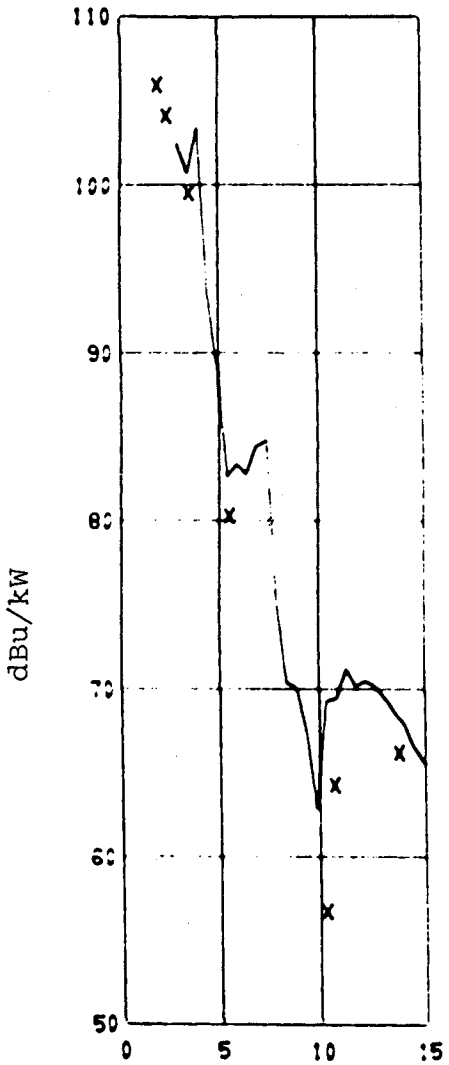

Figure 55. Nevada path at 2 MHz using PROGRAM INTEQ with 500 m spacing of observation points

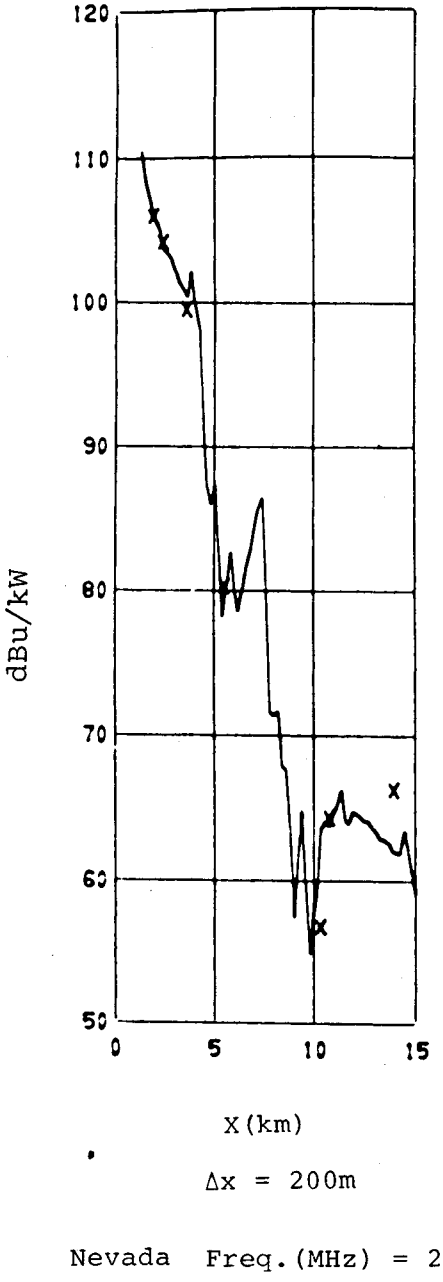

Figure 56. Nevada path at 2 MHz using PROGRAM INTEQ with 200 m spacing of observation points.

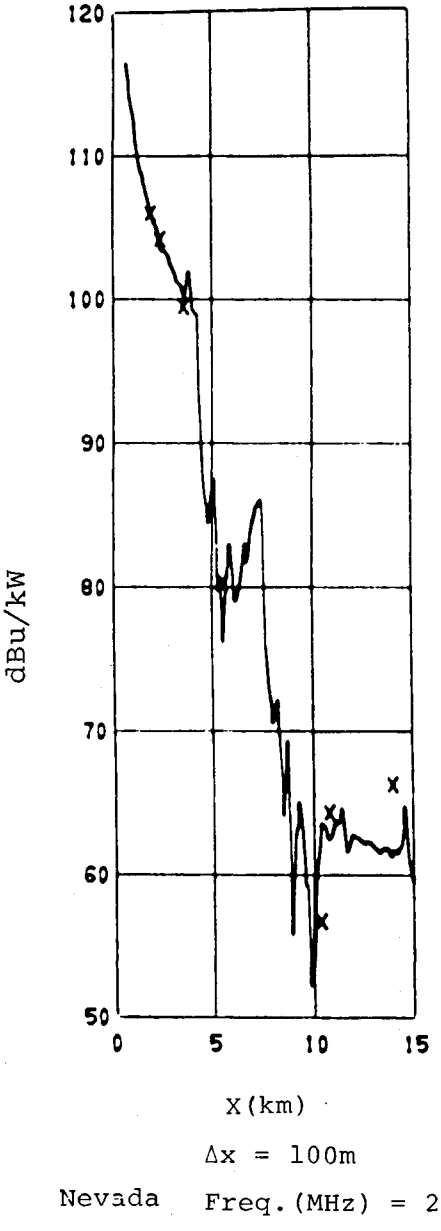

Figure 57. Nevada path at 2 MHz using PROGRAM INTEQ with 100 m spacing of observation points.

At 137 kHz the results in Figures 58, 59, 60, 61, 62, 63, 64, and 65 indicate that both WAGNER and INTEQ have converged using the 500 m spacing, which is nearly three points per wavelength. A conservative estimate for the spacing of points regardless of terrain profile, even for the Colorado Mountain example, might be

Observation interval spacing, $\Delta x \simeq 1/3$ wavelength

6. CONCLUDING REMARKS

Nine examples of measurement/calculation comparison discussed in the previous sections partially verify the applicability of PROGRAMS WAGNER or INTEQ for estimating ground wave propagation over irregular terrain. The predictions appear to follow the general trend of the data except for regions near the transmitter and for large path distances. Further comparisons with other data are obviously needed before the method is completely validated. However, to the authors' knowledge, no other method attempting a detailed prediction for this complex problem has been published. It is hoped that the method presented here will at least partially fulfill the need for a better prediction of propagation effects in telecommunication systems.

Extensions of the model to include off-path terrain effects (the three-dimensional ground wave problem) are planned for the future. A full wave treatment would also provide more accurate estimates of the field, especially in those regions where complex interference phenomena are encountered. Wait (1974) has pointed to the use of alternative methods for evaluating propagation over irregular terrain in cases where the terrain can be considered a single knife-edge or a combination of several knife-like discontinuities, and his approach should be considered, especially when the behaviour of the field in the vicinity of a single terrain feature is desired.

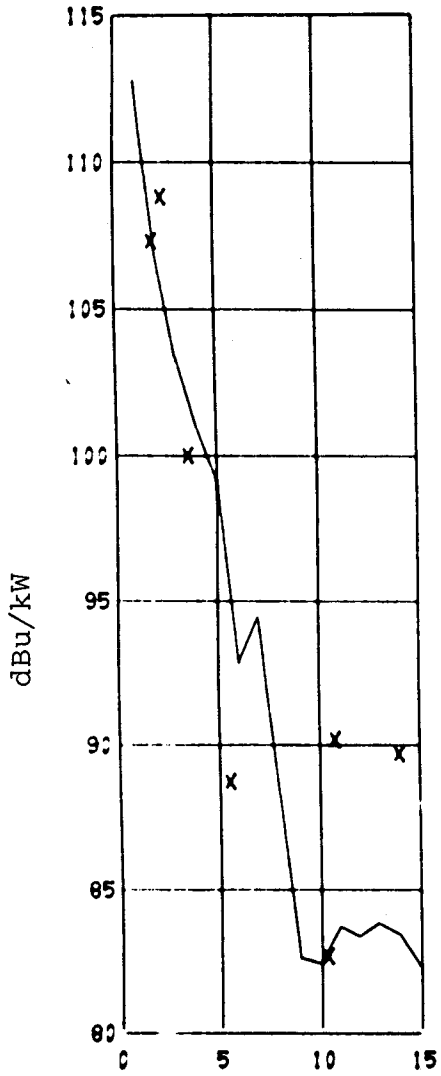

Figure 58. Nevada path at 137 MHz using PROGRAM WAGNER with 1 km spacing of observation points.

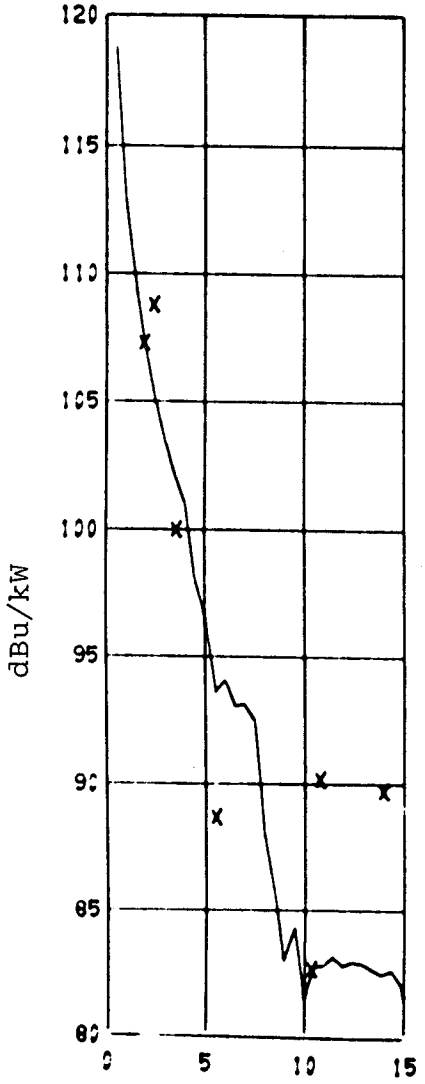

Figure 59. Nevada path at 137 MHz using PROGRAM WAGNER with 500 m spacing of observation points.

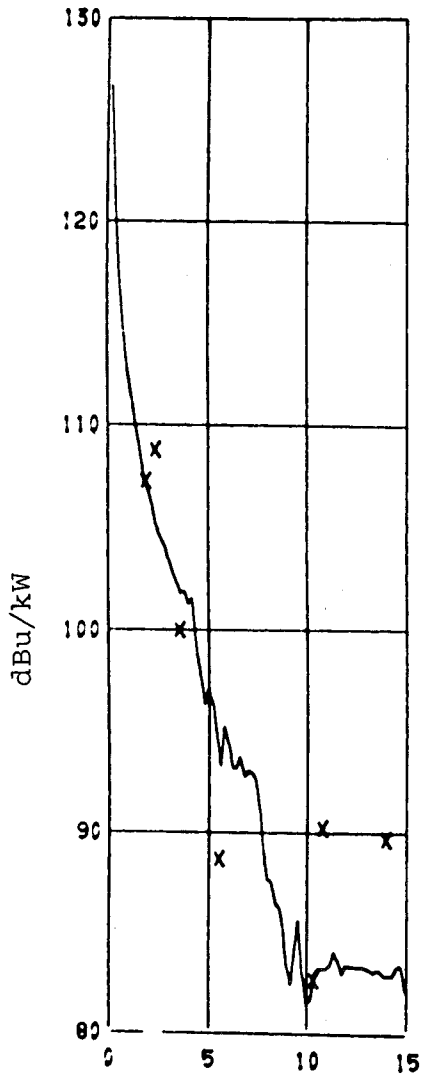

Nevada Freq.(MHz) = 0.137

Figure 60. Nevada path at 137 MHz using PROGRAM WAGNER with 200 m spacing of observation points.

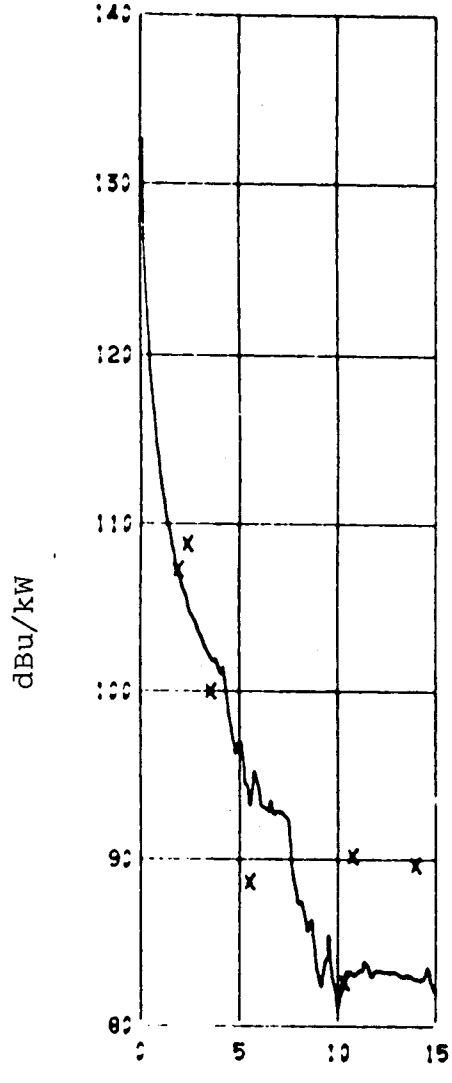

Nevada Freq.(MHz) = 0.137

Figure 61. Nevada path at 137 MHz using PROGRAM WAGNER with 100 m spacing of observation points.

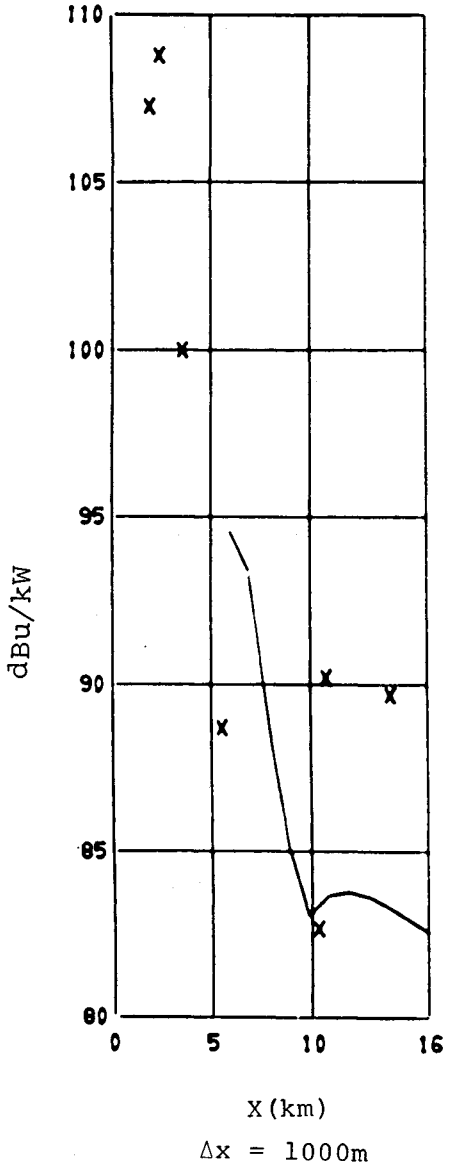

Nevada Freq.(MHz) = 0.137

Figure 62. Nevada path at 137 MHz using PROGRAM INTEQ with 1 km spacing of observation points.

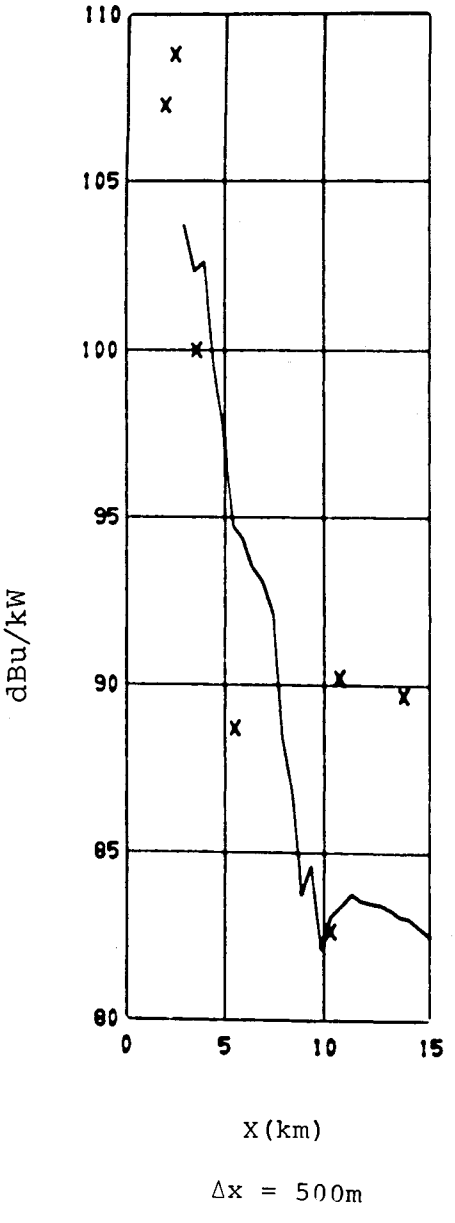

Nevada Freq.(MHz) = 0.137

Figure 63. Nevada path at 137 MHz using PROGRAM INTEQ with 500 m spacing of observation points.

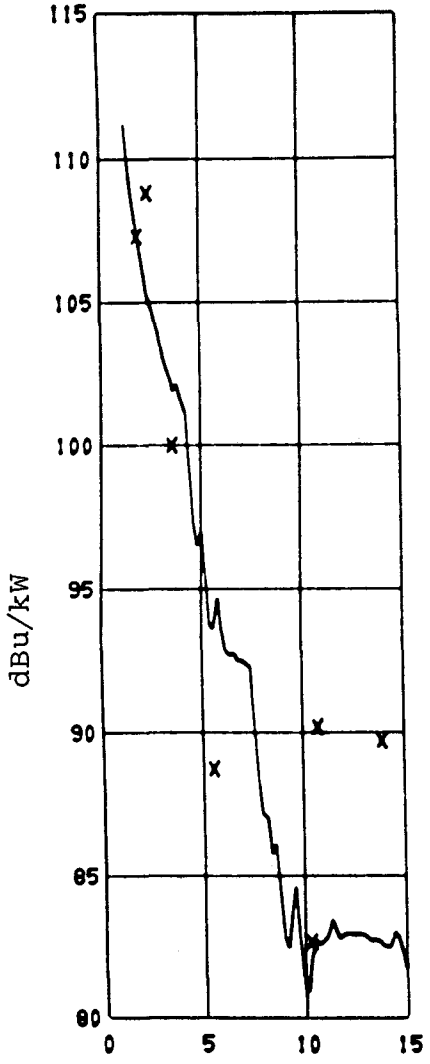

Figure 64. Nevada path at 137 MHz using PROGRAM INTEQ with 200 m spacing of observation points.

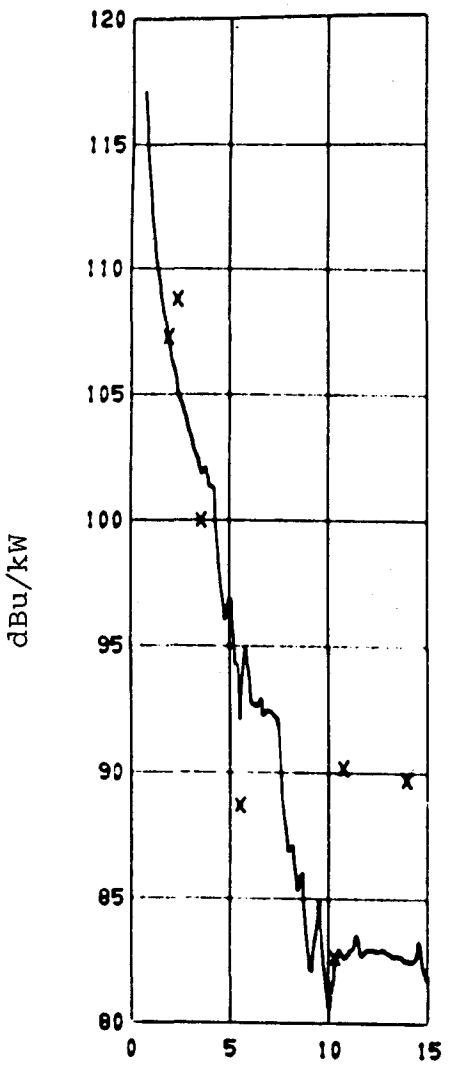

Figure 65. Nevada path at 137 MHz using PROGRAM INTEQ with 100 m spacing of observation points.

7. ACKNOWLEDGEMENT

The Electromagnetic Compatibility Analysis Center (ECAC) supported the research described in this paper. Ms. Jacqueline R. Janoski, Mr. J. A. Zoellner, and Dr. R. A. Whiteman of ECAC initiated the idea to provide ECAC with an up-to-date, efficient prediction algorithm for propagation over irregular, inhomogeneous terrain. Mr. Mark Weissberger of ECAC made many helpful suggestions during the course of the research. Mrs. Rita Reasoner of ITS provided invaluable computer programming assistance. Also, the work was supported in part by the Department of the Air Force, Space and Missile Systems Organization, Norton Air Force Base under the sponsorship of Captains Bob Barrell and Bob Barberg and technical direction from TRW staff and by Mr. J. Cullhane, Dr. Leo Baggerely, and Mr. Jim Wolcott.

8. REFERENCES

Abramowitz, M. and I. A. Stegun (1964), Handbook of Mathematical Functions, National Bureau of Standards, AMS 55, Ch. 7.

CBS Radio (1971), Field intensity measurements to establish performance of directional antenna station KCBS, San Francisco, California, Report E 70704-A, CBS Radio, Columbia Broadcasting System, Inc.

Hansen, P. (1977), Measurements of basic transmission loss for HF ground wave propagation over seawater, Radio Science, 12, No. 3, pp. 397-404, May-June.

Head, H. T. (1958), Field strength measurement survey for Association of Maximum Service Telecasters, Inc., Buffalo, New York; A.D. Ring and Associates, Washington, D. C.

Heckscher, J. (1979), RADC Technical Report, to be published.

Hopkins, M. (1977), ECAC-HDBK-77-07, ECAC's topographic data handbook, IITRI, Annapolis, Md., April; or ECAC's topographic data users manual, ECAC-UM-77-013.

Hufford, G. A. (1952), An integral equation approach to the problem of wave propagation over an irregular terrain, Quart. J. Appl. Math., 9, pp. 391-404.

Johnson, M. E., M. J. Miles, P. L. McQuate, and A. P. Barsis (1967), Tabulcations of VHF propagation data obtained over irregular terrain at 20, 50 and 100 MHz, Part II: Colorado Mountains, ESSA Tech. Report No.: IER 38-ITSA 38-2, U. S. Department of Commerce, Environmental Sciences Services Administration, Institute for Telecommunication Sciences, Boulder, CO 80303.

Kissick, W. A., E. J. Haakinson, and G. H. Stonehocker (1978), Measurements of LF and MF radio propagation over irregular, inhomogeneous terrain, NTIA Report No. 78-12, Boulder, Colorado 80303.

Lytle, R. J. (1974), Measurement of earth medium electrical characteristics: Techniques, results and applications, IEEE Trans. GeoScience and Electronics, GS12, pp. 81-101.

Monteath, G. D. (1973), Applications of the Electromagnetic Reciprocity Principle, (Pergamon Press, New York), p. 116.

Ott, R H. (1970), An alternative integral equation for propagation over irregular terrain, Radio Sci. 5, No. 5 pp. 767-771, May.

Ott, R. H. (1971a), An alternative integral equation for propagation over irregular terrain, 2, Radio Sci., 6, No. 4, pp. 429-435.

Ott, R. H. (1971b), A new method for predicting HF ground wave attenuation over inhomogeneous, irregular terrain, U. S. Dept. of Commerce, Res. Rept. No. OT/TRER 7, Jan. (NTIS Access No. AB721179).

Ott, R. H. (1974), Fock currents for concave surfaces, IEEE Trans. Ant. Prop., AP-22, No. 2, March, pp. 357-360.

Wait, J. R. (1974), Recent analytical investigations of electromagnetic ground wave propagation over inhomogeneous earth models, Proc. IEEE 62, No. 8, Aug., pp. 1061-1072.

APPENDIX A: Effective Surface Impedance for a Two-Layered Ground.

The effective surface impedance, Δ, appearing in Program WAGNER can be modified to account for the effects of stratified layers in the ground as discussed in King and Wait (1976). We will denote the relative (complex and anisotiopic) permittivity and permeability by $\varepsilon(=\varepsilon_r - i60\lambda\sigma)$ and μ. Furthermore, assuming propagation in the x-direction and the positive z-axis in the vertical downward direction, the subscripts, x, y, z, attached to a quantity will refer to that quantity in the x, y, or z directions; the subscripts, 1, 2, 3, etc., refer to layer 1 (the top layer), layer 2, layer 3, etc.

For now, it will be assumed that only two layers are present: a surface layer of height h, and a lower layer of infinite extent downward. With ψ denoting the angle of incidence of the wave with the ground surface, the effective surface impedance for a vertically polarized wave is given by

$$\Delta(\psi) = Z_1(\psi)/\eta_o, \quad Z_1(\psi) = K_1 \frac{K_2 + K_1 \tanh(u_1 h_1)}{K_1 + K_2 \tanh(u_1 h_1)} ,$$

where $$K_1 = (\eta_o/\varepsilon_{x1}) \sqrt{\mu_{y1}\varepsilon_{x1} - (\varepsilon_{x1}/\varepsilon_{z1})\cos^2\psi} ,$$

$$K_2 = (\eta_o/\varepsilon_{x2}) \sqrt{\mu_{y2}\varepsilon_{x2} - (\varepsilon_{x2}/\varepsilon_{z2})\cos^2\psi} ,$$

$$u_1 = \pm ik \sqrt{\mu_{y1}\varepsilon_{x1} - (\varepsilon_{x1}/\varepsilon_{z1})\cos^2\psi} ,$$

and $$\eta_o = \sqrt{\mu_o/\varepsilon_o} \simeq 120\pi \text{ ohms}, \quad k = 2\pi/\lambda .$$

The sign of u_1 is chosen such that the field goes to zero at very large distances.

For horizontal polarization, $\Delta(\psi)$ is obtained by interchanging μ and ε in the preceding equations. Thus,

$$\Delta(\psi) = \eta_o Y_1(\psi), \quad Y_1(\psi) = N_1 \frac{N_2 + N_1 \tanh(v_1 h_1)}{N_1 + N_2 \tanh(v_1 h_1)}$$

where $$N_1 = (1/\eta_o \mu_{x1}) \sqrt{\mu_{x1}\varepsilon_{y1} - (\mu_{x1}/\mu_{z1})\cos^2\psi} \quad ,$$

$$N_2 = (1/\eta_o \mu_{x2}) \sqrt{\mu_{x2}\varepsilon_{y2} - (\mu_{x2}/\mu_{z2})\cos^2\psi} \quad ,$$

$$v_1 = \pm ik \sqrt{\mu_{x1}\varepsilon_{y1} - (\mu_{x1}/\mu_{z1})\cos^2\psi} \quad .$$

Reference

King, R. J., and J. R. Wait (1976), Electromagnetic groundwave propagation theory and experiment, Vol. XVII, Symposia Mathematica, Instituto Nazionale di Alta Matematica, Bologna (published by Academic Press).

APPENDIX B1

USER'S GUIDE, LISTING AND SAMPLE OUTPUT FOR PROGRAM WAGNER

Card 1: KIND, TD (I10, F10.0)
KIND = beginning type of distance at which F(x) will be evaluated
1 is specified on next cards
0 is equidistant
TD = total distance in kilometers

Card 2A: X(I) (8F10.5)
X(I) = specific distances in kilometers at which F(x) will be evaluated.
IF KIND = 1 use these cards to begin giving specific distances until you are done or want to change to equidistant points.
Terminate this set of distances with a 0.

Card 2B1: NED (I2)
NED = number (limited to 50) of consecutive sections with F(x) evaluated at equidistant points. (This should agree with the number of pairs of DEP and FINT).

Card 2B2: (DEP(I), FINT(I), I = 1,NED) (8F10.0)
DEP(I) = distance in kilometers at which this set of equidistant points ends.
FINT(I)= interval of these equidistant points in kilometers
If KIND= 0 use these cards to begin.

N.B. There may be a series of 2A and 2B cards to reach the total distance given on card 1.

Card 3: HA, FREQ, POL, HAR, AKM, MF, IDATA, SF (5F10.5,2I2,F10.0)
HA = transmitter antenna height in kilometers
FREQ = frequency in MHz
POL = polarization; 1 is vertical, 2 is horizontal
HAR = receiver antenna height in kilometers
AKM = earth radius in kilometers

MF = 0 (no microfilm); MF $\neq$ 0 (microfilm)
IDATA = 0(no measured data input); IDATA $\neq$ 0 (measured data input and plot)
SF = scale factor for microfilm

Card 4 ID (8A10)
ID = path identification

```
Card 5:    N, IXUNITS, IZUNITS, REFEL  (3I10,F10.1)
           N = number of points on terrain profile
           IXUNITS = 0, distance input in kilometers
                   = 1, distance input in statute miles
           IZUNITS = 0, height input in meters
                   = 1, height input in feet
           REFEL   = reference elvation in IZUNITS(=height at d=0)

Card 6
   to M:   (X(I), Z(I), I = 1,N)      (4(F10.2,F10.0))
           X(I) = terrain distances in IXUNITS
           Z(I) = terrain heights in IZUNITS
           End with -1. in X field

Card M+1: NGC      (I10)
           NGC = number of sets of DX, SIGX, EPSX
                 (limited to 50)

Card M+2
  to end:  (DX(I), SIGX(I), EPSX(I), I = 1,NGC)
                  (4(F7.0,F7.4,F6.0))
           DX(I) = maximum distance in kilometers for given
                   sigma and epsilon
           SIGX(I) = sigma
           EPSX(I) = epsilon


**Measured data input cards follow last of above cards;
     distances (DD(J), see WAGPL) are in km;
     format: d(km), DBU_m - (8X,6(F6.2,F6.0)
     End with -1. in d_m field.

Output: DBU = 106.92-20log d_km + 20 log2|F(x)|
```

```
      PROGRAM WAGNER(INPUT,OUTPUT,TAPE60=INPUT       )
      DIMENSION IPOL(2)
      DIMENSION ADAB(3),ADGH(3)
      COMMON /0/ F(2000),R13(2000),R14(2000),R15(2000),R16(2000),R17(200
     10),R18(2000),R19(2000),R20(2000),R21(2000)
      COMMON/1/ HA,AKM
      COMMON /2/ D,H,HP
      COMMON /3/ DELTAR,WAVE
      COMMON /4/ FREQ,POL
      COMMON /5/ NG,AB(48),GH(48)
      COMMON /6/ N,X(2001),INDEX
      COMMON /SIN/ SUMP,NIT,SX(501),SZ(501),ALF(501)
      COMMON /INPUT/ DUMM(10320),ID(8),REFEL

      COMMON /GCX/ NGC,DX(50),ETAX(50),DELTAX(50),SIGX(50),EPSX(50)
      COMPLEX ETAX,DELTAX
      DOUBLE PRECISION DAB,DGH
      COMPLEX FEWH,F,ALAMZ,SUM,DELTAR,ETAR
      COMPLEX KERNL,P0,P1,P2,P3,P4,CTMP
      COMPLEX FF,ETA,DELTA
      DATA (NG=5)
      DATA (ADAB=.9061798459,.5384693101,0.)
      DATA (ADGH=.2369268851,.4786286704,.56888888888)
      CANG(Z)=ATAN2(AIMAG(Z),REAL(Z))
      IPOL(1)=8H  VERTIC$IPOL(2)=8HHORIZONT
C
CC              READ GAUSSIAN QUADRATURE ABCISSAS AND WEIGHTS
C
      NR=(NG+1)/2
      DO 1 L=1,NR
      DAB=ADAB(L)
      DGH=ADGH(L)
      J=NG-L+1
      AB(L)=DAB
      AB(J)=-AB(L)
      GH(L)=DGH
1     GH(J)=GH(L)
C
CC          CALL SUBROUTINE TO SET UP DISTANCE ARRAY X IN METERS
CC          START WITH X(2).  X(1)=0. HAS ALREADY BEEN SET.
CC          THE DISTANCES DO NOT HAVE TO BE EQUALLY SPACED.
CC          SUBROUTINE DISTX SHOULD MAKE SURE N ≤ 2000
C
4     X(1)=0.
      F(1)=(1.,0.)
      CALL DISTX
C
C           MAKE SURE THERE ARE AT LEAST 4 DISTANCES
      IF (N.GE.4) GO TO 2
      PRINT 18
      CALL EXIT
C
2     SQRTX2=SQRT(X(2))
      SQRTX3=SQRT(X(3))
      SQRTX4=SQRT(X(4))
      D1=SQRT(X(2)*X(3)*X(4))*(X(2)*(SQRTX4-SQRTX3)+X(3)*(SQRTX2-SQRTX4)
     1+X(4)*(SQRTX3-SQRTX2))
      R1=X(3)*X(4)*(SQRTX4-SQRTX3)/D1
      R2=X(2)*X(4)*(SQRTX2-SQRTX4)/D1
      R3=X(2)*X(3)*(SQRTX3-SQRTX2)/D1
      R4=(X(2)*(SQRTX4**3-SQRTX3**3)+X(3)*(SQRTX2**3-SQRTX4**3)+X(4)*(SQ
     1RTX3**3-SQRTX2**3))/D1
      R5=SQRT(X(3)*X(4))*(X(3)-X(4))/D1
      R6=SQRT(X(2)*X(4))*(X(4)-X(2))/D1
      R7=SQRT(X(2)*X(3))*(X(2)-X(3))/D1
      R8=(SQRTX2*(SQRTX3**3-SQRTX4**3)+SQRTX3*(SQRTX4**3-SQRTX2**3)+SQRT
     1X4*(SQRTX2**3-SQRTX3**3))/D1
      R9=SQRT(X(3)*X(4))*(SQRTX4-SQRTX3)/D1
      R10=SQRT(X(2)*X(4))*(SQRTX2-SQRTX4)/D1
      R11=SQRT(X(2)*X(3))*(SQRTX3-SQRTX2)/D1
```

```
      R12=(SQRTX2*(X(4)-X(3))+SQRTX3*(X(2)-X(4))+SQRTX4*(X(3)-X(2)))/D1
      DO 3 M=5,N
      M1=M-1
      M2=M-2
      DELTA1=X(M)-X(M1)
      DELTA2=X(M)-X(M2)
      D2=(DELTA1-DELTA2)*DELTA1*DELTA2
      R13(M)=X(M1)*X(M2)*(X(M2)-X(M1))/D2
      R14(M)=X(M)*X(M2)*(X(M)-X(M2))/D2
      R15(M)=X(M)*X(M1)*(X(M1)-X(M))/D2
      R16(M)=(X(M1)**2-X(M2)**2)/D2
      R17(M)=(X(M2)**2-X(M)**2)/D2
      R18(M)=(X(M)**2-X(M1)**2)/D2
      R19(M)=(X(M2)-X(M1))/D2
      R20(M)=(X(M)-X(M2))/D2
3     R21(M)=(X(M1)-X(M))/D2
C
C           READ SOURCE HEIGHT, FREQUENCY, AND POLARIZATION
C     COL          DESCRIPTION
C     1-10      SOURCE HEIGHT, KM
C     11-20      FREQUENCY, MHZ
C     21-30      POLARIZATION, 1. = VERTICAL, 2. = HORIZONTAL
C
      READ 19, HA,FREQ,POL,HAR,AKM


      IQT=0
      HAR=HAR*1.E+3
      HA=HA*1.E3
      KPOL=POL
      ALAM=2.997925E2/FREQ
      WAVE=6.283185307/ALAM
      ALAMZ=((0.7071067812,0.7071067812)/SQRT (ALAM))
      TO=SECOND(DUM)
C
C           LOOP ON DISTANCE
C
      DO 14 I=1,N
      INDEX=I
      IF (I .NE. 1) GO TO 51
      CALL TERRAN2(X(I),H,HP,ETA,DELTA,ETAR,DELTAR,COND,EPS)
      PRINT 20, FREQ,IPOL(KPOL),AKM,HA,HAR
      GO TO 52
51    CALL TERRANE (X(I),H,HP,ETA,DELTA,ETAR,DELTAR,COND,EPS)
52    CONTINUE
      IF (I.EQ.1) GO TO 14
      D=X(I)+(H**2)/(2.*X(I))
      F(I)=FEWH(H,X(I))
      IF (I.LE.6) GO TO 13
C
C                J = 2 THROUGH 4
C
      SUM=(0.,0.)
      DO 9 J=2,4
      P0=P1=P2=P3=(0.,0.)
      K=J-1
      XP2=0.5*(X(J)+X(K))
      XM2=0.5*(X(J)-X(K))
      DO 7 M=1,NG
      X0=XP2+AB(M)*XM2
      CTMP=KERNL(X0)*GH(M)
      P1=P1+CTMP*SQRT(X0)
      P2=P2+CTMP*X0
      P3=P3+CTMP*SQRT(X0)**3
      IF (K.NE.1) GO TO 6
      X0=0.25*X(J)*(1.+AB(M))**2
      P0=P0+SQRT(X0)*KERNL(X0)*GH(M)
      GO TO 7
6     P0=P0+CTMP
7     CONTINUE
```

```
      P1=P1*XM2
      P2=P2*XM2
      P3=P3*XM2
      IF (K.NE.1) GO TO 8
      P0=P0*SQRT(X(J))
      GO TO 9
8     P0=P0*XM2
9     SUM=SUM+P0+R4*P1+R8*P2+R12*P3+F(2)*(R1*P1+R5*P2+R9*P3)+F(3)*(R2*P1
     1+R6*P2+R10*P3)+F(4)*(R3*P1+R7*P2+R11*P3)
C
CC                J = 5 THROUGH I-1
C
      I1=I-1
      DO 11 J=5,I1
      P0=P2=P4=(0.,0.)
      XP2=0.5*(X(J)+X(J-1))
      XM2=0.5*(X(J)-X(J-1))
      DO 10 M=1,NG
      X0=XP2+AB(M)*XM2
      CTMP=KERNL(X0)*GH(M)
      P0=P0+CTMP
      P2=P2+CTMP*X0
10    P4=P4+CTMP*X0**2
      P0=P0*XM2
      P2=P2*XM2
      P4=P4*XM2
11    SUM=SUM+F(J-2)*(R15(J)*P0+R18(J)*P2+R21(J)*P4)+F(J-1)*(R14(J)*P0+R
     117(J)*P2+R20(J)*P4)+F(J)*(R13(J)*P0+R16(J)*P2+R19(J)*P4)
C
CC                J=I
C
      THETA=ASIN (SQRT(X(I1)/X(I)))
      CTHETA=COS (THETA)
      P0=P2=P4=(0.,0.)
      DO 12 M=1,NG
      TEMP=1.-0.25*CTHETA**2*(1.+AB(M))**2
      X0=X(I)*TEMP
      CTMP=SQRT(X(I)-X0)*KERNL(X0)*GH(M)
      P0=P0+CTMP
      P2=P2+CTMP*TEMP
12    P4=P4+CTMP*TEMP**2
      P0=P0*CTHETA*SQRT(X(I))
      P2=P2*CTHETA*SQRT(X(I))**3
      P4=P4*CTHETA*SQRT(X(I))**5
      F(I)=(F(I)-ALAMZ*(SUM+F(I-2)*(R15(I)*P0+R18(I)*P2+R21(I)*P4)+F(I1)
     1*(R14(I)*P0+R17(I)*P2+R20(I)*P4)))/(1.+ALAMZ*(R13(I)*P0+R16(I)*P2+
     2R19(I)*P4))
13    AMP=CABS(F(I))
      PHA=CANG(F(I))
      FF=(1.+(0.,1.)*DELTA*WAVE*HAR)*F(I)
      RR1=CABS(FF)
      RR2=20.*ALOG10(WAVE*X(I)/RR1)
      BTL=RR2
      FLDS(I)=139.37+20.*ALOG10(FREQ)-RR2
      DMI=X(I)*.00062137
      DKM(I)=X(I)*.001
      TIME=SECOND(DUM)-TO
      ZFT=(X(I)*X(I)*1.E-3/(2.*AKM)+HA+REFEL+H)*3.2808
      PRINT 22, X(I),H,ZFT,COND,EPS,AMP,PHA,TIME,DMI,FLDS(I),BTL
14    CONTINUE
      DO 16 I=1,NGC
16    DX(I)=DX(I)/1000.


C
      GO TO 4
C
```

```
18     FORMAT (*0NUMBER OF DISTANCES < 4*)
19     FORMAT (5F10.5,2I2,F10.0)
20     FORMAT (*0FREQUENCY =*,F10.2,10X,A8,*AL POLARIZATION*,8X,*EARTH RA
      CDIUS =*F8.0,* KM*/
      C1X,*TRANSMITTER ANTENNA HEIGHT =*F7.3,* METERS*,10X,*RECEIVER ANTE
      CNNA HEIGHT =*F7.3,* METERS*//
      39X,*X*,10X,*Z*,9X,*HT*,5X,*CONDUCTIVITY*,3X,*DIELECTRIC*,15X,*F(X)
      4*,22X,*TIMING*,4X,*FIELD STRENGTH*,2X,*BTL*/
      58X,*(M)*,8X,*(M)*,8X,*FT*,8X,*(MHO/M)*,6X,*CONSTANT*,8X,*MAG*,
      613X,*ARG*,16X,*(SEC)*,5X,*M I*,3X,*   (DBU)*)
22     FORMAT (*0*,F12.2,F10.1,F10.1,F14.6,F13.4,E18.8,E16.8,F15.3,F7.1,
      12F8.2)
       END
```

```
       COMPLEX FUNCTION KERNL(X0)
       COMMON/1/ HA,AKM
       COMMON /2/ D,H,HP
       COMMON /3/ DELTAR,WAVE
       COMMON /4/ FREQ,POL
       COMMON /5/ NG,AB(48),GH(48)
       COMMON /6/ NX,X(2001),I
       COMPLEX FEWH,DELTA,DELTAR,ETA,ETAR
       CALL TERRANE (X0,H0,HP0,ETA,DELTA,ETAR,DELTAR,COND,EPS)
       XMS=X(I)-X0
       HD=H-H0
       R1=SQRT(X0**2+HA**2)
       RW=WAVE*(X0+((H0**2)/(2.*X0))+XMS+((HD**2)/(2.*XMS))-D)
       KERNL=CMPLX(COS (RW),-SIN (RW))*SQRT(X(I)/(R1*XMS))*((HP0+DELTA-DE
      1LTAR)*FEWH(HD,XMS)-(HD/XMS))
       RETURN
       END
```

```
       COMPLEX FUNCTIONFEWH(HD,XD)
       COMMON /3/ DELTAR,WAVE
       COMPLEX TEMP,Q,Z,Z2,ZZ,HWERF,WERFZ,WERF,ZWERF,DELTAR
       TEMP=(0.7071067812,-0.7071067812)*SQRT(.5*WAVE)
       XD2=SQRT(XD)
       Q=-TEMP*HD/XD2
       Z=TEMP*DELTAR*XD2+Q
       ZZ=-Z
       ZI=AIMAG(ZZ)
       IF (ZI.LT.0..OR.(ABS(REAL(ZZ)).LT.6..AND.ZI.LT.6.)) GO TO 1
       Z2=ZZ**2
       HWERF=(Z2-2.)/(ZZ*(Z2-3.5))
       GO TO 2
1      WERFZ=WERF(ZZ)
       HWERF=ZZ-0.5*WERFZ/(ZZ*WERFZ+(0.,-0.56418958))
2      ZWERF=Z+HWERF
       FEWH=(Q*ZWERF-0.5)/(Z*ZWERF-0.5)
       RETURN
       END
```

```
      SUBROUTINE DISTX
C          SUBROUTINE TO FILL DISTANCE ARRAY.  USE EITHER SPECIFIC
C          DISTANCES (KIND = 1) OR COMPUTE DISTANCES AT EQUIDISTANT
C          POINTS (KIND = 0).  A COMBINATION OF THE TWO KINDS CAN BE
C          USED.  ALL VARIABLES ARE READ IN IN KILOMETERS AND THE
C          DISTANCE ARRAY IS FILLED IN METERS.
      COMMON /6/ N,X(2001),INDEX
      DIMENSION DEP(50),FINT(50)
      N=2
      READ 100, KIND,TD
      TDM=TD*1.E+3
      IF (EOF(60)) 8,2
2     IF (KIND) 4,12
4     DO 6 L=N,2001,8
      K=L+7
      READ 101, (X(I), I=L,K)
      DO 6 J=1,8
      N=L+J-1
      IF (X(N) .LE. 0.) GO TO 10
      X(N)=X(N)*1.E+3
6     CONTINUE
7     PRINT 102
8     CALL EXIT
10    IF (X(N-1) .LT. TDM) GO TO 12
      N=N-1
      RETURN
12    READ 103, NED,(DEP(I),FINT(I), I=1,NED)
      DO 20 I=1,NED
      DEPM=DEP(I)*1.E+3
      FINTM=FINT(I)*1.E+3
      SV=.1*FINTM
      DO 14 J=N,2001
      JS=J
      X(J)=FINTM+X(J-1)
      IF (X(J) .GE. (TDM-SV)) GO TO 16
      IF (X(J) .GE. (DEPM-SV)) GO TO 18
14    CONTINUE
      GO TO 7
16    X(JS)=TDM
      N=JS
      RETURN
18    X(JS)=DEPM
      N=JS+1
20    CONTINUE
      GO TO 4
100   FORMAT (I10,F10.0)
101   FORMAT (8F10.5)
102   FORMAT (*0NUMBER OF DISTANCES EXCEEDS DIMENSION*)
103   FORMAT (I2/(8F10.0))
      END
```

```
      COMPLEX FUNCTIONWERF(ZZZ)
      COMPLEX Z,ZZZ,ZV,V,Z2,C,W,S
      DIMENSION C(12), W(5,4)
      EQUIVALENCE (S,C(12))
      LOGICAL LZ2
      DATA (C(1)=(.0,-.5641895835))
      DATA (((W(I,J),I=1,5),J=1,4)=(1.,,0),
     X (3.67879441171442 3E-01,6.0 7157705841393 7E-01),
     X (1.83156388873418E-02,3.40026217066066 2E-01),
     X (1.23409804086678 8E-04,2.01157317037600 4E-01),
     X (1.12535174719264 6E-07,1.45953589900152 8E-01),
     X (4.27583576155807 0E-01,0.00000000000000 0E+00),
     X (3.04744205256912 6E-01,2.08218938202831 6E-01),
     X (1.40239581366277 9E-01,2.22213440179899 1E-01),
     X (6.53177772890469 7E-02,1.73918315416349 0E-01),
     X (3.62814564899886 4E-02,1.35838951000655 1E-01),
     X (2.55395676310505 8E-01,0.00000000000000 0E+00),
     X (2.18492615274890 7E-01,9.29978093926018 6E-02),
     X (1.47952759512015 8E-01,1.31179717084217 8E-01),
     X (9.27107664264433 2E-02,1.28316962228261 5E-01),
     X (5.96869296104459 0E-02,1.13210056124488 2E-01),
     X (1.79001151181393 0E-01,0.00000000000000 0E+00),
     X (1.64261136392986 1E-01,5.01971351352496 6E-02),
     X (1.30757469669852 2E-01,8.11126504774547 2E-02),
     X (9.64025055830443 9E-02,9.12363260042125 8E-02),
     X (6.97909616496475 0E-02,8.93400002403646 1E-02))
      XX=REAL(ZZZ)
      YY=AIMAG(ZZZ)
      X=ABS (XX)
      Y=ABS (YY)
      Z=CMPLX(X,Y)
      LZ2=.FALSE.
      IF (X.GE.4.5.OR.Y.GE.3.5) GO TO 6
      I=X+.5
      J=Y+.5
      V=CMPLX(FLOAT(I),FLOAT(J))
      ZV=Z-V
      C(2)=W(I+1,J+1)
      AI=0.
      DO 1 I=3,12
      AI=AI-.5
      C(I)=(V*C(I-1)+C(I-2))/AI
1     CONTINUE
      J=12
      DO 2 I=2,11
      J=J-1
2     S=S*ZV+C(J)
3     IF (YY.GE.0.) GO TO 4
      IF (.NOT.LZ2) Z2=Z*Z
      S=2.*CEXP(-Z2)-S
      IF (XX.GT.0.) S=CONJG(S)
      GO TO 5
4     IF (XX.LT.0.) S=CONJG(S)
5     WERF=S
      RETURN
6     LZ2=.TRUE.
      Z2=Z*Z
      S=Z*((0.,0.4613135279)/(Z2-0.1901635092)+(0.,0.099992161 68)/
     1(Z2-1.7844927485)+(0.,0.002883938748)/(Z2-5.525343743 79))
      GO TO 3
      END
```

ADJUSTED PATH PROFILE FOLLOWS

	D IN METERS	HT IN METERS
1	0.00000	0.00000
2	885.11500	-8.53440
3	1617.34650	-13.71600
4	1673.67200	-11.58240
5	2092.09000	-11.58240
6	5045.15550	12.80160
7	5246.31800	12.80160
8	5423.34100	15.84960
9	6533.75800	37.18560
10	7290.12900	53.34000
11	7721.42140	75.59040
12	7917.75600	128.62560
13	8046.50000	130.45440
14	8199.38350	125.57760
15	8690.22000	92.04960
16	8835.05700	95.09760
17	9100.59150	103.63200
18	9198.75880	100.58400
19	9659.01860	128.62560
20	10219.05500	135.33120
21	10363.89200	134.72160
22	10870.82150	95.09760
23	11031.75150	63.39840
24	11152.44900	98.14560
25	11400.28120	143.86560
26	11852.49450	147.82800
27	12391.61000	140.81760
28	12785.88850	98.14560
29	12954.86500	94.48800
30	13209.13440	80.46720
31	13389.37600	101.19360
32	13493.98050	102.71760
33	13582.49200	91.74480
34	13679.05000	99.97440
35	13791.70100	105.15600
36	13896.30550	96.62160
37	14274.49100	140.81760
38	14523.93250	105.15600
39	14918.21100	165.20160
40	15119.37350	165.20160
41	15248.11750	149.96160
42	15344.67550	149.96160
43	15529.74500	128.62560
44	16374.62750	100.88880
45	17332.16100	100.88880
46	17380.44000	98.14560
47	17460.90500	98.14560
48	17670.11400	107.28960
49	17959.78800	116.43360
50	18185.09000	116.43360
51	19311.60000	92.04960

BOULDER TO S.E. (DAVIDSON MESA)
NUMBER OF PROFILE DATA POINTS IS 51
REFERENCE ELEVATION IS 1608.73 METERS
PATH PROFILE AS PUT IN FOLLOWS

0.00000	5278.0	.55000	5250.0	1.00500	5233.0	1.04000	5240.0
1.30000	5240.0	3.13500	5320.0	3.26000	5320.0	3.37000	5330.0
4.06000	5400.0	4.53000	5453.0	4.79800	5526.0	4.92000	5700.0
5.00000	5706.0	5.09500	5690.0	5.40000	5580.0	5.49000	5590.0
5.65500	5618.0	5.71600	5608.0	6.00200	5700.0	6.35000	5722.0
6.44000	5720.0	6.75500	5590.0	6.85500	5486.0	6.93000	5600.0
7.08400	5750.0	7.36500	5763.0	7.70000	5740.0	7.94500	5600.0
8.05000	5588.0	8.20800	5542.0	8.32000	5610.0	8.38500	5615.0
8.44000	5579.0	8.50000	5606.0	8.57000	5623.0	8.63500	5595.0
8.87000	5740.0	9.02500	5623.0	9.27000	5820.0	9.39500	5820.0
9.47500	5770.0	9.53500	5770.0	9.65000	5700.0	10.17500	5609.0
10.77000	5609.0	10.80000	5600.0	10.85000	5600.0	10.98000	5630.0
11.16000	5660.0	11.30000	5660.0	12.00000	5580.0		

```
      SUBROUTINE IN(N)
      COMMON /INPUT/X(5000), Z(5000), A(120), B(120), AA(40), AB(40), ID
     1(8),REFEL
      COMMON /GCX/ NGC,DX(50),ETAX(50),DELTAX(50),SIGX(50),EPSX(50)
      COMMON/4/ FREQ,POL
      COMPLEX ETAX,DELTAX
C
CC    INPUT
C
CC    ID = ICENTIFICATION
CC    N = NUMBER OF DATA POINTS
CC    IXUNITS =0, DISTANCES INPUT IN KILOMETERS
CC    IXUNITS =1, DISTANCES INPUT IN MILES
CC    IZUNITS = 0, HEIGHTS INPUT IN METERS
CC    IZUNITS = 1, HEIGHTS INPUT IN FEET
C     REFEL = REFERENCE ELEVATION IN METERS
1502  FORMAT (8A10)
1503  FORMAT (2X,8A10)
1504  FORMAT  (4(F10.5,F10.1))
1505  FORMAT (4(F10.2,F10.0))
1506  FORMAT  (10X,I10,2F15.5)
1510  FORMAT (3I10,F10.1)
1511  FORMAT (2X,*NUMBER OF PROFILE DATA POINTS IS*I10/
     C2X,*REFERENCE ELEVATION IS*F10.2,* METERS*/
     C2X,*PATH PROFILE AS PUT IN FOLLOWS*/)
1512  FORMAT (//* THE NUMBER OF SCALED DATA POINTS HAS EXCEEDED 5000 OR
     1THE NUMBER OF GROUND CONSTANT PAIRS HAS EXCEEDED 50*)
1513  FORMAT (*0ADJUSTED PATH PROFILE FOLLOWS*/23X,* D IN METERS*,3X,
     1*HT IN METERS*)
1514  FORMAT  (1H1)
1515  FORMAT (*0*I2,* DISTANCE AND GROUND CONSTANT PAIRS FOLLOW*/
     111X,*D IN KM*,3X,*SIGMA*,2X,*EPSILON*/
     C(10X,F8.3,F8.4,F9.0))
1516  FORMAT (4(F7.0,F7.4,F6.0))
      FTOM = .3048
      EP = - 5
      Z0 = 1.E-3
      READ 1502, ID
      PRINT 1514
      PRINT 1503, ID
      READ 1510, N,IXUNITS,IZUNITS,REFEL
      IF (IZUNITS .EQ. 1) REFEL=REFEL*FTOM
      IF (N .GT. 5000) GO TO 110
      PRINT 1511, N,REFEL
      READ 1505, (X(I),Z(I), I=1,N)
      PRINT 1504, (X(I), Z(I), I = 1, N)
      IF (N .LT. 1) GO TO 120
      PRINT 1513
      XCONST=1000.
      IF (IXUNITS .EQ. 1) XCONST=1609.3
      ZCONST=1.
      IF (IZUNITS .EQ. 1) ZCONST=FTOM
      DO 105 I = 1, N
      Z(I)=Z(I)*ZCONST-REFEL
      X(I)=X(I)*XCONST
      PRINT 1506, I, X(I), Z(I)
 105  CONTINUE
 120  CONTINUE
      READ 1510, NGC
      IF (NGC .GT. 50) GO TO 110
      READ 1516, (DX(I),SIGX(I),EPSX(I), I=1,NGC)
      PRINT 1515, NGC,(DX(I),SIGX(I),EPSX(I), I=1,NGC)
      DO 130 I=1,NGC
      ETAX(I)=CMPLX(EPSX(I),-17975.*SIGX(I)/FREQ)
      DELTAX(I)=CSQRT(ETAX(I)-1.)
      IF (POL .EQ. 1.) DELTAX(I)=DELTAX(I)/ETAX(I)
130   DX(I)=DX(I)*1000.
      RETURN
 110  CONTINUE
      PRINT 1512
      END
```

```
      SUBROUTINE TERRANE (X,H,HP,ETA,DELTA,ETAR,DELTAR,COND,EPS)
C           SUBROUTINE FOR WAGNER.   DEFINES TERRAIN.
C       SMOOTH SPHERE
      COMMON/INPUT/ TD(5000),THT(5000)
      COMMON /GCX/ NGC,DX(50),ETAX(50),DELTAX(50),SIGX(50),EPSX(50)
      COMMON /TEST2/ SXMIN(100),SXMAX(100)
      COMMON /TERMA/ ICOUNT,X0(100),AN(100),ALPHA(100)
      COMMON/1/ HA,AKM
      COMPLEX ETAX,DELTAX,ETAR,DELTAR,ETA,DELTA
C
C        COMPUTE HEIGHT,SLOPE,CONDUCTIVITY AND DIELECTRIC CONSTANT AT X
7     CONTINUE
      IF (X .GT. TD(N)) X=TD(N)
      A=1000.*AKM
      HP=-X/A
      H=.5*X*HP-HA
      DO 6 I=2,N
      IF (X .GT. TD(I)) GO TO 6
      H=H+THT(I-1)+((X-TD(I-1))/(TD(I)-TD(I-1)))*(THT(I)-THT(I-1))
      HP=HP+(THT(I)-THT(I-1))/(TD(I)-TD(I-1))
      GO TO 9
6     CONTINUE
9     CONTINUE
      DO 2 I=1,50
      IF (X .LE. (DX(I)+.0001)) GO TO 4
2     CONTINUE
4     ETA=ETAX(I)
      DELTA=DELTAX(I)
      COND=SIGX(I)
      EPS=EPSX(I)
      RETURN
      ENTRY TERRAN2
      CALL IN(N)
      ETAR=ETAX(1)
      DELTAR=DELTAX(1)
      GO TO 7
      END
```

1 DISTANCE AND GROUND CONSTANT PAIRS FOLLOW

D IN KM	SIGMA	EPSILON
19.320	.0150	15.

FREQUENCY = 1.49 VERTICAL POLARIZATION EARTH RADIUS = 8500. KM
TRANSMITTER ANTENNA HEIGHT = 45.800 METERS RECEIVER ANTENNA HEIGHT = 6.000 METERS

X (M)	Z (M)	HT FT	CONDUCTIVITY (MHO/M)	DIELECTRIC CONSTANT	F(X) MAG	F(X) ARG	TIMING (SEC)	FIELD STRENGTH MI	FIELD STRENGTH (DBU)	BTL
100.00	-46.8	5274.8	.015000	15.0000	.95756708E+00	-.94645555E-01	.153	.1	132.48	10.35
200.00	-47.7	5271.6	.015000	15.0000	.94279026E+00	-.15583449E+00	.158	.1	126.33	16.50
300.00	-48.7	5268.4	.015000	15.0000	.93238668E+00	-.20385909E+00	.164	.2	122.71	20.12
400.00	-49.7	5265.3	.015000	15.0000	.92377247E+00	-.24450719E+00	.169	.2	120.13	22.70
500.00	-50.6	5262.1	.015000	15.0000	.91613104E+00	-.28027497E+00	.174	.3	118.12	24.71
600.00	-51.6	5259.0	.015000	15.0000	.91339139E+00	-.32187617E+00	.215	.4	116.51	26.32
700.00	-52.6	5255.8	.015000	15.0000	.90767002E+00	-.35311718E+00	.261	.4	115.12	27.72
800.00	-53.6	5252.6	.015000	15.0000	.90227283E+00	-.38219743E+00	.315	.5	113.91	28.93
900.00	-54.5	5249.6	.015000	15.0000	.89800930E+00	-.40852044E+00	.372	.6	112.84	29.99
1000.00	-55.2	5247.3	.015000	15.0000	.89434598E+00	-.43288575E+00	.427	.6	111.89	30.94
1100.00	-55.9	5244.9	.015000	15.0000	.89012764E+00	-.45677281E+00	.501	.7	111.02	31.81
1200.00	-56.6	5242.6	.015000	15.0000	.88584348E+00	-.47976593E+00	.574	.7	110.22	32.61
1300.00	-57.4	5240.3	.015000	15.0000	.88157101E+00	-.50189017E+00	.649	.8	109.49	33.35
1400.00	-58.1	5238.0	.015000	15.0000	.87733580E+00	-.52320986E+00	.734	.9	108.80	34.03
1500.00	-58.8	5235.7	.015000	15.0000	.87314729E+00	-.54379204E+00	.825	.9	108.16	34.67
1600.00	-59.5	5233.3	.015000	15.0000	.86900763E+00	-.56370025E+00	.920	1.0	107.56	35.27
1700.00	-57.6	5239.9	.015000	15.0000	.88645129E+00	-.55880726E+00	1.020	1.1	107.21	35.63
1800.00	-57.6	5239.9	.015000	15.0000	.87413320E+00	-.58556519E+00	1.128	1.1	106.59	36.25
1900.00	-57.6	5239.9	.015000	15.0000	.86949036E+00	-.60438860E+00	1.245	1.2	106.07	36.76
2000.00	-57.6	5239.9	.015000	15.0000	.86545442E+00	-.62207709E+00	1.363	1.2	105.59	37.25
2100.00	-57.6	5240.2	.015000	15.0000	.86304316E+00	-.63736481E+00	1.488	1.3	105.14	37.70
2200.00	-56.8	5242.9	.015000	15.0000	.86437172E+00	-.64759220E+00	1.616	1.4	104.75	38.09
2300.00	-56.0	5245.6	.015000	15.0000	.86285470E+00	-.66085001E+00	1.748	1.4	104.35	38.49
2400.00	-55.2	5248.3	.015000	15.0000	.86067900E+00	-.67458127E+00	1.895	1.5	103.95	38.88
2500.00	-54.4	5251.0	.015000	15.0000	.85816499E+00	-.68841967E+00	2.044	1.6	103.57	39.26

2600.00	-53.6	5253.7	.015000	15.0000	.85544078E+00	-.70222787E+00	2.195	1.6	103.21	39.63
2700.00	-52.8	5256.4	.015000	15.0000	.85257383E+00	-.71594038E+00	2.350	1.7	102.85	39.98
2800.00	-52.0	5259.1	.015000	15.0000	.84960510E+00	-.72952251E+00	2.514	1.7	102.50	40.33
2900.00	-51.2	5261.8	.015000	15.0000	.84656175E+00	-.74295511E+00	2.681	1.8	102.17	40.67
3000.00	-50.4	5264.5	.015000	15.0000	.84346287E+00	-.75622773E+00	2.850	1.9	101.84	40.99
3100.00	-49.6	5267.2	.015000	15.0000	.84032247E+00	-.76933511E+00	3.022	1.9	101.52	41.31
3200.00	-48.8	5269.9	.015000	15.0000	.83715111E+00	-.78227523E+00	3.206	2.0	101.21	41.62
3300.00	-48.0	5272.7	.015000	15.0000	.83395700E+00	-.79504817E+00	3.404	2.1	100.91	41.92
3400.00	-47.3	5275.4	.015000	15.0000	.83074658E+00	-.80765534E+00	3.603	2.1	100.62	42.21
3500.00	-46.5	5278.1	.015000	15.0000	.82752502E+00	-.82009906E+00	3.819	2.2	100.34	42.50
3600.00	-45.7	5280.8	.015000	15.0000	.82429651E+00	-.83238222E+00	4.034	2.2	100.06	42.78
3700.00	-44.9	5283.5	.015000	15.0000	.82106447E+00	-.84450809E+00	4.252	2.3	99.78	43.05
3800.00	-44.1	5286.2	.015000	15.0000	.81783174E+00	-.85648016E+00	4.483	2.4	99.52	43.31
3900.00	-43.3	5288.9	.015000	15.0000	.81460066E+00	-.86830204E+00	4.722	2.4	99.26	43.57
4000.00	-42.6	5291.6	.015000	15.0000	.81137320E+00	-.87997739E+00	4.964	2.5	99.00	43.83
4100.00	-41.8	5294.3	.015000	15.0000	.80815101E+00	-.89150986E+00	5.212	2.5	98.76	44.08
4200.00	-41.0	5297.0	.015000	15.0000	.80493548E+00	-.90290308E+00	5.470	2.6	98.51	44.32
4300.00	-40.2	5299.7	.015000	15.0000	.80172779E+00	-.91416062E+00	5.718	2.7	98.27	44.56
4400.00	-39.5	5302.5	.015000	15.0000	.79852895E+00	-.92528595E+00	5.971	2.7	98.04	44.80
4500.00	-38.7	5305.2	.015000	15.0000	.79533980E+00	-.93628247E+00	6.237	2.8	97.81	45.03
4600.00	-37.9	5307.9	.015000	15.0000	.79216107E+00	-.94715348E+00	6.507	2.9	97.58	45.25
4700.00	-37.1	5310.6	.015000	15.0000	.78899338E+00	-.95790218E+00	6.791	2.9	97.36	45.47
4800.00	-36.4	5313.3	.015000	15.0000	.78583725E+00	-.96853166E+00	7.074	3.0	97.14	45.69
4900.00	-35.6	5316.0	.015000	15.0000	.78269313E+00	-.97904492E+00	7.366	3.0	96.93	45.90
5000.00	-34.8	5318.7	.015000	15.0000	.77956141E+00	-.98944485E+00	7.667	3.1	96.72	46.11
5100.00	-34.5	5319.9	.015000	15.0000	.77129129E+00	-.10067421E+01	7.978	3.2	96.45	46.38
5200.00	-34.6	5319.9	.015000	15.0000	.76650198E+00	-.10202821E+01	8.307	3.2	96.23	46.60
5300.00	-33.7	5323.0	.015000	15.0000	.77207371E+00	-.10191661E+01	8.615	3.3	96.13	46.70
5400.00	-32.1	5328.6	.015000	15.0000	.77130113E+00	-.10244636E+01	8.939	3.4	95.96	46.88

5500.00	-30.3	5334.8	.015000	15.0000	.77210049E+00	-.10283088E+01	9.278	3.4	95.81	47.03
5600.00	-28.4	5341.1	.015000	15.0000	.77160151E+00	-.10338492E+01	9.607	3.5	95.65	47.19
5700.00	-26.5	5347.4	.015000	15.0000	.77040008E+00	-.10402422E+01	9.943	3.5	95.48	47.36
5800.00	-24.7	5353.7	.015000	15.0000	.76886458E+00	-.10470407E+01	10.283	3.6	95.31	47.52
5900.00	-22.8	5360.0	.015000	15.0000	.76710254E+00	-.10540982E+01	10.631	3.7	95.14	47.69
6000.00	-21.0	5366.3	.015000	15.0000	.76517606E+00	-.10613300E+01	10.994	3.7	94.97	47.86
6100.00	-19.1	5372.6	.015000	15.0000	.76312491E+00	-.10686818E+01	11.353	3.8	94.81	48.03
6200.00	-17.3	5378.9	.015000	15.0000	.76097632E+00	-.10761168E+01	11.711	3.9	94.64	48.19
6300.00	-15.4	5385.2	.015000	15.0000	.75874994E+00	-.10836086E+01	12.096	3.9	94.48	48.36
6400.00	-13.6	5391.5	.015000	15.0000	.75646043E+00	-.10911377E+01	12.495	4.0	94.31	48.52
6500.00	-11.7	5397.8	.015000	15.0000	.75411911E+00	-.10986893E+01	12.879	4.0	94.15	48.68
6600.00	-9.8	5404.6	.015000	15.0000	.75284124E+00	-.11046127E+01	13.275	4.1	94.00	48.83
6700.00	-7.7	5411.6	.015000	15.0000	.75118738E+00	-.11110230E+01	13.665	4.2	93.85	48.98
6800.00	-5.6	5418.6	.015000	15.0000	.74915473E+00	-.11178563E+01	14.071	4.2	93.70	49.13
6900.00	-3.6	5425.6	.015000	15.0000	.74700006E+00	-.11248154E+01	14.478	4.3	93.55	49.28
7000.00	-1.5	5432.6	.015000	15.0000	.74476560E+00	-.11318433E+01	14.877	4.3	93.40	49.43
7100.00	.5	5439.6	.015000	15.0000	.74247308E+00	-.11389108E+01	15.308	4.4	93.25	49.58
7200.00	2.6	5446.6	.015000	15.0000	.74013592E+00	-.11460000E+01	15.740	4.5	93.10	49.73
7300.00	4.9	5454.6	.015000	15.0000	.74342757E+00	-.11450462E+01	16.170	4.5	93.02	49.81
7400.00	10.0	5471.5	.015000	15.0000	.75671995E+00	-.11293030E+01	16.611	4.6	93.06	49.78
7500.00	15.1	5488.5	.015000	15.0000	.76164404E+00	-.11249129E+01	17.048	4.7	93.00	49.84
7600.00	20.1	5505.4	.015000	15.0000	.76449450E+00	-.11233491E+01	17.499	4.7	92.91	49.92
7700.00	25.2	5522.3	.015000	15.0000	.76623259E+00	-.11232917E+01	17.981	4.8	92.82	50.01
7800.00	47.4	5595.6	.015000	15.0000	.91675554E+00	-.97624953E+00	18.468	4.8	94.26	48.57
7900.00	74.4	5684.2	.015000	15.0000	.97680880E+00	-.93564700E+00	18.925	4.9	94.71	48.13
8000.00	80.2	5703.8	.015000	15.0000	.82579187E+00	-.10853206E+01	19.387	5.0	93.14	49.70
8100.00	79.1	5700.3	.015000	15.0000	.76934993E+00	-.11518593E+01	19.882	5.0	92.41	50.42
8200.00	75.8	5689.8	.015000	15.0000	.73671488E+00	-.12008081E+01	20.371	5.1	91.93	50.90
8300.00	68.9	5667.4	.015000	15.0000	.68999117E+00	-.12820878E+01	20.847	5.2	91.26	51.58
8400.00	61.9	5645.0	.015000	15.0000	.66415643E+00	-.13360839E+01	21.352	5.2	90.82	52.01

8500.00	55.0	5622.6	.015000	15.0000	.64435374E+00	-.13823602E+01	21.836	5.3	90.46	52.38
8600.00	48.1	5600.2	.015000	15.0000	.62810068E+00	-.14239253E+01	22.345	5.3	90.13	52.70
8700.00	42.0	5580.6	.015000	15.0000	.62819893E+00	-.14362545E+01	22.887	5.4	90.03	52.80
8800.00	44.0	5587.5	.015000	15.0000	.65530870E+00	-.13872433E+01	23.440	5.5	90.30	52.53
8900.00	46.7	5596.8	.015000	15.0000	.66758202E+00	-.13637027E+01	23.967	5.5	90.36	52.47
9000.00	49.8	5607.3	.015000	15.0000	.67430175E+00	-.13502801E+01	24.532	5.6	90.35	52.48
9100.00	52.9	5617.9	.015000	15.0000	.67747167E+00	-.13430412E+01	25.069	5.7	90.30	52.54
9200.00	49.9	5608.2	.015000	15.0000	.64630760E+00	-.13978511E+01	25.628	5.7	89.79	53.04
9300.00	55.9	5628.2	.015000	15.0000	.68442181E+00	-.13350493E+01	26.172	5.8	90.20	52.64
9400.00	61.8	5648.2	.015000	15.0000	.69489619E+00	-.13165227E+01	26.736	5.8	90.24	52.60
9500.00	67.8	5668.1	.015000	15.0000	.70122613E+00	-.13048481E+01	27.305	5.9	90.22	52.61
9600.00	73.8	5688.1	.015000	15.0000	.70551642E+00	-.12966229E+01	27.872	6.0	90.19	52.65
9700.00	77.8	5701.5	.015000	15.0000	.68824375E+00	-.13207305E+01	28.457	6.0	89.88	52.95
9800.00	78.9	5705.5	.015000	15.0000	.67362354E+00	-.13439386E+01	29.041	6.1	89.61	53.23
9900.00	79.9	5709.4	.015000	15.0000	.66588278E+00	-.13578996E+01	29.637	6.2	89.42	53.42
10000.00	81.0	5713.3	.015000	15.0000	.65994386E+00	-.13694405E+01	30.266	6.2	89.25	53.58
10100.00	82.1	5717.3	.015000	15.0000	.65493545E+00	-.13797468E+01	30.890	6.3	89.10	53.73
10200.00	83.2	5721.2	.015000	15.0000	.65049383E+00	-.13893047E+01	31.520	6.3	88.95	53.88
10300.00	82.9	5720.8	.015000	15.0000	.63756912E+00	-.14141394E+01	32.148	6.4	88.70	54.14
10400.00	79.7	5710.7	.015000	15.0000	.60661946E+00	-.14760945E+01	32.786	6.5	88.18	54.65
10500.00	71.8	5685.0	.015000	15.0000	.57705755E+00	-.15485786E+01	33.396	6.5	87.66	55.17
10600.00	63.9	5659.4	.015000	15.0000	.55942110E+00	-.16011956E+01	34.017	6.6	87.31	55.52
10700.00	55.9	5633.7	.015000	15.0000	.54560230E+00	-.16469400E+01	34.643	6.6	87.01	55.82
10800.00	48.0	5608.1	.015000	15.0000	.53399371E+00	-.16884998E+01	35.283	6.7	86.74	56.09
10900.00	36.6	5571.1	.015000	15.0000	.49836122E+00	-.17945700E+01	35.925	6.8	86.06	56.77
11000.00	16.7	5506.5	.015000	15.0000	.45675478E+00	-.19568510E+01	36.582	6.8	85.23	57.61
11100.00	30.0	5550.4	.015000	15.0000	.60721581E+00	-.16383810E+01	37.241	6.9	87.62	55.21
11200.00	53.7	5628.7	.015000	15.0000	.67209473E+00	-.15243834E+01	37.909	7.0	88.43	54.41
11300.00	72.1	5689.2	.015000	15.0000	.69701707E+00	-.14564319E+01	38.591	7.0	88.66	54.17
11400.00	90.4	5749.8	.015000	15.0000	.72077172E+00	-.14035918E+01	39.303	7.1	88.88	53.95

14500.00	50.4	5634.2	.015000	15.0000	.44316065E+00	-.20073215E+01	64.178	9.0	82.57	60.27
14600.00	58.4	5660.9	.015000	15.0000	.53285673E+00	-.18031575E+01	65.116	9.1	84.11	58.73
14700.00	73.5	5710.9	.015000	15.0000	.58170077E+00	-.17098563E+01	66.059	9.1	84.81	58.02
14800.00	88.5	5760.9	.015000	15.0000	.60337610E+00	-.16533234E+01	67.020	9.2	85.07	57.77
14900.00	103.6	5810.8	.015000	15.0000	.61912353E+00	-.16226232E+01	67.976	9.3	85.23	57.60
15000.00	106.2	5819.9	.015000	15.0000	.55517741E+00	-.17159675E+01	68.955	9.3	84.23	58.61
15100.00	106.0	5819.9	.015000	15.0000	.53980183E+00	-.17380105E+01	69.999	9.4	83.93	58.91
15200.00	96.3	5788.6	.015000	15.0000	.47741008E+00	-.18826187E+01	71.060	9.4	82.80	60.03
15300.00	90.4	5769.9	.015000	15.0000	.49461464E+00	-.18566340E+01	72.092	9.5	83.05	59.78
15400.00	83.8	5749.0	.015000	15.0000	.44601608E+00	-.19672979E+01	73.139	9.6	82.10	60.74
15500.00	72.1	5711.2	.015000	15.0000	.43165893E+00	-.20321646E+01	74.186	9.6	81.76	61.08
15600.00	66.2	5692.4	.015000	15.0000	.44188008E+00	-.20150633E+01	75.216	9.7	81.90	60.93
15700.00	62.7	5681.6	.015000	15.0000	.44550369E+00	-.20100308E+01	76.268	9.8	81.92	60.91
15800.00	59.3	5670.8	.015000	15.0000	.44348974E+00	-.20172939E+01	77.327	9.8	81.83	61.01
15900.00	55.8	5660.1	.015000	15.0000	.44074444E+00	-.20270714E+01	78.348	9.9	81.72	61.12
16000.00	52.3	5649.3	.015000	15.0000	.43774913E+00	-.20379752E+01	79.345	9.9	81.60	61.23
16100.00	48.9	5638.5	.015000	15.0000	.43468441E+00	-.20494234E+01	80.350	10.0	81.49	61.35
16200.00	45.4	5627.7	.015000	15.0000	.43162843E+00	-.20611289E+01	81.361	10.1	81.37	61.46
16300.00	41.9	5617.0	.015000	15.0000	.42861701E+00	-.20729362E+01	82.403	10.1	81.26	61.57
16400.00	39.3	5608.9	.015000	15.0000	.43069675E+00	-.20701367E+01	83.428	10.2	81.25	61.59
16500.00	39.1	5608.9	.015000	15.0000	.43646949E+00	-.20548269E+01	84.441	10.3	81.31	61.52
16600.00	38.9	5608.9	.015000	15.0000	.43814361E+00	-.20492396E+01	85.450	10.3	81.29	61.54
16700.00	38.7	5608.9	.015000	15.0000	.43869085E+00	-.20465681E+01	86.495	10.4	81.25	61.58
16800.00	38.5	5608.9	.015000	15.0000	.43865298E+00	-.20454947E+01	87.519	10.4	81.20	61.64
16900.00	38.3	5608.9	.015000	15.0000	.43825398E+00	-.20454603E+01	88.592	10.5	81.14	61.70
17000.00	38.1	5608.9	.015000	15.0000	.43761115E+00	-.20461632E+01	89.676	10.6	81.07	61.76
17100.00	37.9	5608.9	.015000	15.0000	.43679435E+00	-.20474182E+01	90.812	10.6	81.01	61.83
17200.00	37.7	5608.9	.015000	15.0000	.43584872E+00	-.20491018E+01	91.960	10.7	80.94	61.90
17300.00	37.5	5608.9	.015000	15.0000	.43480510E+00	-.20511271E+01	93.080	10.7	80.87	61.97
17400.00	34.5	5599.9	.015000	15.0000	.42893334E+00	-.20711092E+01	94.183	10.8	80.70	62.14

11500.00	91.2	5752.8	.015000	15.0000	.63409268E+00	-.15059253E+01	39.988	7.1	87.69	55.14
11600.00	91.9	5755.7	.015000	15.0000	.61507718E+00	-.15249655E+01	40.697	7.2	87.35	55.48
11700.00	92.6	5758.5	.015000	15.0000	.60419586E+00	-.15366078E+01	41.409	7.3	87.12	55.71
11800.00	93.4	5761.4	.015000	15.0000	.59662999E+00	-.15457102E+01	42.116	7.3	86.94	55.90
11900.00	93.1	5760.9	.015000	15.0000	.58192368E+00	-.15703709E+01	42.851	7.4	86.65	56.19
12000.00	91.6	5756.6	.015000	15.0000	.57142468E+00	-.15912147E+01	43.592	7.5	86.42	56.42
12100.00	90.2	5752.4	.015000	15.0000	.56401120E+00	-.16075461E+01	44.336	7.5	86.23	56.60
12200.00	88.8	5748.1	.015000	15.0000	.55781377E+00	-.16222196E+01	45.064	7.6	86.06	56.77
12300.00	87.3	5743.8	.015000	15.0000	.55238785E+00	-.16358615E+01	45.782	7.6	85.91	56.93
12400.00	85.1	5737.0	.015000	15.0000	.53641632E+00	-.16716802E+01	46.551	7.7	85.58	57.25
12500.00	74.1	5701.4	.015000	15.0000	.49661133E+00	-.17812016E+01	47.311	7.8	84.84	57.99
12600.00	63.1	5665.9	.015000	15.0000	.47715123E+00	-.18519526E+01	48.072	7.8	84.43	58.41
12700.00	52.2	5630.4	.015000	15.0000	.46260250E+00	-.19126164E+01	48.836	7.9	84.09	58.74
12800.00	42.4	5598.9	.015000	15.0000	.46522600E+00	-.19304934E+01	49.629	8.0	84.07	58.76
12900.00	40.1	5591.8	.015000	15.0000	.47987819E+00	-.18965917E+01	50.430	8.0	84.27	58.56
13000.00	36.3	5579.8	.015000	15.0000	.47271444E+00	-.19152656E+01	51.199	8.1	84.07	58.76
13100.00	30.6	5561.7	.015000	15.0000	.46598385E+00	-.19395135E+01	51.984	8.1	83.88	58.95
13200.00	24.9	5543.6	.015000	15.0000	.46128831E+00	-.19599496E+01	52.767	8.2	83.73	59.10
13300.00	34.7	5576.2	.015000	15.0000	.52595444E+00	-.18096914E+01	53.552	8.3	84.80	58.03
13400.00	45.0	5610.4	.015000	15.0000	.54324818E+00	-.17671388E+01	54.373	8.3	85.02	57.81
13500.00	45.5	5612.5	.015000	15.0000	.51363890E+00	-.18151229E+01	55.184	8.4	84.47	58.37
13600.00	36.6	5583.8	.015000	15.0000	.50505737E+00	-.18459625E+01	56.018	8.5	84.26	58.58
13700.00	44.1	5609.1	.015000	15.0000	.52886281E+00	-.17855831E+01	56.854	8.5	84.59	58.24
13800.00	47.5	5620.7	.015000	15.0000	.51897365E+00	-.17981924E+01	57.727	8.6	84.37	58.47
13900.00	39.9	5596.3	.015000	15.0000	.50232221E+00	-.18438343E+01	58.621	8.6	84.02	58.81
14000.00	51.4	5634.7	.015000	15.0000	.55545274E+00	-.17313966E+01	59.531	8.7	84.83	58.00
14100.00	62.9	5673.0	.015000	15.0000	.57626560E+00	-.16862446E+01	60.452	8.8	85.09	57.74
14200.00	74.5	5711.4	.015000	15.0000	.59023836E+00	-.16543930E+01	61.376	8.8	85.24	57.60
14300.00	79.3	5728.0	.015000	15.0000	.54731819E+00	-.17281418E+01	62.315	8.9	84.52	58.31
14400.00	64.9	5681.1	.015000	15.0000	.47491568E+00	-.19006080E+01	63.229	8.9	83.23	59.61

17500.00	36.0	5605.5	.015000	15.0000	.43984776E+00	-.20416220E+01	95.308	10.9	80.87	61.97
17600.00	40.2	5619.9	.015000	15.0000	.44958367E+00	-.20140424E+01	96.453	10.9	81.01	61.83
17700.00	44.0	5633.0	.015000	15.0000	.45207744E+00	-.20032183E+01	97.565	11.0	81.01	61.83
17800.00	47.0	5643.4	.015000	15.0000	.45215430E+00	-.19984860E+01	98.719	11.1	80.96	61.88
17900.00	49.9	5653.7	.015000	15.0000	.45282595E+00	-.19928185E+01	99.916	11.1	80.92	61.91
18000.00	51.6	5659.9	.015000	15.0000	.44506234E+00	-.20075702E+01	101.068	11.2	80.72	62.11
18100.00	51.4	5659.9	.015000	15.0000	.43827815E+00	-.20227858E+01	102.210	11.2	80.54	62.29
18200.00	50.8	5658.9	.015000	15.0000	.43085762E+00	-.20405858E+01	103.357	11.3	80.35	62.49
18300.00	48.4	5651.8	.015000	15.0000	.42229378E+00	-.20649814E+01	104.527	11.4	80.12	62.71
18400.00	46.1	5644.7	.015000	15.0000	.41691939E+00	-.20819894E+01	105.678	11.4	79.97	62.87
18500.00	43.7	5637.6	.015000	15.0000	.41257422E+00	-.20966043E+01	106.814	11.5	79.83	63.01
18600.00	41.3	5630.5	.015000	15.0000	.40881506E+00	-.21098432E+01	107.958	11.6	79.70	63.13
18700.00	38.9	5623.4	.015000	15.0000	.40544527E+00	-.21221549E+01	109.136	11.6	79.58	63.25
18800.00	36.5	5616.3	.015000	15.0000	.40235635E+00	-.21337865E+01	110.318	11.7	79.47	63.36
18900.00	34.1	5609.2	.015000	15.0000	.39948110E+00	-.21448907E+01	111.542	11.7	79.36	63.47
19000.00	31.8	5602.1	.015000	15.0000	.39677468E+00	-.21555699E+01	112.813	11.8	79.26	63.58
19100.00	29.4	5595.0	.015000	15.0000	.39420555E+00	-.21658962E+01	114.051	11.9	79.16	63.68
19200.00	27.0	5587.9	.015000	15.0000	.39175066E+00	-.21759224E+01	115.251	11.9	79.06	63.78
19300.00	24.6	5580.8	.015000	15.0000	.38939259E+00	-.21856888E+01	116.454	12.0	78.96	63.88
19311.60	24.3	5579.9	.015000	15.0000	.38912471E+00	-.21868064E+01	117.707	12.0	78.95	63.89

APPENDIX B2

INPUT, LISTING AND SAMPLE OUTPUT FOR PROGRAM INTEQ 7/24/78

Card 1: LBL (8A10)
LBL = path label

Card 2: NPF, IXU, IZU (3I10)
NPF = number of points on terrain profile
IXU = 0, distance input in kilometers
1, distance input in miles
IZU = 0, height input in meters
1, height input in feet

Cards 3 to M: (PFX(J), PFZ(J), j=1,NPF) (4(F10.2,F10.0)) limited to 500 points
PFX(J) = terrain distances in IXU
PFZ(J) = terrain heights in IZU

Card M+1: HTA, HTB, FMHZ, EN0, IPOL (4F10.0,I3)
HTA = transmitter antenna height in meters
HTB = receiver antenna height in meters
FMHZ = frequency in megahertz
EN0 = N$_0$
IPOL= polarization; 1 vertical; 0 horizontal

Card M+2: NGC (I10)
NGC = number of sets of DX, SIG, EP

Cards M+3 to N: (DX(J), SIG(J), EP(J), J=1,NGC) (4(F7.0,F7.4,F6.0)) limited to 50 sets
DX(J) = maximum distance in kilometers for given sigma and epsilon
SIG(J) = sigma
EP(J) = epsilon

```
      PROGRAM INTEQ(INPUT,OUTPUT)
      COMMON/FIELDD/XI,HTA,D,HTB,F,FIELD,XINTZ,XINTP,NLIMIT
        COMPLEX FIELD
      COMMON /PROFILE/ GE,NPF,PFX(500),PFZ(500)
      COMMON /HEAD/ LBL(8)

      DATA(NLIMIT=200)
      DATA(XZ0=0.5),(XXZ=10.),(NP0=4)
      ADB(Z)=-4.342944819*ALOG(REAL(Z)**2+AIMAG(Z)**2)

      XI=100.
1     CONTINUE
      CALL FILL PF
      PRINT 4, LBL
4     FORMAT (1H1,8A10)
      TLF=20.*ALOG10(F)
      F=F*1.E06
      TO=SECOND(DUM)
      XINTZ=AMAX1(XZ0*XI,XXZ)
      NN=(D-XINTZ)/XI
      XINTZ=D-NN*XI
      XINTP=XINTZ+NP0*XI
      CALL SETFLD
      DD = D
      D=XINTP
2     CALL FIELDS
      DKM=D/1000.
      TIME=SECOND(DUM)-TO
      ATT=ADB(FIELD)
      IF (ATT .LT. -10.) GO TO 1
      ALB=ATT+32.45+20.*ALOG10(DKM)+TLF
      FLDS=139.37+TLF-ALB
      PRINT 5, DKM,ATT,ALB,FLDS,TIME
5     FORMAT (1X,*DKM=*F8.2,*  ADB=*F8.2,*  LB=*F8.2,*  FLDS=*F8.2,
     C*  TIME=*F8.2)
      D=D+XI
      IF (D .LE. DD) GO TO 2
      GO TO 1
      END
```

```
      SUBROUTINE ADVFLD
C
      COMMON/FIELDD/XI,XMTRHT,DIST,RCVRHT,FREQ,FIELD,XINTZ,XINTP,NLIMIT
      COMMON/FLD1/N,FN,XZ,NP,DZTAZ,DZTA(1000)
      COMMON/FLD2/KB2,HT,RTXI,DZTA2,ZTAZ,ZTA(1000),PHIZ,PHI(1000),SECZ,
     X   SEC(1000),RT(1000)
      REAL KB2
      COMMON/FLD3/GAMMA,UZ,U(1000),LDUZ,LDU(1000)
      COMPLEX GAMMA,UZ,U,LDUZ,LDU
      LOGICAL CSGDIF
      COMMON/FLD5/ZR,SQA(2),SQE(2)
      COMPLEX G,DG,PRF,DPRF,Q,QQ,QTEMP
      COMPLEX ZR,FIELD
      COMPLEX CIS,CEXP,CLOG,IGG,IGGI,IGGH,DLTA
      DIMENSION QTEMP(3)
      DATA (ZR=(0.,0.))
      DATA (SQA=.908248291,.09175170),(SQE=.275255128,2.72474487)
C                         HEREWITH IS N ADVANCED
      N=N+1
      FN=FN+1.
      CALL ZETA
      ZTA(N)=ZTA(N-1)+.5*(DZTA(N-1)+DZTA(N))
      TEMP=.5*DZTA(N)*DZTA(N)
      PHI(N)=PHI(N-1)+TEMP+DZTA2
      DZTA2=TEMP
      SEC(N)=1.+DZTA2
      RT(N)=SQRT(FN)
11000                     CONTINUE
C                         BEGINNING THE COMPUTATIONS FOR U(N)
      ZTABR=ZTA(N)
      DZTABR=DZTA(N)
      PHIBR=PHI(N)
12000                     CONTINUE
C                         AT S=0
      Y=FN+XZ
      RTX=SQRT(Y)
      EEZTA=ZTABR-HT
      DDZTA=EEZTA/Y
      TAUX=DZTABR-DDZTA
      TEMP=.5/Y
      PRF=CIS(KB2*(EEZTA*DDZTA-PHIBR))/(RTX*RTXI)
      DPRF=CMPLX(TEMP,KB2*TAUX*TAUX)*PRF
      EEZTA=ZTABR
      DDZTA=EEZTA/Y
      TAU=DZTAZ-DDZTA
      TAUX=DZTABR-DDZTA
      QTEMP(1)=DLTA(0)+TAU
      QTEMP(2)=CMPLX(TEMP,KB2*TAUX*TAUX)
      Q=CMPLX(0.,KB2*TAU*TAU*Y/FN)
13000                     CONTINUE
C                         AT S=X(0)
      Y=FN
      EEZTA=ZTABR-ZTAZ
      DDZTA=EEZTA/Y
      TAU=DZTAZ-DDZTA
      TAUX=DZTABR-DDZTA
      TEMP=.5/Y
      QTEMP(3)=DLTA(0)+TAU
      Q=Q+CLOG(QTEMP(3)/QTEMP(1)*RTX/RT(N))/XZ
      QQ=(SECZ/RT(N))*QTEMP(3)*CIS(KB2*(EEZTA*DDZTA-PHIBR+PHIZ))*UZ
      B=KB2*TAUX*TAUX
      G=IGGI(Q)
      DG=IGGI(Q+CLOG(CMPLX(TEMP,B)/QTEMP(2))/XZ)*CMPLX(TEMP,B)
      Q=CMPLX(0.,KB2*TAU*TAU)+LDUZ
      DO 13001 K=1,2
      TEMP=SQE(K)/Y
      QTEMP(3)=SQA(K)*IGGH(Q+TEMP)
      G=G+QTEMP(3)
      DG=DG+QTEMP(3)*CMPLX(TEMP,B)
13001 CONTINUE
```

```
      G=G*QQ
      DG=-DG*QQ
14000                 CONTINUE
C                     ITERATING WITH S=X(J), FOR J=1...N-2
      J=0
      NJ=N
14010 J=J+1
      NJ=NJ-1
      Y=Y-1.
      IF(NJ.LE.1) GO TO 15000
      EEZTA=ZTABR-ZTA(J)
      DDZTA=EEZTA/Y
      TAU=DZTA(J)-DDZTA
      TAUX=DZTABR-DDZTA
      QQ=(SEC(J)/RT(NJ))*CIS(KB2*(EEZTA*DDZTA-PHIBR+PHI(J)))*
     1     (DLTA(J)+TAU)*U(J)
      Q=CMPLX(0.,KB2*TAU*TAU)+LDU(J)
      B=KB2*TAUX*TAUX
      QTEMP(1)=ZR
      QTEMP(2)=ZR
      DO 14011 K=1,2
      TEMP=SQE(K)/Y
      QTEMP(3)=SQA(K)*IGG(Q+TEMP)
      QTEMP(1)=QTEMP(1)+QTEMP(3)
      QTEMP(2)=QTEMP(2)+QTEMP(3)*CMPLX(TEMP,B)
14011 CONTINUE
      G=G+QTEMP(1)*QQ
      DG=DG-QTEMP(2)*QQ
      GO TO 14010
15000                 CONTINUE
C                     AT S=X(N-1)
      TAU=.5*(DZTA(N-1)-DZTA(N))
      TEMP=KB2*TAU*TAU
      QQ=SEC(N-1)*(DLTA(N-1)+TAU)*CIS(-TEMP)*U(N-1)
      CALL IGGPU(CMPLX(0.,TEMP)+LDU(N-1),QTEMP)
      QTEMP(1)=QTEMP(1)*QQ
      G=G+QTEMP(1)
      DG=DG+QTEMP(1)*LDU(N-1)-QQ*QTEMP(2)
16000                 CONTINUE
C                     AT S=X(N)
      CALL IGGF(PRF-GAMMA*G,-DPRF-GAMMA*DG,2./(GAMMA*DLTA(N)*SEC(N)),
     1     U(N),LDU(N))
      RETURN
      END
```

```
      COMPLEX FUNCTION WERF(ZZZ)
      COMPLEX Z,ZZZ,ZV,V,Z2,C,W,S
      DIMENSION C(12),W(5,4)
      EQUIVALENCE (S,C(12))
      DATA (C(1) = (.0,-.5641895835))
      DATA (((W(I,J),I=1,5),J=1,4)=(1.,.0),
     X (3.67879441171442 3E-01,6.071577058413937E-01),
     X (1.831563888873418E-02,3.400262170660662E-01),
     X (1.234098040866788E-04,2.011573170376004E-01),
     X (1.125351747192646E-07,1.459535899001528E-01),
     X (4.275835761558070E-01,0.000000000000000E+00),
     X (3.047442052569126E-01,2.082189382028316E-01),
     X (1.402395813662779E-01,2.221344017989 91E-01),
     X (6.531777728904697E-02,1.739183154163490E-01),
     X (3.628145648998864E-02,1.358389510006551E-01),
     X (2.553956763105058E-01,0.000000000000000E+00),
     X (2.184926152748907E-01,9.299780939260186E-02),
     X (1.479527595120158E-01,1.311797170842178E-01),
     X (9.271076642644332E-02,1.283169622282615E-01),
     X (5.968692961044590E-02,1.132100561244882E-01),
     X (1.790011511813930E-01,0.000000000000000E+00),
     X (1.642611363929861E-01,5.019713513524966E-02),
     X (1.307574696698522E-01,8.111265047745472E-02),
     X (9.640250558304439E-02,9.123632600421258E-02),
     X (6.979096164964750E-02,8.934000024036461E-02))
      XX=REAL(ZZZ)
      YY=AIMAG(ZZZ)
      X=ABS (XX)
      Y=ABS (YY)
      Z=CMPLX(X,Y)
      LZ2=0
      IF(X.GE.4.5.OR.Y.GE.3.5) GO TO 100
      I=X+.5
      J=Y+.5
      V=CMPLX(FLOAT (I),FLOAT(J))
      ZV=Z-V
      C(2)=W(I+1,J+1)
      AI=0.
      DO 10 I=3,12
      AI=AI-.5
      C(I)=(V*C(I-1)+C(I-2))/AI
   10 CONTINUE
      J=12
      DO 11 I=2,11
      J=J-1
   11 S=S*ZV+C(J)
   20 IF(YY.GE.0.) GO TO 30
      IF(LZ2) 22,21
   21 Z2 = Z*Z
   22 S=2.*CEXP(-Z2)-S
      IF(XX.GT.0.) S=CONJG(S)
      GO TO 200
   30 IF(XX.LT.0.) S=CONJG(S)
  200 WERF=S
      RETURN
  100 LZ2=1
      Z2=Z*Z
      S = Z*((0.,0.4613135279)/(Z2 - 0.1901635092) + (0.,0.09999216168)/
     X(Z2 - 1.7844927485) + (0.,0.002883938748)/(Z2 - 5.525334374379))
      GO TO 20
         END
```

```
      SUBROUTINE FIELDS
      COMMON/FIELDD/XI,XMTRHT,DIST,RCVRHT,FREQ,G,XINTZ,XINTP,NLIMIT
      COMMON/FLD1/N,FN,XZ,NP,DZTAZ,DZTA(1000)
      COMMON/FLD2/KB2,HT,RTXI,DZTA2,ZTAZ,ZTA(1000),PHIZ,PHI(1000),SECZ,
     X   SEC(1000),RT(1000)
      REAL KB2
      COMMON/FLD3/GAMMA,UZ,U(1000),LDUZ,LDU(1000)
      COMPLEX GAMMA,UZ,U,LDUZ,LDU
      COMMON/FLD5/ZR,SQA(2),SQE(2)
      COMPLEX ZR,G,PRF,Q,QQ,QTEMP
      COMPLEX CIS,IGG,IGGI,IGGH,DLTA
      DIMENSION QTEMP(3)
C                          THE RECOMMENCEMENT
      FNX=NX=(DIST-XINTZ)/XI+0.5
52    FORMAT (*0 SYSTEM 52 ERROR*)
20000 IF(NX.LE.N) GO TO 20001
      CALL ADVFLD $ GO TO 20000
20001 CONTINUE
      Y=FNX+XZ
      X=Y*XI
      DIST=X
      Z=RCVRHT/XI
      IF(Z.LT.0.) Z=0.
21000                      CONTINUE
C                          BEGINNING THE COMPUTATIONS FOR W
      ZTABR=ZTA(NX)+Z
      DZTABR=DZTA(NX)
      PHIBR=PHI(NX)
22000                      CONTINUE
C                          AT S=0
      RTX=SQRT(Y)
      EEZTA=ZTABR-HT
      DDZTA=EEZTA/Y
      PRF=CIS(KB2*(EEZTA*DDZTA-PHIBR))/(RTX*RTXI)
      IF(Z.EQ.0) GO TO 26007
      EEZTA=ZTABR
      DDZTA=EEZTA/Y
      TAU=DZTAZ-DDZTA
      QTEMP(1)=DLTA(0)+TAU
      Q=CMPLX(0.,KB2*TAU*TAU*Y/FNX)
23000                      CONTINUE
C                          AT S=X(0)
      Y=FNX
      EEZTA=ZTABR-ZTAZ
      DDZTA=EEZTA/Y
      TAU=DZTAZ-DDZTA
      QTEMP(3)=DLTA(0)+TAU
      Q=Q+CLOG(QTEMP(3)/QTEMP(1)*RTX/RT(NX))/XZ
      QQ=(SECZ/RT(NX))*QTEMP(3)*CIS(KB2*(EEZTA*DDZTA-PHIBR+PHIZ))*UZ
      G=IGGI(Q)
      Q=CMPLX(0.,KB2*TAU*TAU)+LDUZ
      DO 23001 K=1,2
      G=G+SQA(K)*IGGH(Q+SQE(K)/Y)
23001 CONTINUE
      G=G*QQ
24000                      CONTINUE
C                          ITERATING WITH S=X(J), FOR J=1...NX-2
      J=0
      NJ=NX
24010 J=J+1
      NJ=NJ-1
      Y=Y-1.
      IF(NJ.LE.1) GO TO 25000
      EEZTA=ZTABR-ZTA(J)
      DDZTA=EEZTA/Y
      TAU=DZTA(J)-DDZTA
      QQ=(SEC(J)/RT(NJ))*CIS(KB2*(EEZTA*DDZTA-PHIBR+PHI(J)))*(DLTA(J)+TA
     1U)*U(J)
      Q=CMPLX(0.,KB2*TAU*TAU)+LDU(J)
      QTEMP(1)=ZR
```

```
      DO 24011 K=1,2
      QTEMP(1)=QTEMP(1)+SQA(K)*IGG(Q+SQE(K)/Y)
24011 CONTINUE
      G=G+QTEMP(1)*QQ
      GO TO 24010
25000                 CONTINUE
C                     AT S=X(NX-1)
      TEMPA=KB2*Z*Z
      QTEMP(3)=CIS(KB2*2.*DZTABR*Z)
      TAU=.5*(DZTA(NX-1)-DZTA(NX))
      TEMP=KB2*TAU*(TAU-Z-Z)
      QQ=SEC(NX-1)*CIS(-TEMP)*QTEMP(3)*U(NX-1)
      CALL IGZPU(TEMPA,CMPLX(0.,TEMP)+LDU(NX-1),QTEMP)
      G=G+((DLTA(NX-1)+TAU)*QTEMP(1)-Z*QTEMP(2))*QQ
26000                 CONTINUE
C                     AT S=X(NX)
      QQ=SEC(NX)*QTEMP(3)*U(NX)
      CALL IGZU(TEMPA,LDU(NX),QTEMP)
      G=G+(DLTA(NX)*QTEMP(1)-Z*QTEMP(2))*QQ
      G=PRF-GAMMA*G
26008 G=G/PRF
      RETURN
26007 G=2.*U(NX) $ GO TO 26008
      END
```

```
      SUBROUTINE SETFLD
C
      COMMON/FIELDD/XI,XMTRHT,DIST,RCVRHT,FREQ,FIELD,XINTZ,XINTP,NLIMIT
      COMMON/FLD1/N,FN,XZ,NP,DZTAZ,DZTA(1000)
      COMMON/FLD2/KB2,HT,RTXI,DZTA2,ZTAZ,ZTA(1000),PHIZ,PHI(1000),SECZ,
     X   SEC(1000),RT(1000)
      REAL KB2
      COMMON/FLD3/GAMMA,UZ,U(1000),LDUZ,LDU(1000)
      COMPLEX GAMMA,UZ,U,LDUZ,LDU
      COMMON/FLD4/GZCF,BWBG,ABG,BPE,BPE2,RTXZ
      COMPLEX GZCF,BWBG,ABG,BPE,BPE2
      COMPLEX APE,Q1,Q2,Q3,Q4,Q5,Q6,DLTA
      COMPLEX WERF,HWERF,CIS,FIELD
8000  CONTINUE
      HT=XMTRHT/XI
      KB2=FREQ*XI/.953688E8
      XZ=XINTZ/XI
      IF(XZ.LE.0.) XZ=4.
      RTXZ=SQRT(XZ)
      RTXI=SQRT(XI)
      NP=MAX1(1.,XINTP/XI-XZ+.5)
      IF (NP .GT. NLIMIT) PRINT 52
52    FORMAT (*0 SYSTEM 52 ERROR*)
      N=0
      FN=0.
      CALL SETZTA
      ZTAZ=DZTAZ*XZ
      DZTA2=.5*DZTAZ*DZTAZ
      SECZ=1.+DZTA2
      PHIZ=2.*(DZTA2*XZ-DZTAZ*HT)
      T1=SQRT(.5*KB2)
      T2=T1*HT
      APE=CMPLX(T2,T2)
      T2=.56418958*T1
      GAMMA=CMPLX(T2,-T2)
      T2=SECZ*T1
      CALL SETDLTA(0)
      BPE=CMPLX(T2,T2)*DLTA(0)
      BPE2=BPE*BPE
      ABG=APE/RTXZ
      BWBG=BPE*WERF(ABG+BPE*RTXZ)
      T3=KB2*HT*HT
      Q6=2.*APE*BPE
9000  CONTINUE
C                    COMPUTE PLANE EARTH U(N)
      GO TO 9002
9001  N=N+1
      FN=FN+1.
      DZTA(N)=DZTAZ
      ZTA(N)=ZTA(N-1)+DZTAZ
      SEC(N)=SECZ
      PHI(N)=PHI(N-1)+DZTA2+DZTA2
      RT(N)=SQRT(FN)
9002  Y=FN+XZ
      T1=SQRT(Y)
      T2=T3/Y
      Q1=APE/T1
      Q2=BPE*T1
      Q3=Q1+Q2
      Q4=HWERF(Q3)
      Q5=.5/(Q3-Q4)
      U(N)=CIS(T2)/(1.+Q2/(Q1-Q5))/(T1*RTXI)
      LDU(N)=((Q6-Q2*Q4)/(1.-Q1/Q5)-CMPLX(.5,T2))/Y
9080  IF(N.LT.NP) GO TO 9001
      GZCF=CMPLX(AIMAG(CIS(T3/XZ)),-REAL(CIS(T3/XZ)))*(SECZ*1.77245385/
     X      RTXI)/UZ
      RETURN
      END
```

```
      COMPLEX FUNCTION DLTA(J)
      COMMON/FIELDD/XI,XMTRHT,DIST,RCVRHT,FREQ,FIELD,XINTZ,XINTP,NLIMIT
      COMMON /GROUND/ NGC,DX(50),EP(50),SIG(50),IPOL
      DIMENSION DELTA(50),JX(50)
      COMPLEX DELTA,ETA,FIELD
      DO 5 I=1,NGC
      IF (JX(I).GE. J) GO TO 6
5     CONTINUE
      I=NGC
6     DLTA=DELTA(I)
      RETURN
      ENTRY SETDLTA
      DO 10 I=1,NGC
      ETA=CMPLX(EP(I),SIG(I)*.1795 3E11/FREQ)
      DELTA(I)=CSQRT(ETA-1.)
      JX(I) = (DX(I) - XINTZ)/XI + 0.5
10    IF (IPOL .NE. 0) DELTA(I)=DELTA(I)/ETA
      RETURN
      END
```

```
      SUBROUTINE BINET(XX,ALPHA,XBINET)
      COMPLEX ALPHA,XBINET
      COMPLEX A,IX,RTIX,KNL,Q,QQ,RTA,IRTPI
      COMPLEX WERF,CIS
      DIMENSION XBINET(2),KNL(8),Q(2)
      DATA (IRTPI=(0.,1.772453851))
      X=XX
      RTIX=CMPLX(SQRT (.5*X),SQRT (.5*X))
      A=ALPHA
      IF(AMAX1(ABS(REAL(A)),ABS(AIMAG(A))).GT..3542) GO TO 30
      IX=CMPLX(0.,X)
      QQ=CIS(X)
      KNL(1)=IRTPI*QQ*WERF(RTIX)/RTIX
      FK=-.5
      DO 11 K=2,8
      FK=FK+1.
11    KNL(K)=(QQ+IX*KNL(K-1))/FK
      FK=7.
      KK=8
      Q(1)=KNL(KK)
      Q(2)=KNL(KK-1)
      DO 12 K=1,6
      KK=KK-1
      FK=FK-1.
      QQ=A/FK
      Q(1)=KNL(KK)-Q(1)*QQ
12    Q(2)=KNL(KK-1)-Q(2)*QQ
      XBINET(1)=Q(1)
      XBINET(2)=Q(2)
      RETURN
30    CONTINUE
      QQ=CEXP(CMPLX(-.1207822376,X+1.570796327)-A)
      RTA=CSQRT(-A)
      Q(1)=WERF(RTIX+RTA)
      Q(2)=WERF(RTIX-RTA)
      XBINET(1)=QQ*(Q(2)-Q(1))/RTA
      XBINET(2)=QQ*(Q(2)+Q(1))/RTIX
      RETURN
      END
```

```
      SUBROUTINE ZETA
      COMMON /PROFILE/ GE,NPF,PFX(500),PFZ(500)
      COMMON/FLD1/N,FN,XZ,NP,DZTAZ,DZTA(1000)
      COMMON/FIELDD/XI,XXX(9)
      K=KA
      HZ0=HZ1     $     HZ1=0.
      IF(N-NN)10,20,30
10    B=BA        $     XB=XA=XA+XI
      U1=-XI
      GO TO 101
11    HZ1=((B*U*3.+A)*Z+(Y*B+U*A)*0.5*DZ)*V+HZ1
      IF(X1 .LT. XB)100,12
12    IF(B)40,40,13
13    B=-BA       $     KA=K      $     XB=XB+XI
      GO TO 102
20    XB=XA=PFX(NPF)
      U1=-XI*1.5
      ASSIGN 21 TO LS       $     GO TO 101
21    HZ1=((Z-PFZ(NPF))*U+Y*DZ/6.)*V*0.5+HZ1
      IF(X1 .LT. XB)100,22
22    B=HZ1*BA/0.5625
      HZ1=-B*0.5+PFZ(NPF)
      GO TO 40
30    HZ1=HZ0+B
40    DE=DE-DDE
      DZTA(N)=(HZ1-HZ0)/XI+DE
      RETURN
      ENTRY SETZTA
      K=1
      HZ0=PFZ(1)
      HZ1=U1=XA=0.
      XB=(XZ+NP+0.5)*XI
      ASSIGN 61 TO LS       $     GO TO 100
61    HZ1=((Z-PFZ(1))*U+Y*DZ/6.)*V*0.5+HZ1
      IF(X1 .LT. XB)100,62
62    XA=XB-XI*0.5
      DDE=GE*XI
      DE=((PFX(NPF)+XA**2/PFX(NPF))*0.5-XA)*GE
      HZ1=HZ1*3./XB**2
      DZTAZ=HZ1/XB+DE
      HZ1=HZ1+PFZ(1)
      XA=XB
      KA=K
      A=2./XI
      BA=A*0.25/XI
      NN=PFX(NPF)/XI-XZ-0.5
      ASSIGN 11 TO LS
      RETURN
100   CONTINUE
      IF(K .NE. NPF)110,111
111   X1=XB       $     GO TO 102
110   K=K+1
101   CONTINUE
      X1=PFX(K)
      V=X1-PFX(K-1)       $     U=X1-XA
      Z=((V-U)*PFZ(K)+U*PFZ(K-1))/V
      DZ=(PFZ(K)-PFZ(K-1))/V
102   CONTINUE
      U0=U1
      U1=AMIN1(X1,XB)-XA
      U=U1+U0       $     V=U1-U0
      Y=U*U*3.+V*V
      GO TO LS,(11,21,61)
      END
```

```
      SUBROUTINE FILL PF
      COMMON/FIELDD/XI,HTA,D,HTB,FMHZ,FLD,XINTZ,XINTP,NLIMIT
         COMPLEX FLD
      COMMON /PROFILE/ GE,NPF,PFX(500),PFZ(500)
      COMMON /GROUND/ NGC,DX(50),EP(50),SIG(50),IPOL,SF
      COMMON /HEAD/ LBL(8)
      DIMENSION LPOL(2)     $     DATA(LPOL=4HHORZ,4HVERT)
      READ 1001,LBL
      IF(EOF(5LINPUT)) 1,2
1     STOP
2     CONTINUE
      READ 1002, NPF,IXU,IZU,SF
1002  FORMAT (3I10,F10.0)
      IF (NPF .LE. 500) GO TO 3
      PRINT 1006
1006  FORMAT (///*0TROUBLE WITH ARRAY FOR PROFILE OR GROUND CONSTANTS*)
      STOP
3     CONTINUE
      READ 1004, (PFX(J),PFZ(J), J=1,NPF)
1004  FORMAT (4(F10.2,F10.0))
      XK=1000.
      IF (IXU .EQ. 1) XK=1609.3
      DO 4 I=1,NPF
4      PFX(I)=PFX(I)*XK
      IF (IZU .EQ. 0) GO TO 7
      DO 6 I=1,NPF
6     PFZ(I)=PFZ(I)*.3048
7     CONTINUE
      READ 1003,HTA,HTB,FMHZ,ENO,IPOL
      READ 1002, NGC
      IF (NGC .LE. 50) GO TO 9
      PRINT 1006
      STOP
9     CONTINUE
      READ 1005, (DX(I), SIG(I),EP(I), I=1,NGC)
1005  FORMAT (4(F7.0,F7.4,F6.0))
      DO 8 I=1,NGC
8     DX(I)=DX(I)*1000.
      D=PFX(NPF)
      ANT=(PFZ(1)+PFZ(NPF))/2.
      ENS=ENO*EXP(-1.057E-04*ANT)
      GE=(1.-0.04665*EXP(0.005577*ENS))/6370.E03
      IF(ENO .EQ. 0.)     GE=0.
      RETURN
1001  FORMAT (8A10)
1003  FORMAT (4F10.0,I3)
      END
```

```
      COMPLEX FUNCTION CIS(X)
      CIS=CMPLX(COS(X),SIN(X))
      RETURN
      END
```

```
      INTEGER FUNCTION CSGDIF(Z1,Z2)
      COMPLEX Z1,Z2
      ABN(Z)=ABS (REAL(Z))+ABS (AIMAG(Z))
      CSGDIF=1
      IF(ABN(Z1-Z2) .LE. ABN(Z2)*0.5E-08)      CSGDIF=0
      RETURN
      END
```

```
      COMPLEX FUNCTION IGG(ALPHA)
      COMPLEX ALPHA
      COMPLEX A,IPI,PSINH
      DIMENSION A(3)
      DATA (IPI=(0.,3.141592654)),(SQPI=9.869604401)
      A(1)=ALPHA
      A(2)=A(1)-IPI
      A(3)=A(1)+IPI
      T=AIMAG(A(1))
      IF(T.GT.2.) GO TO 2
      IF(T.LT.-2.) GO TO 3
1     IGG=SQPI*PSINH(A(1))/(A(2)*A(3))
      RETURN
2     IGG=-SQPI*PSINH(A(2))/(A(3)*A(1))
      RETURN
3     IGG=-SQPI*PSINH(A(3))/(A(1)*A(2))
      RETURN
      END
```

```
      COMPLEX FUNCTION IGGH(ALPHA)
      COMPLEX ALPHA
      COMPLEX A,B,IPI,PSINH
      DIMENSION A(3)
      DATA (IPI=(0.,3.141592654)),(SQPIB2=4.934802201)
      A(1)=ALPHA
      A(2)=A(1)-IPI
      A(3)=A(1)+IPI
      T=AIMAG(A(1))
      IF(T.GT.2.) GO TO 2
      IF(T.LT.-2.) GO TO 3
1     B=.5*A(1)
      IGGH=(SQPIB2*CEXP(B)*PSINH(B)-A(1))/(A(2)*A(3))
      RETURN
2     B=.5*A(2)
      IGGH=-(SQPIB2*CEXP(B)*PSINH(B)/A(3)+1.)/A(1)
      RETURN
3     B=.5*A(3)
      IGGH=-(SQPIB2*CEXP(B)*PSINH(B)/A(2)+1.)/A(1)
      RETURN
      END
```

```
      COMPLEX FUNCTION IGGI(ALPHA)
      COMPLEX ALPHA,WERF
      COMMON/FLD4/GZCF,BWBG,ABG,BPE,BPE2,RTXZ
      COMPLEX GZCF,BWBG,ABG,BPE,BPE2
      COMPLEX A,AA,AAX
      A=ALPHA
      AA=CSQRT(A)
      AAX=AA*RTXZ
      IGGI=GZCF*(BWBG/(BPE2-A)-.5*(WERF(ABG+AAX)/(BPE-AA)+WERF(ABG-AAX)/
     X    (BPE+AA)))
      RETURN
      END
```

```
      SUBROUTINE IGGPU(ALPHA,XIGGPU)
      COMPLEX ALPHA,XIGGPU
      COMPLEX SHERF
      COMPLEX A,B,Q,ITPI,IHPI
      DIMENSION XIGGPU(2),Q(3)
      DATA (ITPI=(0.,6.283195307)),(IHPI=(0.,1.570796327))
      A=ALPHA
      B=A+A
      A=.7071067812*CEXP(-A)
      Q(1)=SHERF(B)
      Q(2)=SHERF(B+ITPI)
      Q(3)=SHERF(B-ITPI)
      XIGGPU(1)=A*(Q(1)-0.5*(Q(2)+Q(3)))
      XIGGPU(2)=IHPI*A*(Q(2)-Q(3))
      RETURN
      END
```

```
      SUBROUTINE IGGU(ALPHA,XIGGU)
      COMPLEX ALPHA,XIGGU(4)
      COMPLEX A,Q(6)
      COMPLEX IPI,IHPI
      DATA (IPI=(0.,3.141592654)),(IHPI=(0.,1.570796327))
      A=ALPHA
      CALL SHERFP(A,Q(1))
      CALL SHERFP(A+IPI,Q(3))
      CALL SHERFP(A-IPI,Q(5))
      XIGGU(1)=Q(1)-0.5*(Q(3)+Q(5))
      XIGGU(2)=IHPI*(Q(5)-Q(3))
      XIGGU(3)=Q(2)-0.5*(Q(4)+Q(6))
      XIGGU(4)=IHPI*(Q(6)-Q(4))
      RETURN
      END
```

```
      SUBROUTINE IGGF(AA,BB,CC,U,LDU)
      COMPLEX AA,BB,CC,U,LDU
      COMPLEX A,C,D,Z1,Z2,W,DW,GD,XG(4),Q(3)
      DATA(E=1.E-04),(R0=3.),(KT0=100)
      ABN(Z)=ABS (REAL(Z))+ABS (AIMAG(Z))
      A=AA     $     C=CC
      KT=0
      Z1=D=BB/A
      IF(REAL(Z1) .LT. -20.)      Z1=CMPLX(-20.,AIMAG(Z1))
      TA=1.     $     TB=2.
      R2=1.E300
100   KT=KT+1   $  IF (KT .EQ. KT0) PRINT 52
52    FORMAT (*0 SYSTEM 52 ERROR*)
      CALL IGGU(Z1,XG)
      Q(1)=CEXP(-Z1*0.5)
      Q(2)=C/Q(1)
      Q(3)=XG(1)*Q(1)+Q(2)
      W=(Z1-D)*Q(3)+XG(2)*Q(1)
      R1=ABN(W)
      IF(R1*TB .LE. R2)102,101
101   TA=TA*0.5
      TB=EXP(TA*0.693)
      GO TO 108
102   Z2=Z1
      R2=R1
      DW=(Z1-D)*(XG(3)*Q(1)+Q(2))+XG(4)*Q(1)-W*0.5+Q(3)
      GD=W/DW
      T=ABN(GD)
      IF(T .LE. (ABN(Z1)+0.01)*E)      GO TO 110
      IF(TA-1.)103,106,104
103   IF(TA-0.5)105,104,104
104   TA=1.     $     TB=2.     $     GO TO 106
105   TA=TA*2.
      TB=EXP(TA*0.693)
106   IF(T*TA .LE. R0)108,107
107   TA=R0/T
      TB=EXP(TA*0.693)
108   Z1=Z2-GD*TA
      GO TO 100
110   LDU=Z1=Z2-GD
      CALL IGGU(Z1,XG)
      U=A/(XG(1)/(CEXP(Z1)*C)+1.)
      RETURN
      END
```

```
      SUBROUTINE IGZPU(X,ALPHA,XIGZPU)
      COMPLEX ALPHA,XIGZPU
      COMPLEX A,B,Q1,Q2,Q3,ITPI
      DIMENSION XIGZPU(2),Q1(2),Q2(2),Q3(2)
      DATA (ITPI=(0.,6.283185308))
      Y=.5*X
      A=ALPHA
      B=A+A
      A=CEXP(A)*.7071067812
      CALL BINET(Y,B,Q1)
      CALL BINET(Y,B+ITPI,Q2)
      CALL BINET(Y,B-ITPI,Q3)
      XIGZPU(1)=A*(Q1(1)-.5*(Q2(1)+Q3(1)))
      XIGZPU(2)=.5*A*(Q1(2)-.5*(Q2(2)+Q3(2)))
      RETURN
      END
```

```
      SUBROUTINE IGZU(X,ALPHA,XIGZU)
      COMPLEX ALPHA,XIGZU
      COMPLEX A,Q1,Q2,Q3,IPI
      DIMENSION XIGZU(2),Q1(2),Q2(2),Q3(2)
      DATA (IPI=(0.,3.141592654))
      Y=X
      A=ALPHA
      CALL BINET(Y,A,Q1)
      CALL BINET(Y,A+IPI,Q2)
      CALL BINET(Y,A-IPI,Q3)
      DO 30 K=1,2
30    XIGZU(K)=.5*Q1(K)+.25*(Q2(K)+Q3(K))
      RETURN
      END
```

```
      COMPLEX FUNCTION PSINH(ZZ)
      COMPLEX ZZ,Z,Y
      Z=ZZ
      IF(ABS(REAL(Z))+ABS(AIMAG(Z)).GT.1.) GO TO 10
      Z=Z*Z
      PSINH=1.+Z*(.16666667+Z*(.83333333E-2+Z*(.19841270E-3+
     X    Z*.27557319E-5)))
      RETURN
10    Y=CEXP(Z)
      PSINH=(Y-1./Y)/(Z+Z)
      RETURN
      END
```

```
      COMPLEX FUNCTION SHERF(ZZ)
      COMPLEX Z,ZZ,Y
      COMPLEX WERF
      DIMENSION CF(9),CFK(8)
      DATA (CF=.1485805407E-4,.1262934596E-3,.9472009472E-3,
     X   .6156806157E-2,.3386243386E-1,.1523809524,.5333333333,
     X   1.333333333,2.),(CFK=.000983,.01486,.06198,.1520,.2842,.4534,
     X   .6543,.8810)
      Z=ZZ
      T=AMAX1(ABS (REAL(Z)),ABS (AIMAG(Z)))
      DO 11 K=1,8
      IF(T.LT.CFK(K)) GO TO 12
11    CONTINUE
      Y=CSQRT(Z)
      SHERF=1.77245385*(CEXP(Z)-WERF(CMPLX(-AIMAG(Y),REAL(Y))))/Y
      RETURN
12    J=10-K
      SHERF=CMPLX(CF(J-1),0.)
      DO 13 K=J,9
13    SHERF=SHERF*Z+CF(K)
      RETURN
      END
```

```
      SUBROUTINE SHERFP(ZZ,XSH)
      COMPLEX ZZ,XSH(2)
      COMPLEX Z,Y,XS(2),WERF
      DIMENSION CF(9),CFP(9),CFK(8)
      DATA (CF=.148580540 7E-4,.1262934596E-3,.9472009472E-3,
     X    .6156806157E-2,.3386243386E-1,.1523809524,.5333333333,
     X    1.333333333,2.),(CFK=.0009683,.01486,.06198,.1520,.2842,.4534,
     X    .6543,.8810)
      DATA(CFP=.140760512E-4,.118864433E-3,.884054217E-3,
     1      .568320568E-2,.0307840308,.135449735,.457142857,
     2      1.066666667,1.333333333)
      Z=ZZ
      T=AMAX1(ABS (REAL(Z)),ABS (AIMAG(Z)))
      DO 11 K=1,8
      IF(T.LT.CFK(K)) GO TO 12
11    CONTINUE
      Y=CSQRT(Z)
      XS(1)=1.77245385*(CEXP(Z)-WERF(CMPLX(-AIMAG(Y),REAL(Y))))/Y
      XS(2)=((Z-0.5)*XS(1)+1.)/Z
      GO TO 20
12    J=10-K
      XS(1)=CMPLX(CF(J-1),0.)
      XS(2)=CMPLX(CFP(J-1),0.)
      DO 13 K=J,9
      XS(1)=XS(1)*Z+CF(K)
13    XS(2)=XS(2)*Z+CFP(K)
20    XSH(1)=XS(1)
      XSH(2)=XS(2)
      END
```

```
      COMPLEX FUNCTION HWERF(ZZ)
      COMPLEX ZZ,Z,WERF
      Z=ZZ
      IF (AIMAG(Z) .LT. 0. .OR. (ABS(REAL(Z)).LT. 6. .AND. AIMAG(Z) .LT.
     C 6.)) GO TO 10
      HWERF=1./(Z-1.5/(Z-2./Z))
      RETURN
10    HWERF=Z-.5/(Z+(0.,-.56418958)/WERF(Z))
      END
```

```
      G=G*QQ
      DG=-DG*QQ
14000                 CONTINUE
C                     ITERATING WITH S=X(J), FOR J=1...N-2
      J=0
      NJ=N
14010 J=J+1
      NJ=NJ-1
      Y=Y-1.
      IF(NJ.LE.1) GO TO 15000
      EEZTA=ZTABR-ZTA(J)
      DDZTA=EEZTA/Y
      TAU=DZTA(J)-DDZTA
      TAUX=DZTABR-DDZTA
      QQ=(SEC(J)/RT(NJ))*CIS(KB2*(EEZTA*DDZTA-PHIBR+PHI(J)))*
     1     (DLTA(J)+TAU)*U(J)
      Q=CMPLX(0.,KB2*TAU*TAU)+LDU(J)
      B=KB2*TAUX*TAUX
      QTEMP(1)=ZR
      QTEMP(2)=ZR
      DO 14011 K=1,2
      TEMP=SQE(K)/Y
      QTEMP(3)=SQA(K)*IGG(Q+TEMP)
      QTEMP(1)=QTEMP(1)+QTEMP(3)
      QTEMP(2)=QTEMP(2)+QTEMP(3)*CMPLX(TEMP,B)
14011 CONTINUE
      G=G+QTEMP(1)*QQ
      DG=DG-QTEMP(2)*QQ
      GO TO 14010
15000                 CONTINUE
C                     AT S=X(N-1)
      TAU=.5*(DZTA(N-1)-DZTA(N))
      TEMP=KB2*TAU*TAU
      QQ=SEC(N-1)*(DLTA(N-1)+TAU)*CIS(-TEMP)*U(N-1)
      CALL IGGPU(CMPLX(0.,TEMP)+LDU(N-1),QTEMP)
      QTEMP(1)=QTEMP(1)*QQ
      G=G+QTEMP(1)
      DG=DG+QTEMP(1)*LDU(N-1)-QQ*QTEMP(2)
16000                 CONTINUE
C                     AT S=X(N)
      CALL IGGF(PRF-GAMMA*G,-DPRF-GAMMA*DG,2./(GAMMA*DLTA(N)*SEC(N)),
     1     U(N),LDU(N))
      RETURN
      END
```

NEVADA, F=2.0 MHZ, HA=HAR=0., PROGRAM INTEQ

DKM=	.51	ADB=	-5.68	LB=	26.94	FLDS=	118.45	TIME=	.00
DKM=	.61	ADB=	-5.46	LB=	28.71	FLDS=	116.68	TIME=	.02
DKM=	.71	ADB=	-5.53	LB=	29.97	FLDS=	115.42	TIME=	.05
DKM=	.81	ADB=	-5.55	LB=	31.09	FLDS=	114.30	TIME=	.06
DKM=	.91	ADB=	-5.51	LB=	32.14	FLDS=	113.25	TIME=	.08
DKM=	1.01	ADB=	-5.44	LB=	33.12	FLDS=	112.27	TIME=	.10
DKM=	1.11	ADB=	-5.38	LB=	34.00	FLDS=	111.39	TIME=	.12
DKM=	1.21	ADB=	-5.25	LB=	34.88	FLDS=	110.51	TIME=	.14
DKM=	1.31	ADB=	-5.15	LB=	35.66	FLDS=	109.73	TIME=	.17
DKM=	1.41	ADB=	-5.07	LB=	36.38	FLDS=	109.01	TIME=	.19
DKM=	1.51	ADB=	-5.25	LB=	36.80	FLDS=	108.59	TIME=	.21
DKM=	1.61	ADB=	-5.24	LB=	37.37	FLDS=	108.02	TIME=	.24
DKM=	1.71	ADB=	-5.00	LB=	38.13	FLDS=	107.26	TIME=	.27
DKM=	1.81	ADB=	-4.85	LB=	38.78	FLDS=	106.62	TIME=	.29
DKM=	1.91	ADB=	-4.73	LB=	39.36	FLDS=	106.03	TIME=	.32
DKM=	2.01	ADB=	-4.82	LB=	39.71	FLDS=	105.68	TIME=	.35
DKM=	2.11	ADB=	-4.99	LB=	39.97	FLDS=	105.42	TIME=	.38
DKM=	2.21	ADB=	-5.12	LB=	40.23	FLDS=	105.16	TIME=	.41
DKM=	2.31	ADB=	-4.90	LB=	40.84	FLDS=	104.55	TIME=	.43
DKM=	2.41	ADB=	-4.40	LB=	41.71	FLDS=	103.68	TIME=	.46
DKM=	2.51	ADB=	-4.45	LB=	42.02	FLDS=	103.38	TIME=	.49
DKM=	2.61	ADB=	-4.83	LB=	41.97	FLDS=	103.42	TIME=	.52
DKM=	2.71	ADB=	-5.01	LB=	42.12	FLDS=	103.27	TIME=	.55
DKM=	2.81	ADB=	-5.11	LB=	42.33	FLDS=	103.06	TIME=	.58
DKM=	2.91	ADB=	-5.00	LB=	42.74	FLDS=	102.65	TIME=	.60
DKM=	3.01	ADB=	-4.87	LB=	43.17	FLDS=	102.22	TIME=	.63
DKM=	3.11	ADB=	-4.74	LB=	43.59	FLDS=	101.80	TIME=	.66
DKM=	3.21	ADB=	-4.62	LB=	43.98	FLDS=	101.41	TIME=	.69
DKM=	3.31	ADB=	-4.65	LB=	44.22	FLDS=	101.18	TIME=	.72
DKM=	3.41	ADB=	-4.72	LB=	44.41	FLDS=	100.98	TIME=	.75
DKM=	3.51	ADB=	-4.57	LB=	44.81	FLDS=	100.59	TIME=	.78
DKM=	3.61	ADB=	-4.41	LB=	45.21	FLDS=	100.18	TIME=	.81
DKM=	3.71	ADB=	-5.41	LB=	44.45	FLDS=	100.94	TIME=	.85
DKM=	3.81	ADB=	-6.64	LB=	43.45	FLDS=	101.94	TIME=	.88
DKM=	3.91	ADB=	-5.58	LB=	44.74	FLDS=	100.65	TIME=	.91
DKM=	4.01	ADB=	-4.48	LB=	46.05	FLDS=	99.34	TIME=	.94
DKM=	4.11	ADB=	-4.52	LB=	46.23	FLDS=	99.16	TIME=	.98
DKM=	4.21	ADB=	-4.48	LB=	46.47	FLDS=	98.92	TIME=	1.01
DKM=	4.31	ADB=	.34	LB=	51.50	FLDS=	93.89	TIME=	1.04
DKM=	4.41	ADB=	3.47	LB=	54.83	FLDS=	90.56	TIME=	1.08
DKM=	4.51	ADB=	5.13	LB=	56.68	FLDS=	88.71	TIME=	1.12
DKM=	4.61	ADB=	7.11	LB=	58.86	FLDS=	86.53	TIME=	1.16
DKM=	4.71	ADB=	8.08	LB=	60.01	FLDS=	85.38	TIME=	1.19
DKM=	4.81	ADB=	8.85	LB=	60.96	FLDS=	84.43	TIME=	1.23
DKM=	4.91	ADB=	6.93	LB=	59.23	FLDS=	86.16	TIME=	1.27
DKM=	5.01	ADB=	6.28	LB=	58.74	FLDS=	86.65	TIME=	1.32
DKM=	5.11	ADB=	5.23	LB=	57.87	FLDS=	87.52	TIME=	1.35
DKM=	5.21	ADB=	9.68	LB=	62.49	FLDS=	82.90	TIME=	1.39
DKM=	5.31	ADB=	12.65	LB=	65.62	FLDS=	79.77	TIME=	1.44
DKM=	5.41	ADB=	11.55	LB=	64.68	FLDS=	80.71	TIME=	1.48
DKM=	5.51	ADB=	15.89	LB=	69.18	FLDS=	76.21	TIME=	1.56
DKM=	5.61	ADB=	13.92	LB=	67.37	FLDS=	78.02	TIME=	1.61

DKM=	5.71	ADB=	11.49	LB=	65.09	FLDS=	80.30	TIME=	1.66
DKM=	5.81	ADB=	8.63	LB=	62.39	FLDS=	83.00	TIME=	1.70
DKM=	5.91	ADB=	8.83	LB=	62.73	FLDS=	82.66	TIME=	1.75
DKM=	6.01	ADB=	10.29	LB=	64.34	FLDS=	81.05	TIME=	1.80
DKM=	6.11	ADB=	12.08	LB=	66.27	FLDS=	79.12	TIME=	1.85
DKM=	6.21	ADB=	11.99	LB=	66.32	FLDS=	79.07	TIME=	1.89
DKM=	6.31	ADB=	11.11	LB=	65.58	FLDS=	79.81	TIME=	1.94
DKM=	6.41	ADB=	10.60	LB=	65.21	FLDS=	80.18	TIME=	2.00
DKM=	6.51	ADB=	9.11	LB=	63.85	FLDS=	81.54	TIME=	2.04
DKM=	6.61	ADB=	7.44	LB=	62.32	FLDS=	83.07	TIME=	2.09
DKM=	6.71	ADB=	8.70	LB=	63.70	FLDS=	81.69	TIME=	2.14
DKM=	6.81	ADB=	8.10	LB=	63.23	FLDS=	82.16	TIME=	2.19
DKM=	6.91	ADB=	6.62	LB=	61.88	FLDS=	83.52	TIME=	2.24
DKM=	7.01	ADB=	5.62	LB=	61.00	FLDS=	84.39	TIME=	2.29
DKM=	7.11	ADB=	4.88	LB=	60.39	FLDS=	85.00	TIME=	2.34
DKM=	7.21	ADB=	4.28	LB=	59.91	FLDS=	85.48	TIME=	2.39
DKM=	7.31	ADB=	3.89	LB=	59.64	FLDS=	85.75	TIME=	2.45
DKM=	7.41	ADB=	3.48	LB=	59.34	FLDS=	86.05	TIME=	2.49
DKM=	7.51	ADB=	3.89	LB=	59.87	FLDS=	85.52	TIME=	2.55
DKM=	7.61	ADB=	9.57	LB=	65.67	FLDS=	79.72	TIME=	2.61
DKM=	7.71	ADB=	13.32	LB=	69.53	FLDS=	75.86	TIME=	2.67
DKM=	7.81	ADB=	15.77	LB=	72.09	FLDS=	73.30	TIME=	2.73
DKM=	7.91	ADB=	16.97	LB=	73.40	FLDS=	71.99	TIME=	2.80
DKM=	8.01	ADB=	18.30	LB=	74.84	FLDS=	70.55	TIME=	2.86
DKM=	8.11	ADB=	17.37	LB=	74.02	FLDS=	71.37	TIME=	2.91
DKM=	8.21	ADB=	16.44	LB=	73.19	FLDS=	72.20	TIME=	2.97
DKM=	8.31	ADB=	18.58	LB=	75.45	FLDS=	69.95	TIME=	3.02
DKM=	8.41	ADB=	21.63	LB=	78.60	FLDS=	66.79	TIME=	3.08
DKM=	8.51	ADB=	24.29	LB=	81.36	FLDS=	64.03	TIME=	3.14
DKM=	8.61	ADB=	21.34	LB=	78.51	FLDS=	66.88	TIME=	3.19
DKM=	8.71	ADB=	18.84	LB=	76.11	FLDS=	69.28	TIME=	3.24
DKM=	8.81	ADB=	23.44	LB=	80.81	FLDS=	64.58	TIME=	3.30
DKM=	8.91	ADB=	32.12	LB=	89.59	FLDS=	55.80	TIME=	3.36
DKM=	9.01	ADB=	28.18	LB=	85.74	FLDS=	59.65	TIME=	3.42
DKM=	9.11	ADB=	25.18	LB=	82.84	FLDS=	62.55	TIME=	3.49
DKM=	9.21	ADB=	24.23	LB=	81.99	FLDS=	63.40	TIME=	3.55
DKM=	9.31	ADB=	22.50	LB=	80.35	FLDS=	65.04	TIME=	3.61
DKM=	9.41	ADB=	23.56	LB=	81.51	FLDS=	63.88	TIME=	3.67
DKM=	9.51	ADB=	26.02	LB=	84.05	FLDS=	61.34	TIME=	3.72
DKM=	9.61	ADB=	27.74	LB=	85.86	FLDS=	59.53	TIME=	3.78
DKM=	9.71	ADB=	28.13	LB=	86.34	FLDS=	59.05	TIME=	3.84
DKM=	9.81	ADB=	34.81	LB=	93.11	FLDS=	52.28	TIME=	3.91
DKM=	9.91	ADB=	33.61	LB=	92.01	FLDS=	53.39	TIME=	3.98
DKM=	10.01	ADB=	32.08	LB=	90.56	FLDS=	54.83	TIME=	4.05
DKM=	10.11	ADB=	29.91	LB=	88.47	FLDS=	56.92	TIME=	4.13
DKM=	10.21	ADB=	26.12	LB=	84.77	FLDS=	60.62	TIME=	4.20
DKM=	10.31	ADB=	24.58	LB=	83.31	FLDS=	62.08	TIME=	4.27
DKM=	10.41	ADB=	23.04	LB=	81.86	FLDS=	63.53	TIME=	4.34
DKM=	10.51	ADB=	23.03	LB=	81.94	FLDS=	63.46	TIME=	4.41
DKM=	10.61	ADB=	23.17	LB=	82.16	FLDS=	63.23	TIME=	4.49
DKM=	10.71	ADB=	23.72	LB=	82.78	FLDS=	62.61	TIME=	4.56
DKM=	10.81	ADB=	23.75	LB=	82.90	FLDS=	62.49	TIME=	4.64
DKM=	10.91	ADB=	23.57	LB=	82.79	FLDS=	62.60	TIME=	4.71

DKM=	11.01	ADB=	22.83	LB=	82.14	FLOS=	63.25	TIME=	4.78
DKM=	11.11	ADB=	22.28	LB=	81.66	FLOS=	63.73	TIME=	4.83
DKM=	11.21	ADB=	22.35	LB=	81.82	FLOS=	63.57	TIME=	4.90
DKM=	11.31	ADB=	22.10	LB=	81.64	FLOS=	63.75	TIME=	4.98
DKM=	11.41	ADB=	21.12	LB=	80.74	FLOS=	64.65	TIME=	5.05
DKM=	11.51	ADB=	21.78	LB=	81.47	FLOS=	63.92	TIME=	5.13
DKM=	11.61	ADB=	23.31	LB=	83.08	FLOS=	62.31	TIME=	5.20
DKM=	11.71	ADB=	23.96	LB=	83.80	FLOS=	61.59	TIME=	5.28
DKM=	11.81	ADB=	23.58	LB=	83.50	FLOS=	61.89	TIME=	5.35
DKM=	11.91	ADB=	22.74	LB=	82.73	FLOS=	62.66	TIME=	5.43
DKM=	12.01	ADB=	22.56	LB=	82.62	FLOS=	62.77	TIME=	5.49
DKM=	12.11	ADB=	22.58	LB=	82.71	FLOS=	62.68	TIME=	5.58
DKM=	12.21	ADB=	22.59	LB=	82.80	FLOS=	62.59	TIME=	5.65
DKM=	12.31	ADB=	22.61	LB=	82.89	FLOS=	62.50	TIME=	5.72
DKM=	12.41	ADB=	22.64	LB=	82.98	FLOS=	62.41	TIME=	5.78
DKM=	12.51	ADB=	22.66	LB=	83.08	FLOS=	62.31	TIME=	5.86
DKM=	12.61	ADB=	22.70	LB=	83.18	FLOS=	62.21	TIME=	5.94
DKM=	12.71	ADB=	22.59	LB=	83.15	FLOS=	62.24	TIME=	6.02
DKM=	12.81	ADB=	22.48	LB=	83.10	FLOS=	62.29	TIME=	6.10
DKM=	12.91	ADB=	22.47	LB=	83.16	FLOS=	62.23	TIME=	6.18
DKM=	13.01	ADB=	22.61	LB=	83.36	FLOS=	62.03	TIME=	6.26
DKM=	13.11	ADB=	22.67	LB=	83.49	FLOS=	61.90	TIME=	6.33
DKM=	13.21	ADB=	22.67	LB=	83.56	FLOS=	61.84	TIME=	6.41
DKM=	13.31	ADB=	22.78	LB=	83.73	FLOS=	61.66	TIME=	6.49
DKM=	13.41	ADB=	22.89	LB=	83.91	FLOS=	61.48	TIME=	6.57
DKM=	13.51	ADB=	22.57	LB=	83.65	FLOS=	61.74	TIME=	6.65
DKM=	13.61	ADB=	22.40	LB=	83.55	FLOS=	61.84	TIME=	6.73
DKM=	13.71	ADB=	22.42	LB=	83.64	FLOS=	61.75	TIME=	6.81
DKM=	13.81	ADB=	22.28	LB=	83.55	FLOS=	61.84	TIME=	6.89
DKM=	13.91	ADB=	22.50	LB=	83.84	FLOS=	61.55	TIME=	6.97
DKM=	14.01	ADB=	22.72	LB=	84.12	FLOS=	61.27	TIME=	7.05
DKM=	14.11	ADB=	22.28	LB=	83.74	FLOS=	61.65	TIME=	7.13
DKM=	14.21	ADB=	22.25	LB=	83.78	FLOS=	61.61	TIME=	7.22
DKM=	14.31	ADB=	22.30	LB=	83.89	FLOS=	61.51	TIME=	7.30
DKM=	14.41	ADB=	21.91	LB=	83.56	FLOS=	61.83	TIME=	7.38
DKM=	14.51	ADB=	21.72	LB=	83.42	FLOS=	61.97	TIME=	7.46
DKM=	14.61	ADB=	20.29	LB=	82.06	FLOS=	63.33	TIME=	7.55
DKM=	14.71	ADB=	18.77	LB=	80.59	FLOS=	64.80	TIME=	7.63
DKM=	14.81	ADB=	20.54	LB=	82.42	FLOS=	62.97	TIME=	7.72
DKM=	14.91	ADB=	22.15	LB=	84.09	FLOS=	61.30	TIME=	7.81
DKM=	15.01	ADB=	23.19	LB=	85.18	FLOS=	60.21	TIME=	7.89
DKM=	15.11	ADB=	23.79	LB=	85.85	FLOS=	59.54	TIME=	7.97

FORM OT-29
(3-73)

U.S. DEPARTMENT OF COMMERCE
OFFICE OF TELECOMMUNICATIONS

BIBLIOGRAPHIC DATA SHEET

	1. PUBLICATION OR REPORT NO.	2. Gov't Accession No.	3. Recipient's Accession No.
	NTIA Report 79-20		

4. TITLE AND SUBTITLE
Ground Wave Propagation Over Irregular, Inhomogeneous Terrain: Comparisons of Calculations and Measurements.

5. Publication Date
May 1979

6. Performing Organization Code
NTIA/ITS

7. AUTHOR(S)
R.H.Ott, L.E.Vogler, and G.A.Hufford

9. Project/Task/Work Unit No.

8. PERFORMING ORGANIZATION NAME AND ADDRESS
U. S. Department of Commerce
National Telecommunications and Information Administration
Institute for Telecommunication Sciences
325 Broadway, Boulder, Colorado 80303

10. Contract/Grant No.

11. Sponsoring Organization Name and Address
Electromagnetic Compatibility Analysis Center
North Severn, Annapolis, Maryland 21402 and
Dept. of Air Force, Space & Missile Systems Org.(AFSC)
Bldg. 523, Rm. 303, Norton AFB, CA 92409

12. Type of Report and Period Covered

13.

14. SUPPLEMENTARY NOTES

15. ABSTRACT *(A 200-word or less factual summary of most significant information. If document includes a significant bibliography or literature survey, mention it here.)*

An algorithm (PROGRAM WAGNER) that evaluates HF ground-wave attenuation over irregular, inhomogeneous terrain is used to compare calculated field strengths with observed measurements for 9 actual paths and frequencies ranging from 120 kHz to 50 MHz. All comparisons show encouraging agreement between calculations and measurement. The 20 MHz comparisons over the Colorado Mountains provided a challenge for PROGRAM WAGNER.

16. Key Words *(Alphabetical order, separated by semicolons)*

HF-VHF groundwave prediction; integral equation method; irregular terrain; measurement comparisons; radio propagation.

17. AVAILABILITY STATEMENT

☒ UNLIMITED.

☐ FOR OFFICIAL DISTRIBUTION.

18. Security Class *(This report)*
Unclassified

20. Number of pages
137

19. Security Class *(This page)*
Unclassified

21. Price:

☆ U.S. GOVERNMENT PRINTING OFFICE:1979—680-195 / 484

USCOMM-DC 29716-P73